
European Polar Stratospheric Cloud and Lee Wave Experiment

# EUPLEX

A project within the RTD Programme
"Energy, environment, and sustainable development"
Contract No.: EVK2-CT-2001-00119
http://www.nilu.no/euplex

## Final Report
## Reporting Period: 01.05.2002-31.10.2004

**Version 3.1 (Final) 18.02.2005**

**Co-ordinator:**
Dr. Fred Stroh
Forschungszentrum Jülich GmbH

# Contents

# GENERAL EUPLEX PROJECT DESCRIPTION

EUPLEX adressed key questions of Arctic stratospheric ozone depletion that were not answered to a satisfactory extent: How do PSCs form and are observed PSC growth and properties – in both synoptically cold regions and in regions of lee-wave activity – in accord with our current understanding of stratospheric-particle microphysics? How can observed denitrification and dehydration be explained? Are observed halogen activation rates consistent with the current theory of heterogeneous activation on PSC particles? What is the relative importance of synoptic and Lee-wave PSCs for chlorine activation and Arctic ozone loss? Can observed ozone loss rates be explained by the currently accepted ozone loss cycles given simultaneously observed ClO, BrO, and NO/NOy mixing ratios?

Dedicated strategies had been developed to approach these questions, by combining comprehensive in-situ observations of gas-phase composition, aerosol/particle properties, and physical parameters during a field campaign from a high-altitude research aircraft (the *M55-Geophysica*) with LIDAR observations from a lower-flying aircraft (the DLR *Falcon*). Data interpretation was carried out employing a hierarchy of up-to-date microphysical and chemical-dynamical models of the stratosphere.

EUPLEX was a component of the pan-European project **V**alidation of **Inter**national **S**atellites and Study of **O**zone **L**oss (VINTERSOL). The field campaign took place in January/February 2003 in close cooperation with the NASA-led SOLVEII (SAGEIII Validation and Ozone Loss Experiment) campaign.


**International Cooperation in Arena Arctica, Kiruna, Sweden, during the Joint VINTERSOL-EUPLEX / SOLVEII Measurement Activities in January/February 2003. In the foreground the VINTERSOL-EUPLEX carriers the German DLR-Falcon and the Russian M55-Geophysica high altitude aircraft can be seen. In the back the NASA-DC8 of the SOLVEII community is parked. (Photo courtesy of P. Mazzinghi)**

**The M55-Geophysica under take-off preparation during the VINTERSOL-EUPLEX field campaign at Kiruna airport in late January 2003 around noon time. (Photo courtesy of P. Mazzinghi)**

# SECTION 1: MANAGEMENT REPORT FOR THE REPORTING PERIOD

## 1.1 Objectives of the Reporting Period

The graphical presentation of the planned EUPLEX project work flow is shown in Fig. 1.1. In the reporting period which was a six months extension of the regular project period the following main management activities were planned and performed:

1. Coordination of final data analysis for some data products
2. Coordination of ongoing interpretational studies
3. Coordination of publications of project results
4. Presentation of the project results at scientific meetings
5. Preparation and assembly of the final report

Within this final reporting period the EUPLEX consortium has worked out and mostly published additional relevant results on several of its key scientific objectives. Currently 18 publications are accepted by or submitted to peer-review journals. Thereby EUPLEX finishes off providing major new insights on almost all of its scientific objectives, with very few exceptions all planned deliverables have been supplied. Additional results on scientific objectives which had initially been grouped as alternate objectives have been produced or are currently being refined (five major publications are in preparation). A wealth of measurement data obtained under various very interesting and unique atmospheric conditions during the VINTERSOL/SOLVEII Arctic field campaign in 2003 has provided a rich data base that is open to the general scientific community and will certainly foster more scientific studies on processes relevant for the polar and also mid-latitude stratospheric ozone layer.

While many activities within the project were completed in time some deliverables could only be finished within a project extension period mainly due to instrumental upgrades and model refinements and upgrades which needed more work for implementation and/or validation than anticipated.

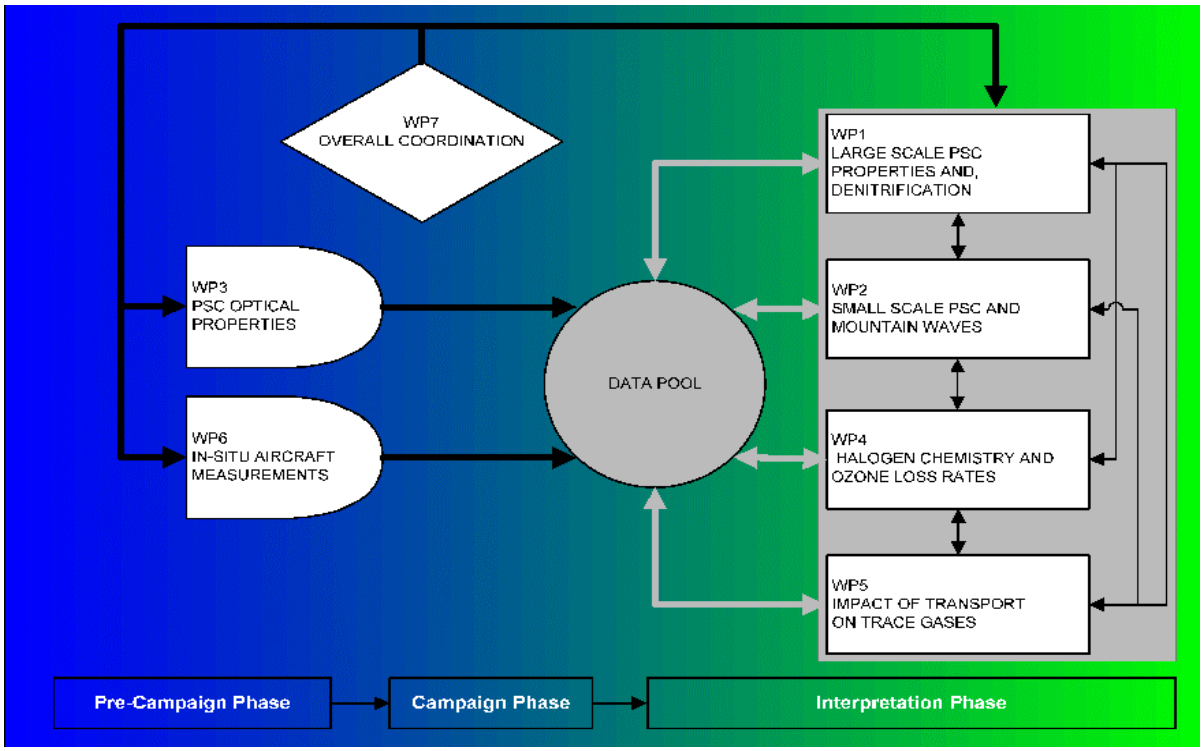


**Fig. 1.1 Graphical Representation of the EUPLEX Project Structure**

An overview of the major new findings obtained within the extension period will be given on the next pages and details are presented in section 2 and section 6 of this report

## 1.2 Scientific and Technical Progress in the Reporting Period

The work flow within the EuPLEx project is represented in the Gantt chart in Fig. 1.2. Good progress was made with the finalization of the data obtained during the field campaign (WP3 and 6) and with the interpretational work (WP1, 2, 4, and 5). At the end of the project period very valuable and interesting new scientific and technical results have been worked out on almost all of the EUPLEX science objectives. Most studies have been published in the peer reviewed literature, primarily in the Atmos. Chem. Phys. SOLVEII/VINTERSOL special issue.

1. A comprehensive data set on the chemical and dynamical evolution of the Arctic polar vortex and its surrounding regions has been measured in the January/February 2003 time period. Data sets consist of meteorological parameters, dynamical tracers (partly with isotopic composition), reactive chemical species involved in ozone destruction, and aerosol physical and chemical properties. With few exceptions all data sets have been finalized and archived on the NILU data base.

2. Observations of particle phase NOy by the SIOUX instrument and particle properties by the FSSP, MAS, and MAL instruments onboard the M55-Geophysica show that in contrast to current understanding small solid particles can form at very small number densities under threshold conditions without prior formation of ice particles. These small NAT particles are a source of large NAT rocks as firstly observed during SOLVE in the arctic winter 1999/2000. This finding is one of the major EUPLEX results and was published in Atmos. Chem. Phys.

3. Observed features of de-/renitrification can be quite well reproduced by the Univ. of Leeds DLAPSE as well as the FZJ CLaMS models assuming a volume dependent NAT nucleation rate. This shows that the development of reliable code for the simulation of this process may be possible. Respective publications have been submitted to Atmos. Chem. Phys.

4. The upgrade of the HALOX instrument from the halogen oxides ClO and BrO towards the simultaneous measurement of the ClO-Dimer, $(ClO)_2$, has yielded a unique data set that allows the study of the respective chlorine partitioning. For the first time reliable laboratory calibrations for the dimer thermal decomposition have been carried out. The study calls for an update of the ClO/ClO dimer equilibrium constant and indicates a problem in our understanding of chlorine chemistry. The study is published in Atmos. Chem. Phys. Disc.

5. Dynamical features of different scale size and intensity as a result of mixing-in of extra vortex air masses were observed on several flights around the vortex boundary region and also deep within the vortex. CLaMS 3D studies have revealed a good model reproduction of these observations and show that central regions of the vortex are hardly affected by these processes. The study is published in Atmos. Chem. Phys.

6. ClO measurements by the HALOX instrument onboard the M55-Geophysica aircraft in connection with chemical modelling employing the FZJ CLaMS model allow a study of ongoing Cl activation. Good reproduction of the activation process by the CLAMS model have been found, however the initialization of the model runs needs to be refined still.

7. Based on ozone-tracer correlations the development of chemical ozone loss over the mid January to mid March period was monitored in the 15 to 20km altitude range. This study is currently being finalized.

8. HALOX measurements of enhanced ClO mixing ratios in the UTLS region between 12 and 14km in altitude are under investigation in order to study the importance of chlorine activation on cirrus clouds.

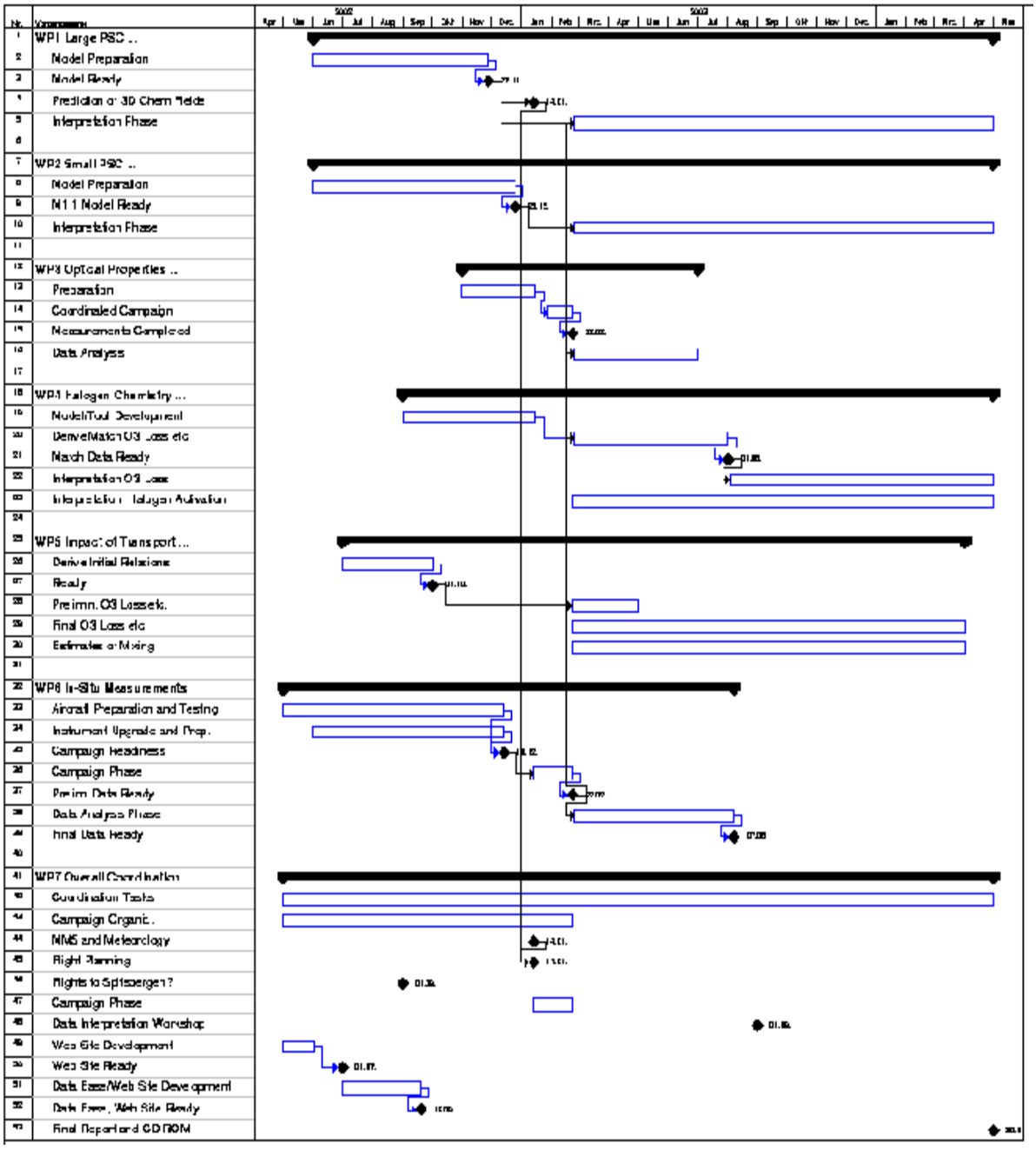


**Fig. 1.2 Gantt Chart of the EuPLEx project work flow. Major work flows extending beyond this point are in WP5 (halogen photochemistry and activation on cirrus particles), WP6 (mixing studies and ozone loss), and WP7 (calibration of ClO dimer and $ClONO_2$ measurements.).**

A preliminary list of the used financial resources per project partner is given in Tab. 1.1. For most partners some resources were still available within the extension period, e.g. since in several cases personnel could only be hired with significant delays from project start. A final table will be supplied as soon as the respective partners (empty rows) have supplied their cost statements to the coordinator. Obviously several administrations face severe problems finishing up statements towards the end of the year and early in the new year.

.

| Partner | Per-sonnel | Durable Equipm. | Sub-con-tract-ing | Travel + Subsist. | Cosumables | Com-put-ting | Other Costs | Over-head | Total |
|---|---|---|---|---|---|---|---|---|---|
| **FZJ** | 27524 | 0 | 0 | 4567 | 0 | 0 | 0 | 23049 | **55140** |
| **DLR** | 30088 | 0 | 0 | 1805 | 0 | 0 | 0 | 18035 | **49928** |
| **IPA-UMZ** | 0 | 0 | 0 | 527 | 0 | 0 | 763 | 258 | **1548** |
| **JWG-IMG** | 0 | 0 | 0 | 3070 | 172 | 0 | 0 | 648 | **3188** |
| **ON** | Swiss Partner | | | | | | | | |
| **AWI** | 21047 | 0 | 0 | 1190 | 0 | 0 | 0 | 16837 | **39074** |
| **CNR-IFA** | Cost Statement issued together with Partner 7 (CNR-IFA) | | | | | | | | |
| **INOA** | 6054 | 0 | 6200 | 1245 | 0 | 0 | 0 | 1460 | **11639** |
| **CAO** | 0 | 0 | 0 | 5600 | 4100 | 0 | 0 | 1940 | **11640** |
| **ULANC** | 17610 | 0 | 0 | 3956 | 0 | 0 | 0 | 4313 | **25879** |
| **ETHZ** | 31099 | 0 | 0 | 2300 | 0 | 0 | 0 | 0 | **33399** |
| **UNI-LEEDS** | 8134 | 277 | 0 | 45 | 0 | 0 | 0 | 1691 | **10882** |
| **NILU** | 15791 | 0 | 6188 | 0 | 0 | 0 | 0 | 10973 | **32952** |
| **STM** | 4031 | 0 | 0 | 0 | 0 | 0 | 0 | 3225 | **7256** |
| **CNR-ISAO** | 22426 | 0 | 0 | 2763 | 0 | 0 | 0 | 17937 | **43126** |

**Tab. 1.1 Preliminary Resource Allocation Table: Used financial resources per partner. All numbers are in €. Note that in the Total adjustments to costs previously reported are included.**

## 1.3 Milestones and Deliverables Obtained

Tab 1.2 and Tab 1.3 give complete lists of the project deliverables and milestones. With the exception of the aircraft MATCH flights and the dependent items (see EUPLEX Mid-Term Report), some results related to ice formation in PSC, and related to halogen photochemistry and ozone loss all deliverables and milestones have been timely delivered within the regular project period. All major scientific results are either published in the peer reviewed literature or publications are in preparation.

| Deliv. # | Deliverable Title | Deliv. Date[1] | Nature[2] | Status[3] |
|---|---|---|---|---|
| **D1.1** | $NO_y$ abundance in PSC particles of different types including NAT rocks | 12 | Da | OK |
| **D1.2** | Calculated synoptically produced PSC size distributions and $HNO_3$ content along Geophysica flight tracks | 8 | Da | OK |
| **D1.3** | Calculated gas phase $HNO_3$ fields | 8 | Da | OK |
| **D1.4** | Calculated denitrification fields and evaluation of model against observations | 8 | Da | OK |
| **D1.5** | Evaluation and revision of synoptic PSC nucleation mechanisms in written reports | 22 | Re | OK |
| **D2.1** | Documented case studies of mountain wave PSC encounters – in-situ data, co-located lidar data, and dynamical analysis. | 22 | Da | OK |
| **D2.2** | Improved algorithms for growth and phase change (nucleation of ice) of mountain wave PSC particles | 22 | Me | NO/R |
| **D2.3** | Microphysical simulations of aerosol phase and surface area for WP4. | 14 | Da | OK |
| **D2.4** | Test of the hypothesis: there is a single sequence of PSC composition for lee wave clouds. Reported in refereed literature. Connected issue: could mountain PSCs initialise NAT-rock formation? | 22 | Da | NO/R |
| **D3.1** | 2-D real time information of location, extension, internal structure of PSCs from Falcon flight level (12 km) to top of aerosol layer (30 km) | 8 | Da | OK |
| **D3.2** | Temperature fluctuations inferred from Falcon lidar profiles | 10 | Da | OK |
| **D3.3** | Data set of range-corrected backscatter signal and volume depolarisation ratio within 2 km above and below the Geophysica. | 12 | Da | OK |

[1]month in which the deliverables were made available. Month 0 marking the start of the project, and all delivery dates being relative to this start date
[2]nature of the deliverable; Re = Report, Da = Data set, Me = Methodology
[3]status of the deliverable, OK = available, P = in preparation, NO = cannot be delivered due to missing data because of meteorological situation during campaign, R=Related results available, no entry = not yet available.

**Tab. 1.2 Complete list of Deliverables and Status of Delivery**

| | | | | |
|---|---|---|---|---|
| **D4.1** | Two sets of trajectories connecting measurements of two flights within 5-7 days | 8 | Da | OK |
| **D4.2** | Ozone loss and other chemically induced changes for two matches | 12 | Da | NO |
| **D4.3** | Box model simulations with respect to ozone loss and/or de-/rehydration and de-/renitrification or $HNO_3$ photolysis or chlorine deactivation. | 18 | Da | OK |
| **D4.4** | Results for chlorine activation from box model simulations. | 24 | Da | OK |
| **D4.5** | Chemical fields from a 3D-CTM including information on de-nitrification | 8 | Da | OK |
| **D4.6** | High-resolution simulations of chemical fields | 8 | Da | OK |
| **D4.7** | Vortex average chemical ozone loss from ozone sondes | 24 | Da | OK |
| **D5.1** | Initial relations for $Cl_y$:$N_2O$, $Br_y$:CFC-11 valid for the time of the mission | 8 | Da | OK |
| **D5.2** | Initial relations for $O_3$:$N_2O$, $O_3$:$CH_4$ and $NO_y$:$N_2O$ in the early vortex | 8 | Da | OK |
| **D5.3** | Total inorganic chlorine and bromine along the Geophysica flight track | 12 | Da | OK |
| **D5.4** | Estimates of integrated ozone loss, denitrification and dehydration, and their uncertainties | 14 | Da | OK |
| **D5.5** | Estimates of the amount and character of mixing across the vortex edge | 24 | Da | OK |
| **D6.1** | 2-D Quick-look data from all instruments within 12 hr after flight for strategy identification. | 8 | Da | OK |
| **D6.2** | Validated concentrations of active chemical species ClO, BrO | 18 | Da | OK |
| **D6.3** | Validated data of the tracer species N2O, CH4, O3, H2O, CO2, and CFC F11 | 16 | Da | OK |
| **D6.4** | Validated data of reactive nitrogen species NOy | 12 | Da | OK |
| **D6.5** | Validated cloud particle size distributions with optical particle counter | 12 | Da | OK |
| **D6.6** | Validated background aerosol particle number density | 12 | Da | OK |
| **D6.7** | Validated cloud backscatter and depolarisation data | 12 | Da | OK |
| **D6.8** | Validated meteorological base parameters | 12 | Da | OK |
| **D7.1** | PSC climatology for campaign site selection | 3 | Da | OK |
| **D7.2** | Alternative scientific objectives | 5 | Da | OK |
| **D7.3** | Supply trajectories for different flight scenarios | 8 | Da | OK |
| **D7.4** | Experimental and flight diary | 9 | Re | OK |
| **D7.5** | Collection of meteorological forecasts and analyses during campaign | 9 | Re | OK |
| **D7.6** | Web site, news paper reports, press release | 0 | Re | OK |
| **D7.7** | Scientific campaign overview paper | 24 | Re | P |
| **D7.8** | Final Report | 26 | Re | OK |
| **D7.9** | Data CD ROM | 24 | Da | P |

**(Tab. 1.2 continued)**

| MS. # | MS title | Date | Status |
|---|---|---|---|
| **M1.1** | Models ready for campaign forecasting and data analysis | 7 | OK |
| **M1.2** | Evaluation of models against observations and testing of synoptic PSC hypotheses | 24 | OK |
| **M2.1** | Definition of 'default' model parameters, and variations | 3 | OK |
| **M2.2** | Definition of case studies | 10 | OK |
| **M2.3** | First test of hypothesis | 15 | OK |
| **M2.4** | Test of hypothesis with refined models | 22 | OK |
| **M3.1** | Lidar measurements completed | 8 | OK |
| **M3.2** | Lidar and scatterometer final data available | 12 | OK |
| **M4.1** | Final set of trajectory sets ready | 10 | OK |
| **M4.2** | Ozone loss deduced from aircraft measurements | 13 | OK |
| **M4.3** | Results of model calculations for the Match trajectory set finished and analysed | 23 | NO |
| **M4.4** | Simulation of halogen activation events for the PSC flights finished and analysed | 24 | OK |
| **M5.1** | Definition of appropriate relations for Cly:$N_2O$, Bry:CFC-11 | 8 | OK |
| **M5.2** | Definition of initial relations $O_3$:$N_2O$, $O_3$:$CH_4$ and NOy:$N_2O$ | 6 | OK |
| **M5.3** | First estimates of ozone loss, denitrification and dehydration | 10 | OK |
| **M5.4** | Refined estimates of ozone loss, denitrification and dehydration | 24 | OK |
| **M5.5** | Estimates of mixing across vortex edge | 24 | OK |
| **M6.1** | Modifications of in-situ NOy instrument for detection of particle NOy completed | 6 | OK |
| **M6.2** | Calibrated instruments ready for aircraft measurement campaign | 7 | OK |
| **M6.3** | Preliminary data ready (12h after return of the aircraft) | 8 | OK |
| **M6.4** | Final data ready on data base | 12 | OK |
| **M7.1** | Kick-Off meeting | 0 | OK |
| **M7.2** | Campaign site selected | 3 | OK |
| **M7.3** | Campaign group meeting | 4 | OK |
| **M7.3** | Campaign Infrastructure secured | 5 | OK |
| **M7.4** | End of Co-ordinated field campaign | 8 | OK |
| **M7.5** | Data interpretation workshop | 15 | OK |
| **M7.6** | Final project meeting | 23 | OK |
| **M7.7** | Final Report | 26 | OK |

**Tab. 1.3 Complete list of Milestones and Status of Work (same coding as for Tab 1.1, see footnotes there)**

## 1.4 Deviations from the Work Plan

A detailed task list for the extension period was set-up and is listed in the yearly report 2004. The delayed work was related to the following subjects:

1. Halogen chemistry: Due to the upgrade of the FZJ HALOX instrument to also measure the ClO dimer and chlorine nitrate (in addition to ClO and BrO) the timely availability of the deliverable D6.2 could not be realized. Now sophisticated laboratory calibrations for the ClO dimer have been carried out in order to finalize the data for the associated model studies (D4.3, D5.4). The delivery of calibrated data for $ClONO_2$ may not be possible subject to ongoing laboratory calibrations.
2. Ozone loss: As reported in the Mid-Term Report (p.15) direct measurements of ozone loss rates within one air mass (the so-called aircraft MATCH experiment, D4.2) could not be carried out due to unfavorable meteorological conditions. However, a study of ozone loss derived from tracer correlations (D5.2) had been launched by partner 4 in connection with partner 1 but could not be finished until the end of the regular project period.
3. PSC formation: Partner 10 has been developing a new non-equilibrium model for stratospheric aerosol. However, the model has only recently been completed and deliverables D2.2 and D2.3 had not been finalized within the regular project period. These are crucial to the finalization of the hypothesis test D2.4.
4. High-resolution tracer data: Due to instrumental problems the high time resolution $N_2O$ measurements of Partner 8 needed much more time for data analysis than anticipated. Therefore this part of D6.3 is still finalized through intercomparisons. This data is crucial for the final model treatment of dynamical features (D5.5).

No further deviation from this task list was encountered and at the end of the extension period the related deliverables have been supplied either as data to the data base or in the form of publications. Some publications are not yet accepted but have been submitted.

Since several data sets have only been submitted quite recently the data CD ROM has not yet been completed. It will become available within the next three months. It is planned to have it ready for the EGU meeting in Vienna in April in order to promote and distribute it there to interested scientists.

## 1.5 Co-ordination of the Information and Communication Activities

The major tool for the exchange of information within the EUPLEX project is email. Therefore the mailing lists:

- euplex_all@nilu.no (all people involved in the EUPLEX project) and
- euplex_cg@nilu.no (EUPLEX core group)

were set-up and have been updated regularly in order to have easy access to all project participants or just the core group.

### 1.5.1 EUPLEX Data Base and Web Page

A VINTERSOL-EUPLEX database was be set up under NADIR at NILU (zardoz.nilu.no path: /nadir/projects/vintersol/data/euplex/) for acquisition and storage of all experimental and theoretical data sets. Common data format is the NASA-Ames format widely used in the stratospheric scientific community. A project web page (http://www.nilu.no/euplex) was also established at NILU in order to communicate non-urgent information to all project members through a restricted access area. In addition a public access section was maintained to supply information on the objectives, progress, and first results to the interested public. A data CD ROM is in prepa-

ration and will become available within the next three months. It is planned to have it ready for the EGU meeting in Vienna in April in order to promote and distribute it there to interested scientists.

### 1.5.2 Meetings

In order to ensure the proper flow of information between the partners and to readily initiate project tasks within the different work packages project meetings were planned and held as scheduled in the Description of Work and detailed in Table 6.2. Minutes of the project meetings are available from the EUPLEX web site.

Within the reporting period the Final Project Workshop was held on 14./15. Sept. 2004 at University of Leeds, UK, focussing on the final data status and results of the data interpretation work within the project. A very productive two day meeting was held and many well worked out results were presented. Some problems with data quality were discussed and mainly solved. The preparation of the final report was organized and tasks and deadlines were defined.

Very interesting data was gathered during the Arctic campaign also in the UTLS region enabling new stufies into NOy partitioning in the presence of ice particles in the form of cirrus clouds and also on their potential for halogen activation. These subjects have not been primary scientific objectives of EUPLEX but alternate objectives in case of unfavourable meteorological conditions. However, since these data are available anyway, the consortium will keep working on their exploitation. The further plans for the analysis and interpretation of this data and first studies were discussed on 10. Jan. 2005 at a dedicated meeting at DLR, Oberpfaffenhofen.

### 1.5.3 Further Communication Activities

An abstract for an overview presentation of the EUPLEX project results and the implications for the Arctic ozone problem has been submitted to the Polar ozone session for the EGU meeting 2005 in Vienna. The possibility of an overview paper in the peer reviewed literature (Atmos. Chem. Phys.) is currently being investigated.

Currently a broad press release on the EUPLEX project results and the implications for the Arctic ozone problem is discussed within the consortium. The activity will be lead by the coordinator even so the official project period is finished.

The EUPLEX campaign and the results with emphasis on the ones obtained at FZJ was recently featured in the Yearly Report of the HGF (Helmhotz-Gemeinschaft Deutscher Großforschungszentren).

### 1.5.4 Difficulties encountered at co-ordination level

A problem arose with the end of the project period with the timeliness of the contributions from several project partners for the final report. Obviously such reports are even harder to assemble towards the end of a year. However, with the submission of this report this problem isn't relevant anymore within this project. A viable solution could be to grant an automatic extension for the submission of any major report if the holiday season falls within the preparation period.

# SECTION 2: EXECUTIVE SUMMARY FOR THE REPORTING PERIOD

| Contract n° | EVK2-CT-2001-00119 | Reporting period: | 01.05.2004 – 31.10.2004 |
|---|---|---|---|
| Title | EuPLEx - European polar stratospheric cloud and lee wave experiment | | |

**Objectives**

General objectives are critical tests of current hypotheses for the three key processes of Arctic stratospheric ozone depletion chemistry through measurement-model intercomparisons:

1. PSC formation and properties in Lee-wave and synoptic scale PSC;
2. Halogen activation on PSC, and;
3. Chemical ozone loss.

These tests should lead to an improvement of the model reproduction of these crucial processes.

During the project extension period the following tasks were to be completed:

1. Finalization of data products from the field campaign;
2. Finalization of interpretational studies concerning PSC formation and halogen activation.
3. Publication of the results in the peer reviewed literature.

**Scientific achievements completed in the extension period**

1. A comprehensive data set on the chemical and dynamical evolution of the Arctic polar vortex and its surrounding regions has been measured in the January/February 2003 time period. Data sets consist of meteorological parameters, dynamical tracers (partly with isotopic composition), reactive chemical species involved in ozone destruction, and aerosol physical and chemical properties. With few exceptions all data sets have been finalized and archived on the NILU data base and are available to the VINTERSOL and SOLVE-II communities as well as to the public.
2. Observations of particle phase NOy and particle properties under threshold conditions show that small NAT particles can form at very small number densities without pre-existence of ice particles. Since homogeneous nucleation can also be excluded for the probed scenarios the observed NAT rock embryos (most probably a source of large NAT rocks) are likely to form by heterogeneous nucleation (e.g. on meteoritic dust particles).
3. However, the formation of NAT containing particles within lee-wave events was shown to also have a significant potential for the formation of synoptic NAT PSCs and subsequent denitrification in the Arctic region.
4. A good quantitative model reproduction of observed de-/renitrification in the Arctic polar vortex 2002/03 was attained when regarding non-equilibrium conditions for the growth of NAT particles. Observations of lee-wave PSCs confirm the importance of non-equilibrium liquid particles, as predicted by detailed PSC models; the quasi-lagrangian sampling of particle composition within these PSCs provides a stringent test of the models.
5. The HalogenOxides (HALOX) instrument (ClO, BrO) was upgraded towards the measurement of the ClO-Dimer (ClOOCl) and of chlorine nitrate, $ClONO_2$. For the first time ClO dimer laboratory calibrations were performed to ensure proper dimer measurements.
6. Independent studies of the measured ClO and dimer concentrations for just one flight and a suitable ensemble of flights, respectively, have consistently revealed more nighttime ClO than predicted from the established (JPL) equilibrium constant, calling for a smaller equilibrium constant Keq. This points to the fact that there still is a major challenge in the understanding of stratospheric reactive chlorine partitioning.
7. Intercomparison of measured and modelled ClO suggest that ongoing Cl activation on liq-

uid aerosol particles has been observed and can be reproduced by CLaMS reasonably well.

8. Accumulated observed ozone loss around the 450K potential temperature level from early December 2002 to mid March 2003 amounts to about 1200 ppb. This is somewhat higher than the modelled integrated ozone loss employing standard (JPL) kinetics. However, employing the new ClO/ClO dimer equilibrium constant derived from the EUPLEX measurements and simultaneously higher Bry mixing ratios (as recently reported by Pundt et al.) integrated ozone loss in the observed magnitude can be reproduced within a simple box model.
9. Dynamical features of different scale size and intensity as a result of mixing in of extra vortex air masses can be reasonably modelled and even predicted employing the Lagrangian CLaMS model.
10. For a flight tailored to the observation of the equilibrium between ClO and its dimer in the same air mass measured at daylight and night-time CN measurements show that at some points the air masses have been exactly reencountered in agreement with the meteorological analysis. This experiment shows that such self-Match and consequently also Match flights are possible under appropriate meteorological conditions.
11. During a flight in cirrus clouds at 10km altitude preliminary data from the HALOX instrument indicate enhanced levels of ClO compared to outside the cloud. Also on several ascent and descent manoeuvres shallow enhancements in ClO have been observed between 12 and 14km in altitude. These observations very relevant for the UTLS region are still under investigation.

**Socio-economic relevance and policy implications**

The thinning of the ozone layer is a global problem and therefore affects all of Europe. The substantial ozone loss that has been observed in the Arctic has affected Europe more than other regions of the Northern Hemisphere. This is due to the fact that the polar vortex often is shifted towards the European sector of the Arctic because of the Aleutian high (a high pressure system over Alaska and Easter Siberia). Therefore it is of strategic importance to Europe to obtain a better understanding of the ozone layer problem in order to enable reliable predictions of its future state. GCM calculations [Shindell et al., Nature, 392, 589 (1998)] predict that the coupling of ozone and climate may lead to far more dramatic ozone loss during the decade from 2010 to 2020 than has been observed during the 1990s. Especially in the Northern hemisphere, the potential for increasing ozone losses exist [Waibel et al., Science, 283, 2064 (1998)]. Thinning of the ozone layer leads to increased levels of UV-B radiation on the ground that has adverse effects on human health, the marine environment, as well as agriculture. The crucial uncertainties for predicting the future development of the Arctic winter ozone layer are those addressed by EUPLEX.

The scientific results from EUPLEX considerably enhance in various aspects the potential for improved modelling and even short term prediction of Arctic polar ozone losses to be expected in any ongoing winter season. This in the longer run may enable short term (weeks to months) warnings in case of extremely low ozone columns and consequently elevated UV exposures above the European region in early spring. This is a major contribution to the actions quality of life and health and security.

**Conclusions**

The results obtained within the EuPLEx project improve our understanding of the processes of PSC formation, denitrification, halogen activation, and ozone loss in the Arctic polar winter and spring. The results provide a major step forward in the representation of the related processes in our models of the Arctic polar winter and spring stratospheric ozone destruction. This means a significantl improvement of our capability to predict short term evolutions of the northern hemisphere ozone layer and consequently UV exposure on ground and therefore may enable

policy decisions for mitigation in case of severe events.

Keywords

Stratospheric ozone, polar stratospheric clouds, NAT particles, stratospheric denitrification, halogen activation, halogen partitioning, arctic ozone depletion, polar vortex dynamics.

## 2.1 List of peer reviewed and submitted publicatons from the project

Bogdan, A., M. Kulmala, A. R. MacKenzie, A. Laaksonen, M. J. Molina, and A. Avramenko, The study of finely divided aqueous systems as a clue to understanding the formation mechanisms of polar stratospheric clouds: 1. $HNO_3/H_2O$ and $H_2SO_4/H_2O$ systems, *J. Geophys. Res.*, **108** (D10), 4302, doi:10.1029/2002JD002605.

Bogdan, A., M. Kulmala, A. R. MacKenzie, A. Laaksonen, M. J. Molina, and A. Avramenko, The study of finely divided aqueous systems as a clue to understanding the formation mechanisms of polar stratospheric clouds: 2. $HCl/H_2O$ and $HNO_3/HCl/H_2O$ systems, *J. Geophys. Res.*, **108** (D10), 4303, doi:10.1029/2002JD002606.

Curtius, J., R. Weigel, H.-J. V?ssing, C.-M. Volk, A. Werner, H. Schlager, A. Roiger, C. Schiller, H. Wernli, V. Dreiling, and S. Borrmann, In-situ aerosol measurements covering the 10 nm to 30 microm size range in the Arctic lower stratosphere during winter 2003 onboard the high altitude research aircraft Geophysica, submitted to Atmos. Chem. Phys, 2004.

Davies, S., G. W. Mann, K. S. Carslaw, M. P. Chipperfield, J.A. Kettleborough, M.L. Santee, H. Oelhaf, G. Wetzel, Y. Sasano, T. Sugita, 3-D microphysical model studies of Arctic denitrification: Comparison with observations, submitted to Atmos. Chem. Phys. Disc., 2004.

Feng, W., , M.P. Chipperfield, S. Davies, B. Sen, G. Toon, J.F. Blavier, C.R. Webster, C.M. Volk, A. Ulanovsky, F. Ravegnani, P. von der Gathen, H. Jost, E.C. Richard, H. Claude, Three-Dimensional Model Study of the Arctic Ozone Loss in 2002/03 and Comparison with 1999/2000 and 2003/04, Atmos. Chem. Phys. Discuss, 4, 5045-5074, 2004.

Grooß J.-U., G. Günther, R. Müller, P. Konopka, S. Bausch, H. Schlager, C. Voigt, C. M. Volk, G. C. Toon, Simulation of denitrification and ozone loss for the Arctic winter 2002/2003, Atmos. Chem. Phys. Discuss., 4, 8069-8101, 2004.

Hobe, M. von, J.-U. Grooß, R. Müller, S. Hrechanyy, U. Winkler, F. Stroh, A re-evaluation of the ClO/ $Cl_2O_2$ equilibrium constant based on stratospheric in-situ observations, , Atmos. Chem. Phys. Discuss., 4, 5075-5102, 2004

Mann, G.W., K.S. Carslaw, M.P. Chipperfield, S.D. Eckermann, Large NAT particles and denitrification caused by mountain waves in the Arctic stratosphere, accepted for publication in J. Geophys. Res., 2005.

Davies, S., G. W. Mann, K. S. Carslaw, M. P. Chipperfield, J.A. Kettleborough, M.L. Santee, H. Oelhaf, G. Wetzel, Y. Sasano, T. Sugita, 3-D microphysical model studies of Arctic denitrification: Comparison with observations, submitted to Atmos. Chem. Phys. Disc., 2004.

Kleinboehl, A., J. Kuttippurath, M. Sinnhuber, B.-M. Sinnhuber, H. Kuellmann, K. Kuenzi, J. Notholt, Rapid meridional transport of tropical airmasses to the Arctic during the major stratospheric warming in January 2003, Atmos. Chem. Phys. Discuss., 4, 7121-7138, 2004.

Konopka, P., H.-M. Steinhorst, J.-U. Grooß, G. G¨unther, R. M¨uller, J. W. Elkins, H.-J. Jost, E. Richard, U. Schmidt, G. Toon and D. S. McKenna, 2004: Mixing and ozone loss in the 1999-2000 arctic vortex: Simulations with the 3-dimensional Chemical Lagrangian Model of the Stratosphere (CLaMS). *J. Geophys. Res.*, **109**(D2), doi:10.1029/2003JD003792.

Lowe, D., A. R. MacKenzie, N. Nikiforakis, and J. Kettleborough, A condensed-mass advection based model of liquid polar stratospheric clouds, *Atmos. Chem. Phys.*, **3**, 29-38, 2003.

Lowe, D., A. R. MacKenzie, H. Schlager, C. Voigt, A. Dörnbrack, M. J. Mahoney, and F. Cairo, Liquid particle composition and heterogeneous reactions in a mountain-wave Polar Stratospheric Cloud, *Atmos. Chem. Phys. Discuss.*, submitted November 2004.

MacKenzie, A. R., Recent advances in the study of polar stratospheric and tropical tropopause clouds, *Recent Res. Developments in Geophysics*, **4**, 439-462, 2002.

Steinhorst, H.-M., P. Konopka, G. G¨unther and R. M¨uller, 2004: How permeable is the edge of the Arctic vortex - Model studies of winter 1999-2000. *J. Geophys. Res.*, accepted.

Tilmes, S., R. Müller, J.-U. Grooß, M. Ho¨pfner, G. C. Toon, and J. M. Russell III, Very early chlorine activation and ozone loss in the Arctic winter 2002 – 2003, Geophys. Res. Lett., 30(23), 2201, doi:10.1029/2003GL018079, 2003.

Voigt, C., H. Schlager, B. Luo, A. Dörnbrack, A. Roiger, P. Stock, J. Curtius, H. Vössing, S. Borrmann, S. Davies, P. Konopka, C. Schiller, G. Shur, T. Peter, NAT formation of low Nat supersaturations, Atmos. Chem. Phys. Discuss., 4, 8579-8607, 2004.

## 2.2 List of publicatons from the project in preparation

Davies, S., G. W. Mann, K. S. Carslaw, M. P. Chipperfield, J. J. Remedios, A. M. Waterfall, Arctic denitrification during winter 2002/03: using satellite observations to interpret a 3-D microphysical model, manuscript in preparation.

Grooß, J.U., Rolf Müller, Fred Stroh, Marc von Hobe, Observation and simulation of air with recent chlorine activation, in preparation for Atmos. Chem. Phys, 2005.

Günther, G., R. Müller, P. Konopka, F. Stroh, C. M. Volk, Quantification of Mixing and Transport across the Boundary of the Lower Vortex during the Winter 2002/03, in preparation for Atmos. Chem. Phys., 2005.

Remedios, J.J. Remedios, A.M. Waterfall, R. Spang, G.Mann, S.Davies, K.Carslaw, Nitric acid distributions observed by the MIPAS on ENVISAT during the Vintersol campaign of 2002/3 and comparisons to a denitrification model, manuscript in preparation.

Schlager, H., et al., Observations of denitrification and renitrification in the 2002-2003 Arctic winter stratosphere, in preparation for Atmos. Chem. Phys., 2005.

Stroh, F., Marc von Hobe, Serhiy Hrechanyy, Ulf Winkler, Gebhard G?nther, Paul Konopka, Michael Volk, Hans Schlager, Francesco Cairo, Valentin Mitev and Renaud Matthey, Observations of Enhanced ClO in the Arctic Polar Winter UTLS in the Arctic Polar Winter UTLS, in preparation for Atmos. Chem. Phys, 2005.

## 2.3 Other publicatons from the project

A high number of talks and posters on the results obtained in the EUPLEX project have been given at a variety of scientific meetings and as seminar talks etc. For the sake of conciseness these are not listed here.
Meetings with significant contributions from the EUPLEX project were:

- EGU, Nice, April 2003
- Joint SOLVEII/VINTERSOL Science Meeting, Orlando, Oct. 2003
- AGU, San Francisco, Dec. 2003
- EGU, Nice, April 2004
- Quadrennial Ozone Symposium, Kos, June 2004

# SECTION 3: PROGRESS MADE IN THE REPORTING PERIOD

## 3.1 Introduction

Towards the end of the project and in the extension period the work flows as schematically shown in Fig. 1.1 naturally converged and the scientific interpretation of the initial topics within the work packages as listed in Tab. 3.1 overlapped increasingly. The separation into the initial work package structure seemed rather artificial and therefore some grouping was performed: The section is structured into the progress made within the PSC work packages (WP1, WP2, and WP3), the work packages dealing with gas phase chemical and dynamical processes (WP4 and WP5), and finally the in-situ measurement work package (WP6). The major results obtained within the extension period are described in detail in section 6 of this report while this section will focus more on the technical work progress. For sake of conciseness most figures with major results have been included within section 6 and referred to here rather than reproducing the figures in two sections.

The major work load on some project partners was naturally finished already within the regular project duration so that these are not included in this section of the report.

| | **WP Title and objectives** | **Lead, Co-lead** | **Partners** |
|---|---|---|---|
| **WP1** | Large scale PSC properties, denitrification and dehydration<br>Microphysical modelling<br>3D modelling<br>Hypotheses testing 'NAT rocks' | Carslaw,<br>Schlager | FZJ, DLR (C), Umainz, INO, ETH, ULeeds (L) |
| **WP2** | Small scale PSC microphysics and mountain waves<br>Microphysical modelling<br>Lagrangian modelling<br>Hypotheses testing 'PSC composition in Lee waves' | MacKenzie,<br>Dörnbrack | FZJ, DLR (C), Umainz, CNR, INO, CAO, Ulanc (L), ETH |
| **WP3** | PSC optical properties<br>Lidar-based NAT rock identification<br>Lidar interpretation<br>Optical properties | Peter,<br>Flentje | DLR (C), ON, CNR, ETH (L) |
| **WP4** | Halogen Activation and Ozone Loss Rates<br>Match Analysis<br>Lagrangian 2D and 3D modelling<br>Hypotheses testing on Cl activation rates<br>Hypotheses testing on ozone loss rates<br>Vortex average ozone loss | Müller,<br>von der Gathen | FZJ (L), AWI (C), ULeeds, NILU |
| **WP5** | Tracer Relationships, Subsidence, and Dynamics<br>Set up correlations (Tracer-Tracer, Tracer-O3, –NOy, Cly, total H)<br>Lagrangian mixing studies | Volk,<br>Konopka | FZJ (C), DLR, Ufrank (L), INO |
| **WP6** | M55 Geophysica Aircraft Measurements<br>Instrument preparation, testing, calibration, deployment<br>Data analysis<br>Data intercomparison and validity checks<br>Generate master data sets for each flight | Borrmann,<br>Mazzinghi | FZJ, DLR, UMainz (L), UFrank, ON, CNR, INO (C), CAO, CNR |

| | | | |
|---|---|---|---|
| **WP7** | Overall Co-ordination, Aircraft Flight Planning<br>Scientific campaign and flight planning<br>Tools for flight planning (MM5,...), Met support<br>Logistics for campaign and flights<br>Data base management<br>Meteorological Data Support<br>Meetings, Reports, etc. | Stroh,<br>Balestri | FZJ (L), DLR, UMainz, AWI, CNR, ULanc (C), ETH, ULeeds, NILU, STM |

**Work package structure of the EUPLEX project. Letters in parantheses indicate institution of the work package leader (L) and co-leader(C).**

## 3.2 Progress within the PSC Work Packages (WP1-WP3)

### 3.2.1 Partner 2: Deutsches Zentrum für Luft- und Raumfahrt (DLR)

In the reporting period, we performed a final data analysis for 11 Geophysica flights in January/February 2003 of the SIOUX NOy and FOX ozone data. In addition, NOy measurements in cirrus clouds have been evaluated. The error in airborne lidar data (OLEX) of PSC observations has been determined.

On 6 February 2003, SIOUX observed low number densities of solid nitric acid containing particles with diameters up to 6 micrometers in the Arctic stratosphere. We use these measurements to constrain the theories of NAT formation (Voigt et al., 2004). We can exclude homogeneous NAT formation in binary or ternary solutions, heterogeneous NAT formation on ice and sedimentation of NAT from above for that case. In contrast, the observations demand a slow but persistent NAT nucleation mechanism at temperatures near TNAT. We derive a NAT nucleation rate on meteoritic particles by combining in-situ measurements of the meteoritic surfae area in the stratosphere and laboratory data of heterogeneous NAT nucleation on micrometeorites. In contrast to previous work, we show that NAT nucleation on meteoritic particles may present a pathway for solid particle formation above the ice frostpoint and can explain the observations of low number density NAT clouds.

A comparison of microphysical and optical data of the liquid ternary PSCs measured on 8 February shows a good agreement (Lowe et al., 2004). During a cirrus flight on 11 February 2004, an increase in NOy uptake on cirrus particles has been measured when temperatures are below 206K. The detection limit of volume depolarisation of the OLEX lidar has been determined to 1%.

### 3.2.2 Partner 10: University of Lancaster (ULANC)

During the reporting period the PSC observations made on the 8$^{th}$ February 2003 were continued.

To investigate particle compositions and chlorine activation within the mountain wave aircraft flight data have been employed to create a quasi-lagrangian trajectory along which the ULANC box model was run. However the aircraft trajectory within the mountain wave was not isentropic, so the aerosols sampled during this section of the flight are unlikely to have the same temperature histories. To study the effect this would have on our simulations we used four isentropic trajectories at 445K, 450K, 455K and 460K, derived from MTP data, along which we run our

microphysical model. The results of these model runs were then interpolated onto the quasi-lagrangian. The dynamical models reproduce the magnitude and, to a lesser extent, the shape of the $NO_y$ observations reasonably well. There is little difference between results produced using the quasi-lagrangian trajectory and those interpolated from the isentropic trajectories, indicating that the assumptions made for the quasi-lagrangian trajectory are reasonable.

### 3.2.3 Partner 11: Swiss Federal Institute of Technology (ETHZ)

Optical models have been developed to simulate the optical properties of the measured PSCs. They are based on a T-matrix computation of scattering efficiencies to estimate the optical properties of particles. The code allows for modelling a wide range of particle compositions (i.e. refractive indices) and asphericities. Combined with the microphysical model which takes into count of the $HNO_3$ and $H_2O$ uptake of background sulphuric aerosol particles, the optical properties can be calculated using the output of the microphysical modelling (see Fig. 6.21). The observed backscattering ratios by MAS and condensed phase $HNO_3$ by SIOUX shown in Figure 3.6 are indicated in Fig. 6.21. The model result shows good agreement with the observed value, indicating a liquid cloud.

Also extinction coefficients measured by SAGE III indicate the need for an yet unknown heterogeneous mechanism. We calculated extinciton coefficients (using backward trajectories) with different types of nuclei, which nucleate at different supersaturation.

### 3.2.4 Partner 12: University of Leeds (UNIVLEEDS)

Throughout the duration of EuPLEx we have continually developed and used the coupled DLAPSE/SLIMCAT model to investigate denitrification of the Arctic lower stratosphere. In January 2003 the coupled model was updated to include the full SLIMCAT chemistry scheme. This version of the model was used to provide daily maps of NOy partitioning and denitrification to aid flight planning. One member of the group was always present in Kiruna for the duration of EuPLEx to assist in this process.

Following the campaign phase, DLAPSE has been extensively compared with observations of NOy and denitrification from the Geophysica and the MIPAS-E instrument aboard ENVISAT. In conjunction with the EU MAPSCORE project, additional comparisons have also been made between DLAPSE and a wide variety of observations of NOy and denitrification from three previous Arctic winters -1999/2000, 1996/97 and 1994/95.

We have also heavily modified the DLAPSE/SLIMCAT model to simulate denitrification of the Arctic stratosphere by large NAT particles sourced from NAT “mother clouds” which are produced downwind of mountain wave ice clouds (Fueglistaler, 2002). The computational expense of such simulations means that the potential role of the “mother cloud” mechanism in causing Arctic denitrification has been explored for one winter only (1999/2000). This work places important constraints on the contribution of mountain wave induced “mother clouds” to Arctic denitrification.

## 3.3 Progress within the Gas Phase Work Packages (WP4, WP5)

### 3.3.1 Partner 1: Forschungszentrum Jülich GmbH (FZJ)

During the extension period modelling studies of chemistry and dynamics partly including NAT particle sedimentation were carried out employing the 2D and 3D versions of the CLAMS model. Several studies have been refined and finished and results have been published in the peer reviewed literature (Grooß et al. 2004, , Günther et al. 2004, Hobe at al. 2004, Konopka et al. 2004, Steinhorst et al. 2004). Due to the wealth of data gathered during the EUPLEX campaign not all studies that have been launched could be completely finished until now and are still under investigation (Stroh et al. 2005) or publications are in preparation (Grooß et al. 2005).

For the CLaMS simulation for the winter 2002/2003 chemical ozone depletion was investigated. The simulation was initialized using ozone mixing ratios derived from ENVISAT-MIPAS data on 17 November 2002. To verify that CLaMS is simulating ozone mixing ratios correctly the simulated ozone mixing ratios were compared to observations in March. One example is the comparison with the observations by FOX on the Geophysica that are displayed in Fig. 6.26. These observations were made during the EnviSat validation campaign between 28 February and 16 March. The average difference of the ozone mixing ratios (CLaMS-FOX) is very low −0.06 ppm ± 0.18 ppm (1 sigma). The remaining differences may be explained by small-scale structures below the resolution of CLaMS.

Further, the impact of denitrification on the simulated ozone depletion was investigated through an additional simulation in which the sedimentation scheme was deactivated. In general, the simulated ozone depletion is very similar to the reference simulation. The largest effect of the denitrification was found towards the end of the simulation in mid-March when the deactivation of active chlorine species is hindered by the denitrification. The maximum of the ozone depletion due to denitrification averaged over the vortex as defined by Nash et al. (1996) was determined to be 100 ppb at 460 K potential temperature corresponding to 10% of the ozone depletion of the reference simulation.

Data analysis of the HALOX ClO and ClO dimer measurements has been completed (see 3.4.1) and he study of the ClO/ClO dimer equilibrium has been much refined (Hobe et al. 2004). Results suggest that the thermal equilibrium between the dimer formation and dissociation is shifted significantly towards the monomer compared to the current JPL 2002 recommendation which extrapolates laboratory studies to stratospheric temperatures. Detailed analysis of observations made in darkness was used to re-evaluate the magnitude and temperature dependence of the equilibrium constant. A fit of the JPL format for equilibrium constants yields $K_{EQ} = 3.49 \times 10^{-27} \exp(8174/T)$, a factor of 4 to 8 smaller than JPL 2002 (see Fig. 6.28).

### 3.3.2 Partner 4: Johann-Wolfgang Goethe University Frankfurt (JWG-IMG)

Partner 4 has been working on i) the analysis of ozone loss during EUPLEX using the correlation of measured ozone and tracers, and ii) the analysis of vortex descent and mixing across the vortex edge using tracer-tracer correlations.

Cumulative ozone loss over the 2002/03 winter was derived from the $O_3$-$N_2O$ and $O_3$-$CO_2$ relations as a function of the respective tracer mixing ratio, which can be converted to the "spring equivalent" potential temperature. Fig. 6.42 shows that deduced ozone loss between mid January and mid February amounts to roughly 800 ppb between spring equivalent potential temperatures of 415 K and 435 K (similarly at 435 to 460 K, not shown), and 600 ppb between 400 K and 415

K (with no detectable loss below 400 K, not shown). Thereafter slower ozone loss, about 200 ppb until mid March, was observed above 400 K, with an apparent increase of ozone for three flights in late February/early March found only by the FOZAN instrument. The total ozone loss throughout the winter until mid March is estimated to be 1200 ppb for equivalent spring potential temperatures between 415 K and 460 K.

For the analysis of descent and mixing in the 2002/03 Arctic vortex tracer measurements have been refined and validated and the evolution of tracer correlations have been studies. Detailed studies of descent and mixing have been performed in collaboration with Partner 1 emplying the CLAMS model. Details are given in section 6.5.2 and results have been published.

### 3.3.3 Partner 6: Alfred Wegener Institute (AWI)

Model runs have been performed with updated reaction kinetics that has been derived from the in-situ measurements during the self-match flight. The box model was used to quantify the impact of these changes in reaction kinetics on chemical ozone loss rates. The results have been compared with Match measurements of the ozone loss rate.

### 3.3.4 Partner 11: Swiss Federal Institute of Technology (ETHZ)

A box model study of the ClO/ClO dimer on the basis of one flight on 30.01.93 yielded an equilibrium constant that was used to study its effect on chemical ozone loss depletion. An example trajectory (see Fig. 6.34) started on 590K on 1 Dec 1999 and calculated onwards until end of March 2000 shows hardly any differences in ozone depletion for the "old" ($K_{jpl}$ and the "new" ($K_{euplex}$) equilibrium constant (black and blue stars in Fig. 6.34), which is 30% for this case. This changes when higher amounts of BrO ($10 \cdot 10^{-12}$) (Pundt et al., 2002) are assumed. Ozone depletion is 33% during the winter assuming this higher amount of BrO and $K_{jpl}$(red line in Fig. 6.34), but further increases to 36% (green line in Fig. 6.34) using the "new" equilibrium constant $K_{euplex}$.

## 3.4 Progress within the Measurement Work Package (WP6)

### 3.4.1 Partner 1: Forschungszentrum Jülich GmbH (FZJ)

The HALOX measurements of ClO dimer and chlorine nitrate were closely characterized and for the first-time reliable ClO dimer laboratory calibrations could be carried out (Fig. 6.55 ). The efficiency of the thermal dissociation in the heated inlet nozzle was determined to be in excess of 80% and mostly close to 100% giving high confidence in the ClO dimer data obtained during the campaign (For details see section 6.6.2). Fig. 3.1 shows the final ClO and ClO dimer data for a flight on 30. Jan. 2003 that was specially designed to remeasure air observed on the first flight leg a second time at higher solar zenith angles (sza) on the second leg. The dimerization of ClO with increasing sza is obvious from the evolution of the respective mixing ratios.

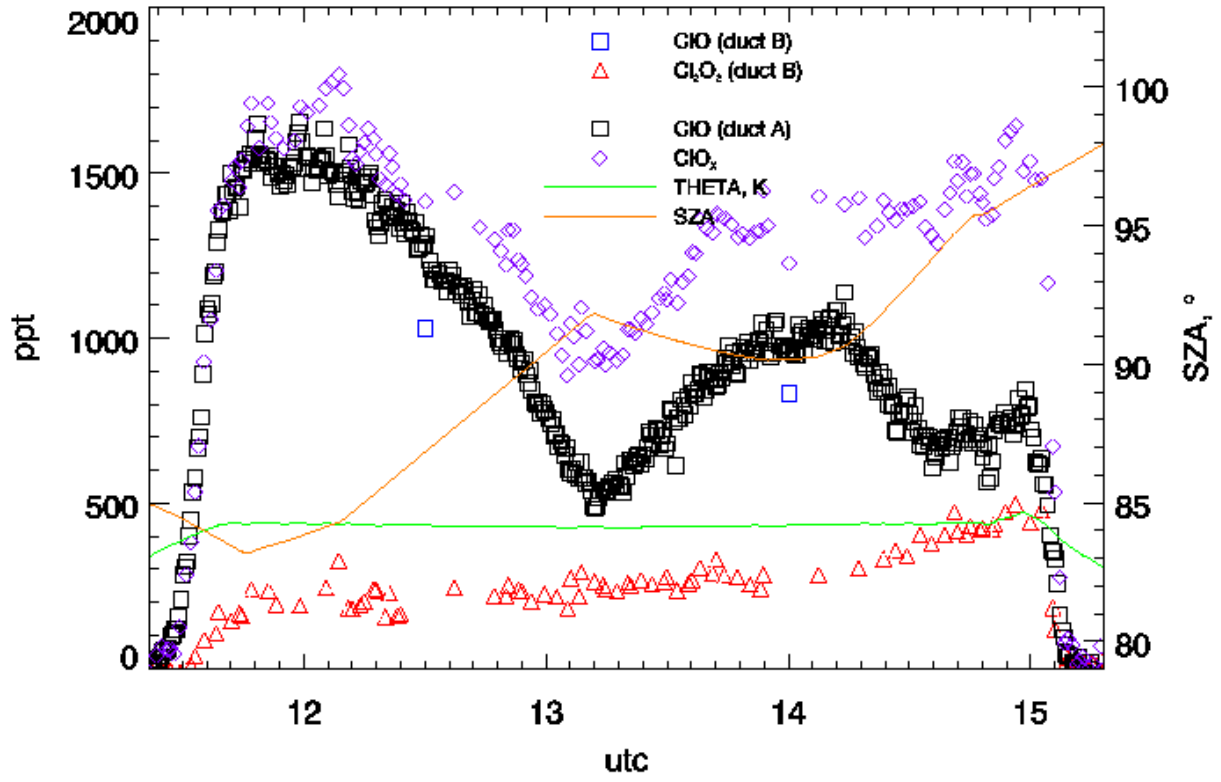


**Fig. 3.1 Final calibrated HALOX ClO and ClO dimer data for the so called Self-Match flight on 30. Jan. 2003. A small systematic difference within the measurement uncertainty between the measurements of ClO in the parallel measurement ducts A and B still exists.**

### 3.4.2 Partner 3: University of Mainz (IPA-UMZ)

During the reporting period both COPAS instruments were calibrated at IFT Leipzig at the World Calibration Centre for physical aerosol measurements (WCCAP) of the Global Atmospheric Watch program.

The COPAS and FSSP data of the EUPLEX campaign were analysed in-depth and a manuscript for ACP was written. This manuscript is currently circulated among the co-authors and is close to submission. The results of the data analysis were also presented at the EUPLEX final data workshop in Leeds (for details of the results see also Yearly EUPLEX Report for 1.5.2003-1.5.2004).

In July the FSSP and COPAS instruments took part in a field campaign at Kleiner Feldberg, Germany. In these measurements FSSP-100 and FSSP-300 were inter-compared with other optical aerosol sizers (Grimm OPC and Pallas aerosol spectrometer) and COPAS was compared against standard TSI CN-Counters.

### 3.4.3 Partner 8: Italian National Institute of Optics (INOA)

During the extension period the work of the TDL team comprised of the final data analysis, intercomparison with the HAGAR GC $N_2O$ and other higher time resolution data, and interpretation of the TDL data from the Arctic winter campaign.

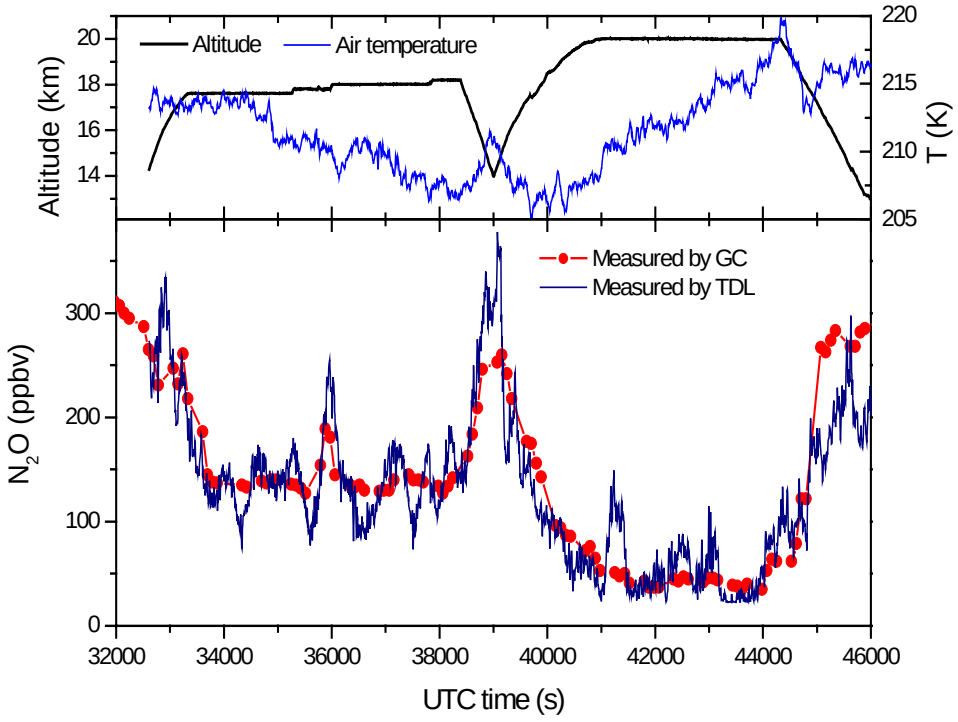


**Fig. 3.2 $N_2O$ mixing ratios measured during flight 26/01/2003 by HAGAR and TDL instrument.**

*Fast measurements of tracers by TDL for the detection of fine structures in the polar vortex*

During the EUPLEX project the Mid InfraRed TDL spectrometer, already installed in the aircraft for the measurement of the concentration of $HNO_3$ in the evaporated particles, was converted for the measurement of $N_2O$ in the gas phase installing a new isokinetic probe provided by the University of Mainz. The instrument time resolution in this configuration resulted to be about 6 s, limited by the gas sampling flow from the probe.

The fast measurement of $N_2O$ is of crucial importance to classify an air mass in the transition from the interior of the polar vortex to the mid latitude stratosphere. High resolution data of this tracer allows to detect thin filaments of air which have been spun off the polar vortex. These filaments carry the characteristics of the vortex (as for instance low ozone due to chemical ozone destruction) into the mid latitudes when dissolving there. Quantification of this process is one of the major result of the project in order to explain the observed but still unresolved decadal decline of ozone in the mid latitude stratosphere. Without such a tracer it is not possible to determine whether a low ozone value in an air mass sampled by Geophysica is due to the chemical destruction of ozone, or due to the dynamical transport of ozone poor air of low latitude origin to the location of the flight. The combined use of the two instruments onboard of the Geophysica measuring $N_2O$ is a unique possibility to exploit both the high precision and accuracy provided by the HAGAR gas chromato-graph, but with limited time resolution, with the lower accuracy, but higher time resolution provided by the TDL technique. The comparison of the results of the two instruments in a typical flight in Fig. 3.2 shows their basic agreement within the declared accuracy. The main differences occur during the fast transients, as expected. The main part of the processing and interpretation of the TDL data was then devoted to the analysis of such transients, concentrating on that occurring in the transition region from inside-outside of the vortex and to the effect of orography. Interpretation of these structures was done making use of the data of other instruments, measuring other tracers correlated or anticorrelated with $N_2O$, but having similar time resolution, mainly FOZAN for $O_3$ and SIOUX for NOy.

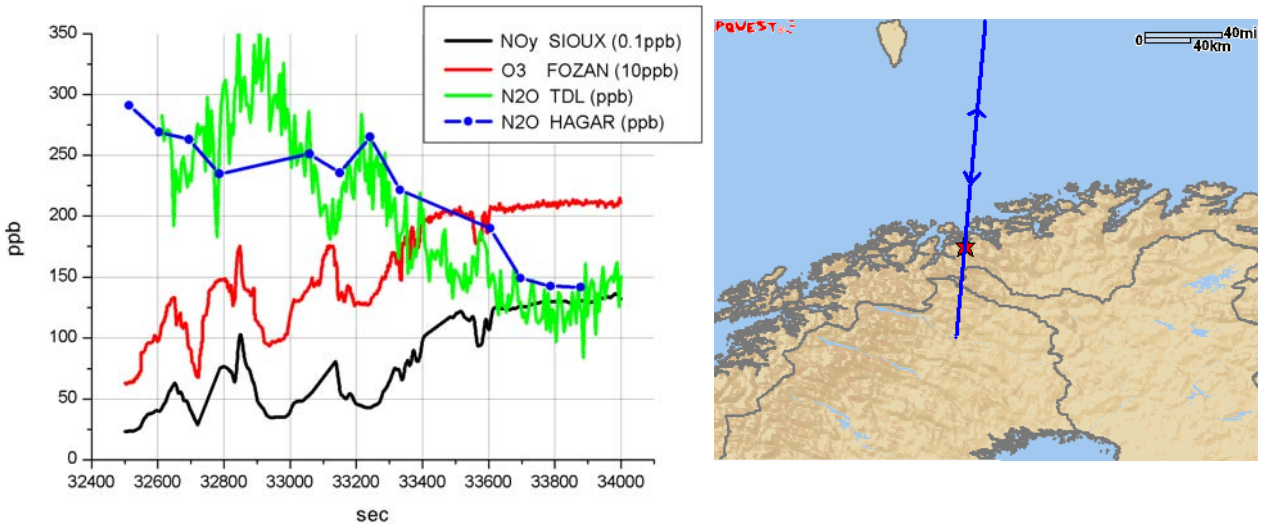


**Fig. 3.3 Comparison of tracer measurements performed by different instruments during flight 26/01/2003, with geographic localization. Flight altitude 16 km.**

An example is the investigation of a detail of the same flight profile in Fig 3.1 showing that the fast variation (on a time scale of about 20 seconds) in the $N_2O$ concentration observed by TDL, is also detected by both FOZAN and SIOUX as an anticorrelated fast variation in the concentration of $O_3$ and NOy (Fig. 3.3). This transient may be related to the orography (crossing of the land-sea interface), which can be sensed even at a flight altitude of 16 km by fast instruments, but cannot be detected by the gas chromatograph. The relation of fast transient with ground structures was also observed in several other flights. The most outstanding was found in the flight of 23/01/2003, where a similar feature was detected twice over the Svalbard islands, both on the way in and in return flight.

In all the these occurrences the correlation coefficient between TDL-$N_2O$, $O_3$ and NOy ranges from 0.86 to 0.95, demonstrating that all the instruments were measuring the same behaviour.

The importance of these effect in the polar microchemistry is still to be assessed and future mission could be addressed to this investigation, with dedicated flight profiles and a compete set of high time resolution instrument. However, the relationship with structures in the vortex edges is very likely, as shown in Fig 3.4, where the situation as observed on 23/01/03 is compared with the potential vorticity, showing that the transient is very close to a transition between inside and outside the vortex.

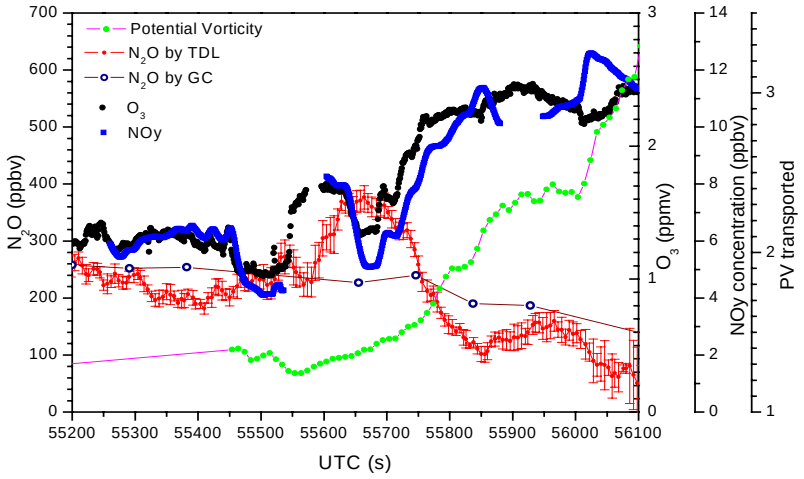


**Fig. 3.4 Comparison of tracer measurements with potential vorticity during flight 23/01/2003.**

## 3.5 References

Grooß J.-U., G. Günther, R. Müller, P. Konopka, S. Bausch, H. Schlager, C. Voigt, C. M. Volk, G. C. Toon, Simulation of denitrification and ozone loss for the Arctic winter 2002/2003, Atmos. Chem. Phys. Discuss., 4, 8069-8101, 2004.

Grooß, J.U., Rolf Müller, Fred Stroh, Marc von Hobe, Observation and simulation of air with recent chlorine activation, in preparation for Atmos. Chem. Phys, 2005.

Hobe, M. von, J.-U. Grooß, R. Müller, S. Hrechanyy, U. Winkler, F. Stroh, A re-evaluation of the ClO/ $Cl_2O_2$ equilibrium constant based on stratospheric in-situ observations, , Atmos. Chem. Phys. Discuss., 4, 5075-5102, 2004

Konopka, P., H.-M. Steinhorst, J.-U. Grooß, G. G¨unther, R. M¨uller, J. W. Elkins, H.-J. Jost, E. Richard, U. Schmidt, G. Toon and D. S. McKenna, 2004: Mixing and ozone loss in the 1999-2000 arctic vortex: Simulations with the 3-dimensional Chemical Lagrangian Model of the Stratosphere (CLaMS). *J. Geophys. Res.*, **109**(D2), doi:10.1029/2003JD003792.

Steinhorst, H.-M., P. Konopka, G. G¨unther and R. M¨uller, 2004: How permeable is the edge of the Arctic vortex - Model studies of winter 1999-2000. *J. Geophys. Res.*, accepted.

Stroh, F., Marc von Hobe, Serhiy Hrechanyy, Ulf Winkler, Gebhard G?nther, Paul Konopka, Michael Volk, Hans Schlager, Francesco Cairo, Valentin Mitev and Renaud Matthey, Observations of Enhanced ClO in the Arctic Polar Winter UTLS in the Arctic Polar Winter UTLS, in preparation for Atmos. Chem. Phys, 2005.

Voigt, C., H. Schlager, and B. Luo, Nitric acid in Cirrus and Polar Stratospheric Clouds, AGU - General assembly, San Francisco, USA, 11-18 Dec 2004.

## SECTION 4: TECHNICAL IMPLEMENTATION PLAN

The Technical Implementation Plan was completed online on CORDIS and submitted. It can be found as an appendix to the hardcopies of this document. It is also available from the project web site as PDF file.

# SECTION 5: EXECUTIVE SUMMARY FOR THE OVERALL PROJECT DURATION

| Contract n° | EVK2-CT-2001-00119 | Project Duration: | 01.05.2002 – 31.10.2004 |
|---|---|---|---|
| Title | EuPLEx - European polar stratospheric cloud and lee wave experiment | | |

**Objectives**

General objectives are critical tests of current hypotheses for the three key processes of Arctic stratospheric ozone depletion chemistry through measurement-model intercomparisons:

1. PSC formation and properties in Lee-wave and synoptic scale PSCs;
2. Halogen activation on PSC, and;
3. Chemical ozone loss.

Airborne in-situ and remote sensing observations based on dedicated flight strategies and intercomparison with state of the art microphysical and chemical models should yield improved or new parameterisations or corroborate established concepts.

The outcome of the EUPLEX project is a major improvement of the model reproduction of several crucial processes which are prerequisites to the reliable prediction of the evolution of stratospheric ozone in the Arctic polar winter. Many of the new findings have been published in a wealth of peer-reviewed papers and several more are close to submission or in preparation.

**Scientific achievements**

- A comprehensive data set on the chemical and dynamical evolution of the Arctic polar vortex and its surrounding regions has been measured in the January/February 2003 time period. Data sets consist of meteorological parameters, dynamical tracers (partly with isotopic composition), reactive chemical species involved in ozone destruction, and aerosol physical and chemical properties. With few exceptions all data sets have been finalized and archived on the NILU data base and are available to the VINTERSOL and SOLVE-II communities as well as to the public.
- Observations of particle phase NOy and particle properties under threshold conditions show that small NAT particles can form at very small number densities without pre-existence of ice particles. Since homogeneous nucleation can also be excluded for the probed scenario the observed NAT rock embryos (most probably a source of large NAT rocks) are likely to form by heterogeneous nucleation (e.g. on meteoritic dust particles).
- However, the formation of NAT containing particles within lee-wave events was shown to also have a significant potential for the formation of synoptic NAT PSCs and subsequent denitrification in the Arctic region.
- A good quantitative model reproduction of observed de-/renitrification in the Arctic polar vortex 2002/03 was attained when regarding non-equilibrium conditions for the growth of NAT particles. Observations of lee-wave PSCs confirm the importance of non-equilibrium liquid particles, as predicted by detailed PSC models; the quasi-lagrangian sampling of particle composition within these PSCs provides a stringent test of the models.
- The HalogenOxides (HALOX) instrument (ClO, BrO) was upgraded towards the measurement of the ClO-Dimer (ClOOCl) and of chlorine nitrate, $ClONO_2$. For the first time ClO dimer laboratory calibrations were performed to ensure proper dimer measurements.
- Independent studies of the measured ClO and dimer concentrations for just one flight and a suitable ensemble of flights, respectively, have consistently revealed more nighttime ClO than predicted from the established (JPL) equilibrium constant, calling for a smaller equilib-

rium constant Keq. This points to the fact that there still is a major challenge in the understanding of stratospheric reactive chlorine partitioning.

- Intercomparison of measured and modelled ClO suggest that ongoing Cl activation on liquid aerosol particles has been observed and can be reproduced by CLaMS reasonably well.

- Accumulated observed ozone loss around the 450K potential temperature level from early December 2002 to mid March 2003 amounts to about 1200 ppb. This is somewhat higher than the modelled integrated ozone loss employing standard (JPL) kinetics. However, employing the new ClO/ClO dimer equilibrium constant derived from the EUPLEX measurements and simultaneously higher Bry mixing ratios (as recently reported by Pundt et al.) integrated ozone loss in the observed magnitude can be reproduced within a simple box model.
- Dynamical features of different scale size and intensity as a result of mixing in of extra vortex air masses can be reasonably modelled and even predicted employing the Lagrangian CLaMS model.
- For a flight tailored to the observation of the equilibrium between ClO and its dimer in the same air mass measured at daylight and night-time CN measurements show that at some points the air masses have been exactly reencountered in agreement with the meteorological analysis. This experiment shows that such self-Match and consequently also Match flights are possible under appropriate meteorological conditions.
- During a flight in cirrus clouds at 10km altitude preliminary data from the HALOX instrument indicate enhanced levels of ClO compared to outside the cloud. Also on several ascent and descent manoeuvres shallow enhancements in ClO have been observed between 12 and 14km in altitude. These observations very relevant for the UTLS region are still under investigation.

**Socio-economic relevance and policy implications**

The thinning of the ozone layer is a global problem and therefore affects all of Europe. The substantial ozone loss that has been observed in the Arctic has affected Europe more than other regions of the Northern Hemisphere. This is due to the fact that the polar vortex often is shifted towards the European sector of the Arctic because of the Aleutian high (a high pressure system over Alaska and Easter Siberia). Therefore it is of strategic importance to Europe to obtain a better understanding of the ozone layer problem in order to enable reliable predictions of its future state. GCM calculations [Shindell et al., Nature, 392, 589 (1998)] predict that the coupling of ozone and climate may lead to far more dramatic ozone loss during the decade from 2010 to 2020 than has been observed during the 1990s. Especially in the Northern hemisphere, the potential for increasing ozone losses exist [Waibel et al., Science, 283, 2064 (1998)]. Thinning of the ozone layer leads to increased levels of UV-B radiation on the ground that has adverse effects on human health, the marine environment, as well as agriculture. The crucial uncertainties for predicting the future development of the Arctic winter ozone layer are those addressed by EUPLEX.

The scientific results from EUPLEX considerably enhance in various aspects the potential for improved modelling and even short term prediction of Arctic polar ozone losses to be expected in any ongoing winter season. This in the longer run may enable short term (weeks to months) warnings in case of extremely low ozone columns and consequently elevated UV exposures above the European region in early spring. This is a major contribution to the actions quality of life and health and security.

**Conclusions**

The results obtained within the EuPLEx project improve our understanding of the processes of

PSC formation, denitrification, halogen activation, and ozone loss in the Arctic polar winter and spring. The results provide major improvements in the representation of the related processes in our models of the Arctic polar winter and spring stratospheric ozone column. This means a significantly improvement of our capability to predict short term evolutions of the northern hemisphere ozone layer and consequently UV exposure on ground and therefore may enable policy decisions for mitigation in case of severe events.

**Keywords**

Stratospheric ozone, polar stratospheric clouds, NAT particles, stratospheric denitrification, halogen activation, halogen partitioning, arctic ozone depletion, polar vortex dynamics.

## 5.1 List of peer reviewed and submitted publicatons from the project

Bogdan, A., M. Kulmala, A. R. MacKenzie, A. Laaksonen, M. J. Molina, and A. Avramenko, The study of finely divided aqueous systems as a clue to understanding the formation mechanisms of polar stratospheric clouds: 1. $HNO_3/H_2O$ and $H_2SO_4/H_2O$ systems, *J. Geophys. Res.*, **108** (D10), 4302, doi:10.1029/2002JD002605.

Bogdan, A., M. Kulmala, A. R. MacKenzie, A. Laaksonen, M. J. Molina, and A. Avramenko, The study of finely divided aqueous systems as a clue to understanding the formation mechanisms of polar stratospheric clouds: 2. $HCl/H_2O$ and $HNO_3/HCl/H_2O$ systems, *J. Geophys. Res.*, **108** (D10), 4303, doi:10.1029/2002JD002606.

Curtius, J., R. Weigel, H.-J. V?ssing, C.-M. Volk, A. Werner, H. Schlager, A. Roiger, C. Schiller, H. Wernli, V. Dreiling, and S. Borrmann, In-situ aerosol measurements covering the 10 nm to 30 microm size range in the Arctic lower stratosphere during winter 2003 onboard the high altitude research aircraft Geophysica, submitted to Atmos. Chem. Phys, 2004.

Davies, S., G. W. Mann, K. S. Carslaw, M. P. Chipperfield, J.A. Kettleborough, M.L. Santee, H. Oelhaf, G. Wetzel, Y. Sasano, T. Sugita, 3-D microphysical model studies of Arctic denitrification: Comparison with observations, submitted to Atmos. Chem. Phys. Disc., 2004.

Feng, W., , M.P. Chipperfield, S. Davies, B. Sen, G. Toon, J.F. Blavier, C.R. Webster, C.M. Volk, A. Ulanovsky, F. Ravegnani, P. von der Gathen, H. Jost, E.C. Richard, H. Claude, Three-Dimensional Model Study of the Arctic Ozone Loss in 2002/03 and Comparison with 1999/2000 and 2003/04, Atmos. Chem. Phys. Discuss, 4, 5045-5074, 2004.

Grooß J.-U., G. Günther, R. Müller, P. Konopka, S. Bausch, H. Schlager, C. Voigt, C. M. Volk, G. C. Toon, Simulation of denitrification and ozone loss for the Arctic winter 2002/2003, Atmos. Chem. Phys. Discuss., 4, 8069-8101, 2004.

Hobe, M. von, J.-U. Grooß, R. Müller, S. Hrechanyy, U. Winkler, F. Stroh, A re-evaluation of the ClO/ $Cl_2O_2$ equilibrium constant based on stratospheric in-situ observations, , Atmos. Chem. Phys. Discuss., 4, 5075-5102, 2004

Mann, G.W., K.S. Carslaw, M.P. Chipperfield, S.D. Eckermann, Large NAT particles and denitrification caused by mountain waves in the Arctic stratosphere, accepted for publication in J. Geophys. Res., 2005.

Davies, S., G. W. Mann, K. S. Carslaw, M. P. Chipperfield, J.A. Kettleborough, M.L. Santee, H. Oelhaf, G. Wetzel, Y. Sasano, T. Sugita, 3-D microphysical model studies of Arctic denitrification: Comparison with observations, submitted to Atmos. Chem. Phys. Disc., 2004.

Kleinboehl, A., J. Kuttippurath, M. Sinnhuber, B.-M. Sinnhuber, H. Kuellmann, K. Kuenzi, J. Notholt, Rapid meridional transport of tropical airmasses to the Arctic during the major stratospheric warming in January 2003, Atmos. Chem. Phys. Discuss., 4, 7121-7138, 2004.

Konopka, P., H.-M. Steinhorst, J.-U. Grooß, G. G¨unther, R. M¨uller, J. W. Elkins, H.-J. Jost, E. Richard, U. Schmidt, G. Toon and D. S. McKenna, 2004: Mixing and ozone loss in the 1999-2000 arctic vortex: Simulations with the 3-dimensional Chemical Lagrangian Model of the Stratosphere (CLaMS). *J. Geophys. Res.*, **109**(D2), doi:10.1029/2003JD003792.

Lowe, D., A. R. MacKenzie, N. Nikiforakis, and J. Kettleborough, A condensed-mass advection based model of liquid polar stratospheric clouds, *Atmos. Chem. Phys.*, **3**, 29-38, 2003.

Lowe, D., A. R. MacKenzie, H. Schlager, C. Voigt, A. Dörnbrack, M. J. Mahoney, and F. Cairo, Liquid particle composition and heterogeneous reactions in a mountain-wave Polar Stratospheric Cloud, *Atmos. Chem. Phys. Discuss.*, submitted November 2004.

MacKenzie, A. R., Recent advances in the study of polar stratospheric and tropical tropopause clouds, *Recent Res. Developments in Geophysics*, **4**, 439-462, 2002.

Steinhorst, H.-M., P. Konopka, G. G¨unther and R. M¨uller, 2004: How permeable is the edge of the Arctic vortex - Model studies of winter 1999-2000. *J. Geophys. Res.*, accepted.

Tilmes, S., R. Müller, J.-U. Grooß, M. Ho¨pfner, G. C. Toon, and J. M. Russell III, Very early chlorine activation and ozone loss in the Arctic winter 2002 – 2003, Geophys. Res. Lett., 30(23), 2201, doi:10.1029/2003GL018079, 2003.

Voigt, C., H. Schlager, B. Luo, A. Dörnbrack, A. Roiger, P. Stock, J. Curtius, H. Vössing, S. Borrmann, S. Davies, P. Konopka, C. Schiller, G. Shur, T. Peter, NAT formation of low Nat supersaturations, Atmos. Chem. Phys. Discuss., 4, 8579-8607, 2004.

## 5.2 List of publicatons from the project in preparation

Davies, S., G. W. Mann, K. S. Carslaw, M. P. Chipperfield, J. J. Remedios, A. M. Waterfall, Arctic denitrification during winter 2002/03: using satellite observations to interpret a 3-D microphysical model, manuscript in preparation.

Grooß, J.U., Rolf Müller, Fred Stroh, Marc von Hobe, Observation and simulation of air with recent chlorine activation, in preparation for Atmos. Chem. Phys, 2005.

Günther, G., R. Müller, P. Konopka, F. Stroh, C. M. Volk, Quantification of Mixing and Transport across the Boundary of the Lower Vortex during the Winter 2002/03, in preparation for Atmos. Chem. Phys., 2005.

Remedios, J.J. Remedios, A.M. Waterfall, R. Spang, G.Mann, S.Davies, K.Carslaw, Nitric acid distributions observed by the MIPAS on ENVISAT during the Vintersol campaign of 2002/3 and comparisons to a denitrification model, manuscript in preparation.

Schlager, H., et al., Observations of denitrification and renitrification in the 2002-2003 Arctic winter stratosphere, in preparation for Atmos. Chem. Phys., 2005.

Stroh, F., Marc von Hobe, Serhiy Hrechanyy, Ulf Winkler, Gebhard G?nther, Paul Konopka, Michael Volk, Hans Schlager, Francesco Cairo, Valentin Mitev and Renaud Matthey, Observations of Enhanced ClO in the Arctic Polar Winter UTLS in the Arctic Polar Winter UTLS, in preparation for Atmos. Chem. Phys, 2005.

## 5.3 Other publicatons from the project

A high number of talks and posters on the results obtained in the EUPLEX project have been given at a variety of scientific meetings and as seminar talks etc. For the sake of conciseness these are not listed here.
Meetings with significant contributions from the EUPLEX project were:

- EGU, Nice, April 2003
- Joint SOLVEII/VINTERSOL Science Meeting, Orlando, Oct. 2003
- AGU, San Francisco, Dec. 2003
- EGU, Nice, April 2004
- Quadrennial Ozone Symposium, Kos, June 2004

# SECTION 6: DETAILED REPORT ON THE SCIENTIFIC FINDINGS FROM EUPLEX

In order to guarantee efficient co-operation between the different groups within the project and as a consequence of the timing and nature of the tasks within the project, EUPLEX was subdivided into seven work packages (WP). An overview of the WPs is given in Tab. 6.1, and a schematic view of the structure of the project and the links between the work packages is shown in Fig. 1.1.

The work packages 3 (long range lidar instrument on the Falcon and short range lidar on the Geophysica) and 6 (in-situ measurements on the Geophysica) are measurement work packages. They include instrument preparation, calibration, operation during the campaign, and data analysis. They are separated due to the different nature of the data they deliver and the different data analysis methods, e.g. the sophisticated optical T-Matrix methods for the lidar measurements. WPs 3 and 6 fed their data into a data pool, which interpretation work packages 1, 2, 4, and 5 utilised. There was a close communication between the interpretation work packages, e.g., the provision of tracer correlations from WP5 to the other three WPs, so that consistent initial conditions were used in the microphysical and chemical models. WP7 was an infrastructure work package mainly concerned with co-ordinating and service tasks, such as campaign planning, logistics, and data base management. Results obtained within the work packages and their relevance for the Arctic ozone problem are detailed in the following subsections.

| WP | WP Title and objectives | Lead, Co-lead | Partners |
|---|---|---|---|
| **WP1** | Large scale PSC properties, denitrification and dehydration<br>Microphysical modelling<br>3D modelling<br>Hypotheses testing 'NAT rocks' | Carslaw, Schlager | FZJ, DLR (C), Umainz, INO, ETH, ULeeds (L) |
| **WP2** | Small scale PSC microphysics and mountain waves<br>Microphysical modelling<br>Lagrangian modelling<br>Hypotheses testing 'PSC composition in Lee waves' | MacKenzie, Dörnbrack | FZJ, DLR (C), Umainz, CNR, INO, CAO, Ulanc (L), ETH |
| **WP3** | PSC optical properties<br>Lidar-based NAT rock identification<br>Lidar interpretation<br>Optical properties | Peter, Flentje | DLR (C), ON, CNR, ETH (L) |
| **WP4** | Halogen Activation and Ozone Loss Rates<br>Match Analysis<br>Lagrangian 2D and 3D modelling<br>Hypotheses testing on Cl activation rates<br>Hypotheses testing on ozone loss rates<br>Vortex average ozone loss | Müller, von der Gathen | FZJ (L), AWI (C), ULeeds, NILU |
| **WP5** | Tracer Relationships, Subsidence, and Dynamics<br>Set up correlations (Tracer-Tracer, Tracer-O3, –NOy, Cly, total H)<br>Lagrangian mixing studies | Volk, Konopka | FZJ (C), DLR, Ufrank (L), INO |

| | | | |
|---|---|---|---|
| **WP6** | M55 Geophysica Aircraft Measurements<br>Instrument preparation, testing, calibration, deployment<br>Data analysis<br>Data intercomparison and validity checks<br>Generate master data sets for each flight | Borrmann, Mazzinghi | FZJ, DLR, UMainz (L), UFrank, ON, CNR, INO (C), CAO, CNR |
| **WP7** | Overall Co-ordination, Aircraft Flight Planning<br>Scientific campaign and flight planning<br>Tools for flight planning (MM5,...), Met support<br>Logistics for campaign and flights<br>Data base management<br>Meteorological Data Support<br>Meetings, Reports, etc. | Stroh, Balestri | FZJ (L), DLR, UMainz, AWI, CNR, ULanc (C), ETH, ULeeds, NILU, STM |

**Tab. 6.1 Work package structure of the EUPLEX project. Letters in parantheses indicate institution of the work package leader (L) and co-leader(C).**

In order to provide a results overview section that can be read stand-alone only a minimum of references are made to other sections of this report. At a few places in this section figures are rather reproduced in slightly modified versions in order to make the arguments clearer and avoid searching through the document. This increases the length slightly but hopefully contributes to the ease of reading.

## 6.1 WP1: Synoptic-scale PSC properties and their effect on denitrification

### 6.1.1 Objectives

Analyse NOy ($HNO_3$) in PSC particles of different types including NAT rocks. Develop 3-D particle growth and sedimentation models for the simulation of synoptic scale PSCs. Run 3-D PSC models during the aircraft campaign to aid in flight planning. Calculate 3-d fields of gas phase nitric acid and denitrification for comparison with observations. Use synoptic PSC models to test synoptic PSC particle formation hypotheses.

### 6.1.2 Methodology and scientific achievements

The Arctic winter of 2002/03 was colder than the climatological mean and characterised by an unusually early onset of temperatures sufficiently low for the existence of PSCs. Widespread PSCs were remotely observed from early-December until mid-January but a stratospheric warming event increased temperatures above the threshold for PSC formation in mid-January. The vortex cooled again in late January however temperatures were infrequently low enough for the formation of PSCs during the EuPLEx field campaign. The absence of in unperturbed NOy:$N_2O$ relation because of the early onset of denitrification meant that NOy* was derived following Popp et al. (2001) from 1999/2000 .

### 6.1.3 Measurement of NAT in air at low NAT-supersaturations

A polar stratospheric cloud (PSC) was observed on 6 February 2003 in the Arctic stratosphere by in-situ measurements onboard the high-altitude research aircraft Geophysica (Voigt et al., 2004). Low number densities (~$10^{-4}$ $cm^{-3}$) of nitric acid ($HNO_3$) containing particles - probably NAT - with diameters up to 6 µm were measured at altitudes between 18 and 20 km. The particle size distribution derived by Monte Carlo simulations from the NOy data (DLR, thick line) is compared to simultaneous FSSP measurements (University of Mainz, thin line) in Fig. 6.1.

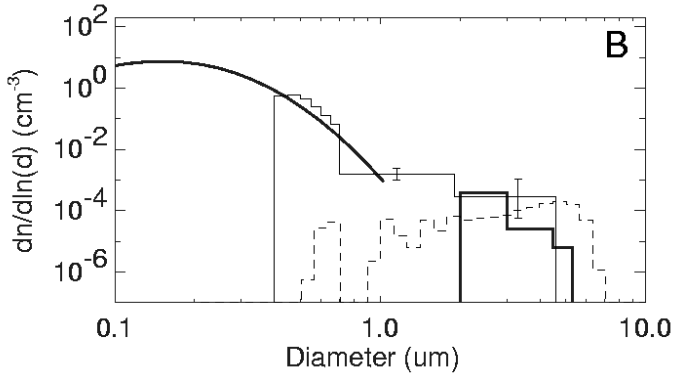


**Fig. 6.1 Particle size distribution measured on 6 February 2003 in a NAT PSC. Data from the NOy instrument (thick line), the FSSP (thin line) and results of DLAPSE model simulations (dashed line) are shown.**

In addition, results of a vortex wide simulation of NAT particles using the DLAPSE model (University of Leeds) show the existence of $1.5 \times 10^{-4}$ $cm^{-3}$ NAT particles with diameters up to 7 µm (dashed line in Fig. 6.1) near the flight track on 6 February 2003 in good agreement with the observations.

These particles may be considered as precursors of NAT-rocks. They have the potential to grow further and to remove $HNO_3$ from the stratosphere, thereby enhancing polar ozone loss.

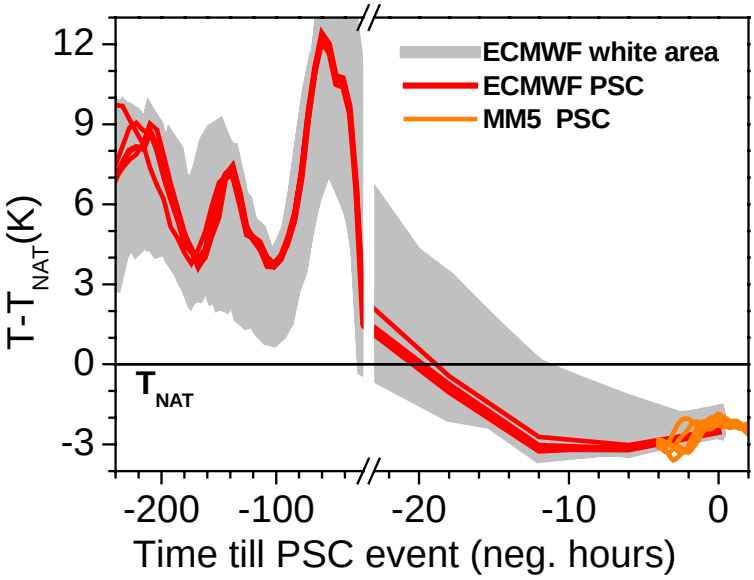


**Fig. 6.2 Temperature difference of the backward trajectories to TNAT versus time till PSC event. Red (ECMWF trajectories) and orange lines (MM5 trajectories are the trajectories ending in the PSC event, the gray shaded area indicates trajectories ending in a larger region around the flight track.**

Interestingly, the NAT particles formed in less than a day at temperatures $T > T_{NAT}$ - 3.5 K, just slightly below the NAT equilibrium temperature $T_{NAT}$. **Fig. 6.2** shows the difference of ECMWF- and mesoscale MM5-trajectory temperatures to $T_{NAT}$. Red and orange lines are the trajectories ending in the PSC event.

Given the trajectories remain 20 hours below $T_{NAT}$ (red lines in **Fig. 6.2**), we derive an average NAT nucleation rate of $8 \times 10^{-6}$ cm$^{-3}$ air h$^{-1}$ for the late Arctic winter 2002/2003, which reasonably reproduces our observations of NAT particle number density, size distribution and additionally of denitrification. This rate is slightly higher compared to the rate derived by Carslw et al., (2002) for the winter 1999/2000.

This unique measurement of PSC formation at extremely low NAT saturation ratios ($S_{NAT} \lesssim 11$) constrains current NAT nucleation theories. In particular, NAT formation on ice can for certain be excluded. In addition, homogeneous NAT nucleation from liquid binary or ternary solutions or surface nucleation cannot explain the observed NAT particle number densities. By combining in-situ data of the meteoritic surface area in the stratosphere and laboratory data of freezing of STS on micro-meteorites, we estimate a rate for NAT nucleation on meteoritic particles, which coincides with our measurements.

Thus, NAT nucleation on ubiquitous meteoritic smoke particles may present a pathway for solid particle formation at temperatures above the ice frost point. In particular, it may explain the origin of low number density NAT PSC observed in winter 2002/2003 and in previous winters (Fahey et al., 2001). However, the detailed mechanism and the spatial and temporal variation of the meteoritic smoke particles as well as the temperature dependence of the NAT nucleation rate on these remain a challenge for future laboratory and field studies.

### 6.1.4 Measurements of $HNO_3$ in mountain wave PSC encounters

On 8 February 2003, moderate mountain wave activity led to the formation of PSCs over northern Scandinavia. To find the PSCs, MM5 mesoscale model predictions were used as first estimate to design the flight path of Geophysica and Falcon. In addition, the OLEX Lidar measurements onboard the Falcon served as path finder for Geophysica and some flight legs of the Geophysica could be adjusted during the flight to the regions where PSCs were detected by the OLEX Lidar. This procedure enabled coordinated flights with both aircraft in mountain wave PSCs even under highly non-stationary mountain wave conditions. Fig. 6.3 (A) shows temperatures analysed with MM5 together with the Geophysica flight track. Flight sections with PSC measurements are marked in red, cirrus measurements in blue.

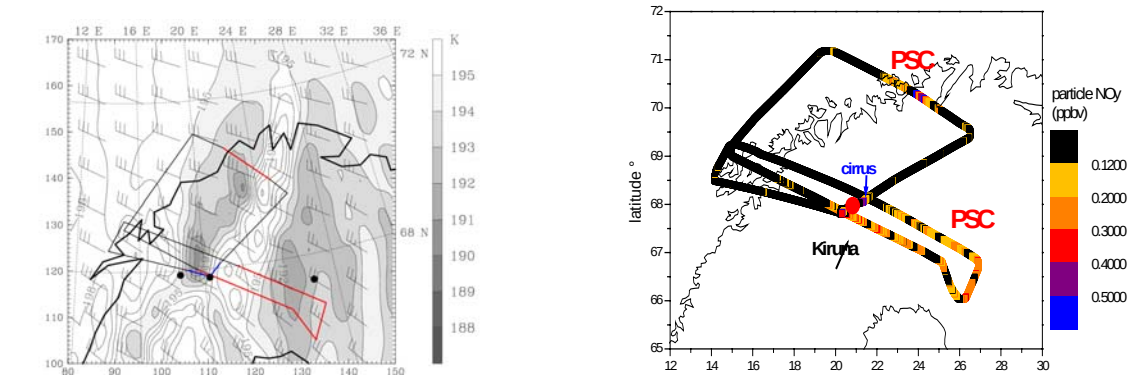


(A) longitude °E (B) longitude °E

**Fig. 6.3 (A) Temperature field at 55 hPa on 8 February 2003, 16.00 UT, analysed with the mesoscale MM5 model (DLR) together with the flight path of the Geophysica. PSC and cirrus measurements are marked in red and blue, respectively. (B) Particulate NOy detected in PSCs and cirrus.**

In the northern flight leg, the Geophysica penetrated into a mountain wave PSC, which contained up to 0.5 ppbv NOy (Fig. 6.3B). Highly correlated increases in particlulate NOy (DLR) and backscatter ratios measured with a backscatter sonde (CNR-ISAC) and a Micro-joule Lidar (UNIV-Neuchatel) show the presence of a supercooled ternary solution (STS) PSC (Fig. 6.4). These observations are further supported by the simultaneous detection of non-depolarising PSC particles with the OLEX Lidar (DLR) onboard the Falcon.

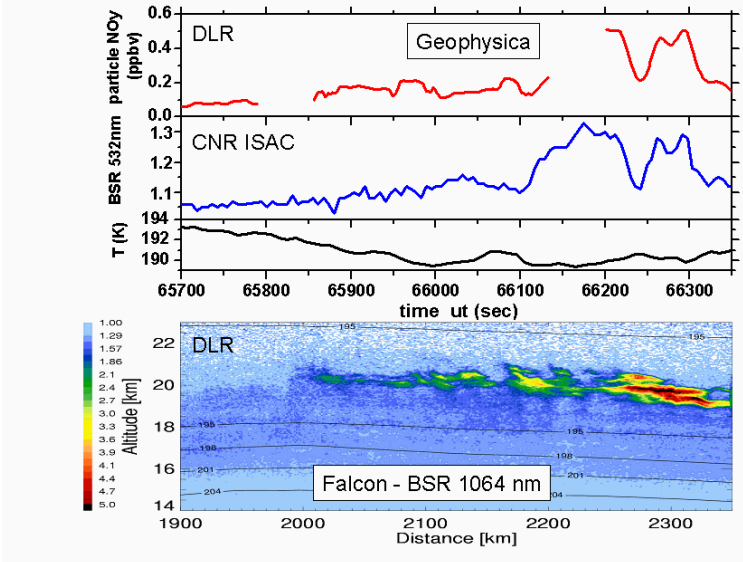


**Fig. 6.4 Coordinated in-situ and remote sensing measurements of a mountain-wave PSC on 8 February 03 (Upper panel: Particle NOy (DLR) and backscatter ratio at 532 nm (CNR-ISAC) from Geophysica measurements. Lower panel: Backscatter ratio at 1064 nm from OLEX (DLR) measured in the same region from the Falcon.**

Microphysical equilibrium modelling of the quasi-Lagrangian measurement of the liquid PSC (WP2) overestimates the nitric acid content of the PSC particles. Conversely, the particle composition is in agreement with results from a non-equilibrium model (University of Lancester).

In addition, in a region west of Kiruna on 8 February (Fig. 6.3) and during a flight into Russia on 9 February, a slight increase in particulate NOy and elevated backscatter ratios indicate supercooled ternary solution PSCs, which were slightly enhanced in nitric acid (<0.3ppbv $HNO_3$). The measurements of liquid PSCs were compared to chemical and optical models of particle growth and chlorine activation in PSCs (WP2, WP3 and WP4).

### 6.1.5 Model calculations of $HNO_3$ and denitrification.

The coupled DLAPSE/SLIMCAT model was used to provide daily maps of NOy partitioning and denitrification to aid flight planning. DLAPSE calculated denitrification was used to intialise CLaMS for detailed studies of transport and ozone loss (WP3 and 4). Maps of model $HNO_3$, denitrification and particle phase $HNO_3$ are available on the internet (http://www.env.leeds.ac.uk/~stewart/EUPLEX/EUPLEX_NRT.html).

### 6.1.6 Model comparisons with observations

Both DLAPSE (Leeds) and CLaMS (FZJ) have been extensively compared with observations of NOy and denitrification from the Geophysica as shown in Fig. 6.5. DLAPSE has also been compared with MIPAS-E observations of $HNO_3$ and denitrification during the Arctic winter of 2002/03. The result is visualized in Fig. 6.6. Both models use similar Lagrangian microphysical volume-averaged denitrification schemes (Carslaw et al., 2002) for the growth and sedimentation of large NAT particles (Fahey et al., 2001). Model particle nucleation rates of $3.2 \times 10^{-9}$ and $2.2 \times 10^{-9}$ particles $cm^{-3}$ $s^{-1}$ , respectively are required to reproduce the observed denitrification from SIOUX/HAGAR.

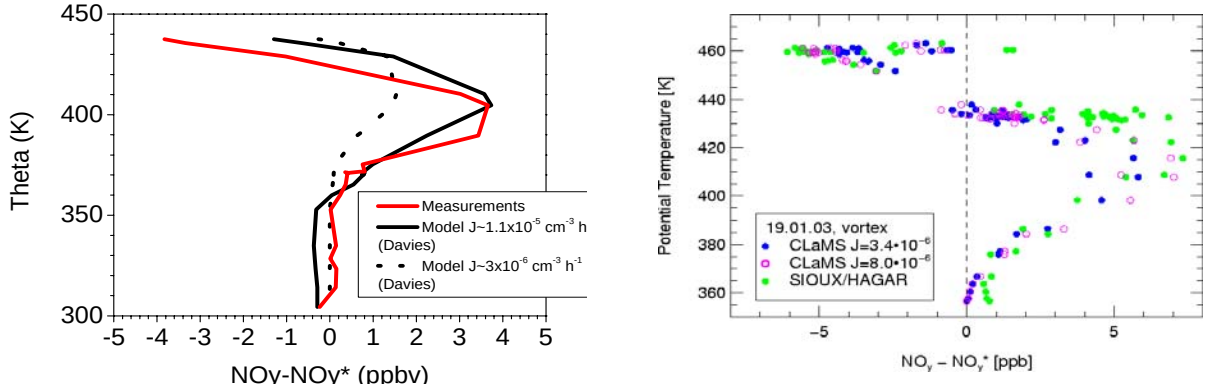


**Fig. 6.5 Comparison of model and observed denitrification from Geophysica for i) DLAPSE (Leeds) on February 6, 2003 and ii) CLaMS (FZJ) on January 19, 2003.**

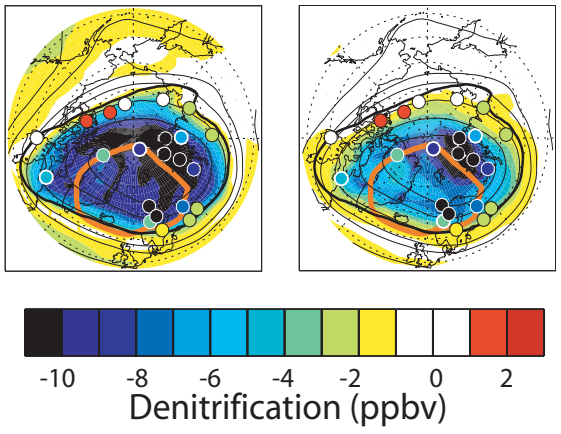


**Fig. 6.6 Contour plot of DLAPSE (right) and equilibrium (left) denitrification at 465K for January 3, 2003. MIPAS observed denitrification is shown as filled circles.**

Using an equilibrium denitrification scheme (common in CTMs) 'smeared out' the denitrification over a wide region of the vortex whereas DLAPSE produced strongest denitrification in the core of the vortex. MIPAS observations indicate that strong denitrification is also confined to the vortex core, providing observational evidence for earlier theoretical studies (Mann et al., 2002).

In co-operation with the MAPSCORE EU project, additional comparisons were also been made between DLAPSE and observations of NOy and denitrification from three previous Arctic winters: 1999/2000 (ER2, MLS), 1996/97 (ILAS) and 1994/95(MIPAS-B, MLS). In general, DLAPSE was able to reproduce the observed denitrification within the constraints of the observations when a volume averaged NAT particle nucleation rate was used. A nucleation rate of $3.2 \times 10^{-9}$ $cm^{-3}$ $s^{-1}$ agreed best with all observations apart from 1999/2000, where $J=0.8 \times 10^{-9}$ $cm^{-3}$ $s^{-1}$ compared most favourably. These comparisons demonstrate that Arctic denitrification in a number of winters may be successfully simulated by assuming a simple volume-averaged nucleation rate for NAT particles, as used in DLAPSE and CLaMS.

### 6.1.7 Model studies of mountain-wave induced synoptic denitrification.

The Leeds DLAPSE denitrification model has been modified to examine the potential for mountain wave induced NAT clouds to produce large NAT particles and denitrification of the polar vortex. NAT clouds at high particle number densities (mother clouds) are produced in the model immediately downwind of mountain wave ice clouds which are advected away from the source and release low concentrations of NAT particles (Fueglistaler et al., 2002). These studies indicate that wave-induced NAT „mother clouds" may occupy 5-10% of the volume of the NAT-supersaturated region of the vortex. The NAT rocks produced by growth and sedimentation from „mother clouds" may occupy a much larger volume (up to 60% of the NAT-supersaturated region). For the Arcitic winter of 1999/2000, this study indicates that this mechanism may be responsible for a significant proportion (although not all) of the observed denitrification. Fig. 6.7 shows some resulting denitrification profiles.

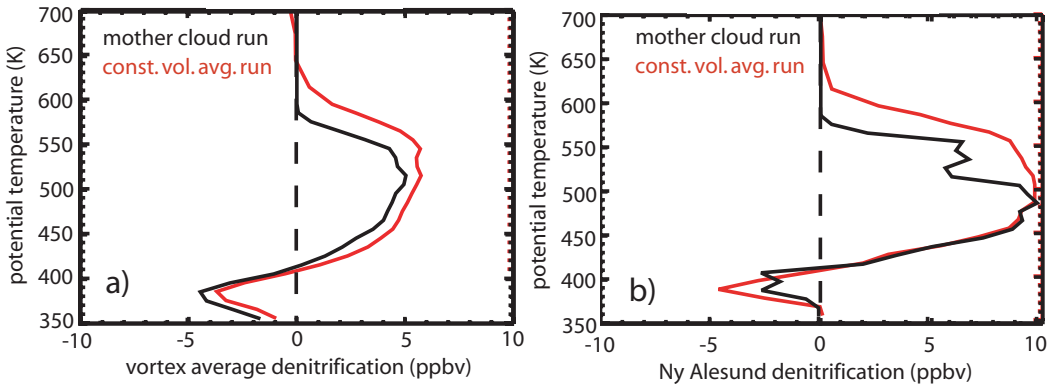


**Fig. 6.7 Profiles of denitrification at 12UT on January 20, 2000 for the mountain wave induced „mother cloud" run (black line) and the constant volume-averaged nucleation run (red line) a) as a vortex average, b) at Ny Alesund (79N, 12E).**

### 6.1.8 Socio-economic relevance and policy implication

An understanding of the physico-chemical processes which control the ozone layer forms the basis for political decisions about the phase-out of ozone depleting substances. WP1 demonstrates the world-leading position of EU science in the provision of data and model simulations

of these processes. WP1 aims to deliver information which will aid in the development of PSC parameterisations for use in GCM predictions of the future state of the ozone layer.

### 6.1.9 Discussion and conclusions

Unique observations of the existence of NAT particles at low number densities at very low NAT saturation ratios were made during EuPLEx. These observations challenge current NAT nucleation theories as NAT formation on ice may be excluded. Homogeneous NAT nucleation from liquid binary or ternary solutions or surface nucleation using currently available rates cannot explain the observed NAT particle number densities. The heterogeneous nucleation of NAT on ubiquitous background meteoritic material is the most plausible explanation of these observations. This nucleation mechanism may account for the original observations of large NAT particles and denitrification in 1999/2000 (Fahey et al., 2001) although the detailed mechanism requires further study. Modelling studies have shown that while NAT particle formation by lee wave induced „motherclouds“ may play a significant role in Arctic denitrification, an additional contribution is required from other mechanisms to fully explain observations of denitrification.

Model simulations of Arctic denitrification are most realistic when based upon full-microphysical calculations of NAT particle growth and sedimentation. The alternative assumption, almost universally used in current chemical transport models, that NAT is in equilbrium with gas phase nitric acid, does not produce realistic denitrification patterns. Microphysical denitrification schemes based on straightforward volume-averaged NAT particle nucleation rates produce denitrification which is broadly consistent with the degree of observed denitrification in 2002/03 and earlier winters. The model particle nucleation rates used to simulate seasonal denitrification are similar to those inferred from the observations of NAT particles at low supersaturations described above ($J \sim 3 \times 10^{-9}$ $cm^{-3}$ $s^{-1}$). In contrast, simple thermodynamic equilibrium schemes (as often used in CTMs and GCMs) tend to produce excess denitrification in the outer regions of the vortex. Development of a parameterisation for GCMs?

### 6.1.10 Publications from the project

Voigt, C., H. Schlager, B. Luo, A. Dörnbrack, A. Roiger, P. Stock, J. Curtius, H. Vössing, S. Borrmann, S. Davies, P. Konopka, C. Schiller, G. Shur, T. Peter, NAT formation of low Nat supersaturations, Atmos. Chem. Phys. Discuss., 4, 8579-8607, 2004.

Grooß J.-U., G. Günther, R. Müller, P. Konopka, S. Bausch, H. Schlager, C. Voigt, C. M. Volk, G. C. Toon, Simulation of denitrification and ozone loss for the Arctic winter 2002/2003, Atmos. Chem. Phys. Discuss., 4, 8069-8101, 2004.

Mann, G.W., K.S. Carslaw, M.P. Chipperfield, S.D. Eckermann, Large NAT particles and denitrification caused by mountain waves in the Arctic stratosphere, accepted for publication in J. Geophys. Res., 2005.

Davies, S., G. W. Mann, K. S. Carslaw, M. P. Chipperfield, J.A. Kettleborough, M.L. Santee, H. Oelhaf, G. Wetzel, Y. Sasano, T. Sugita, 3-D microphysical model studies of Arctic denitrification: Comparison with observations, submitted to Atmos. Chem. Phys. Disc., 2004.

Davies, S., G. W. Mann, K. S. Carslaw, M. P. Chipperfield, J. J. Remedios, A. M. Waterfall, Arctic denitrification during winter 2002/03: using satellite observations to interpret a 3-D microphysical model, manuscript in preparation.

Feng, W., , M.P. Chipperfield, S. Davies, B. Sen, G. Toon, J.F. Blavier, C.R. Webster, C.M. Volk, A. Ulanovsky, F. Ravegnani, P. von der Gathen, H. Jost, E.C. Richard, H. Claude, Three-Dimensional Model Study of the Arctic Ozone Loss in 2002/03 and Comparison with 1999/2000 and 2003/04, Atmos. Chem. Phys. Discuss, 4, 5045-5074, 2004.

Schlager, H., et al., Observations of denitrification and renitrification in the 2002-2003 Arctic winter stratosphere, in preparation for Atmos. Chem. Phys., 2005.

Nitric acid distributions observed by the MIPAS on ENVISAT during the Vintersol campaign of 2002/3 and comparisons to a denitrification model, J.J. Remedios, A.M. Waterfall, R. Spang, G.Mann, S.Davies, K.Carslaw, manuscript in preparation.

C. S. Singleton,C. E. Randall,M. P. Chipperfield,S. Davies,W. Feng,R. M. Bevilacqua, K. W. Hoppel, M. D. Fromm, G. L. Manney, V. L. Harvey, 2002–2003 Arctic ozone loss deduced from POAM III satellite observations and the SLIMCAT chemical transport model, Atmos. Chem. Phys. Discuss., 4, 7011-7045, 2004.

## 6.2 WP2: Small-scale polar stratospheric clouds and mountain waves

### 6.2.1 Objectives

To test the hypothesis: *there is a single sequence of PSC composition for mountain wave clouds*. That is, to produce a data-consistent microphysical description of the evolution of stratospheric aerosol particles passing through large-amplitude gravity waves. To investigate the potential role of mountain wave clouds in the *formation sequence of large $HNO_3$ hydrate particles (NAT rocks).*

### 6.2.2 Methodology and scientific achievements

The focus of WP2 was the field campaign in January-February 2003; the activity in the current reporting period consists of data analysis. An overview of the campaign is given above. Here we focus on interpretation of the mountain-wave-induced PSCs, observed during the campaign.

On 8 February 2003, mountain waves were present above Scandinavia (Fig. 6.8, below). These waves produced temperatures below 190 K at the Geophysica flight altitude (Fig. 6.9, below), which, in turn, produced PSCs. These PSCs are nitric acid containing particles (Fig. 6.9, top panel). The resulting larger particles gave a higher return signal in the MAS and OLEX measurements of scattering ratio (Fig. 6.9, middle and lower panels, and Fig. 6.10). This increase in scattering ratio was accompanied by a very small observed particle depolarisation (not shown), suggesting that, in the main, the particles were liquid and spherical. Using measurements of the particle NOy from SIOUX, and of particle from the combination of FISH and FLASH, it will be possible to examine the change in mean composition of these particles through the cloud event. The formation of high number density NAT clouds (PSC 1b-enh) was not observed as the required low temperature for the formation of ice clouds, which provide surfaces for heterogeneous NAT nucleation, were not reached during the campaign period. We were also not able to test the mother cloud mechanism for NAT rocks formation. The nucleation of low number density NAT particles under threshold NAT supersaturation was observed during the filed campaign period and was reported in WP 1 in detail.

Short descriptions of WP2 activities from individual partners follow:

*FZJ: FISH measurements of total water*

These have been described in WP1, see above. No water ice stratospheric clouds were observed in-situ during EuPLEx. FISH measurements provided boundary conditions for the modelling study described above (Lowe et al., 2004).

*DLR: Mesoscale models of stratospheric dynamics*

On 8$^{th}$ February 2003 two co-located flights of the Geophysica and Falcon were performed under moderate, but highly non-stationary mountain wave conditions. The flight path of the Geophysica was designed based on MM5 mesoscale model predictions, including the flexibility to adjust some flight legs during the flight to the regions with lowest temperatures. This was decided by the mission scientist onboard the Falcon, which has been used as path finder for PSCs, on the basis of the OLEX Lidar measurements. This procedure enabled coordinated flights with both aircraft in mountain wave PSCs. Fig. 1 shows analysed temperatures with MM5 together with the Geophysica flight track.

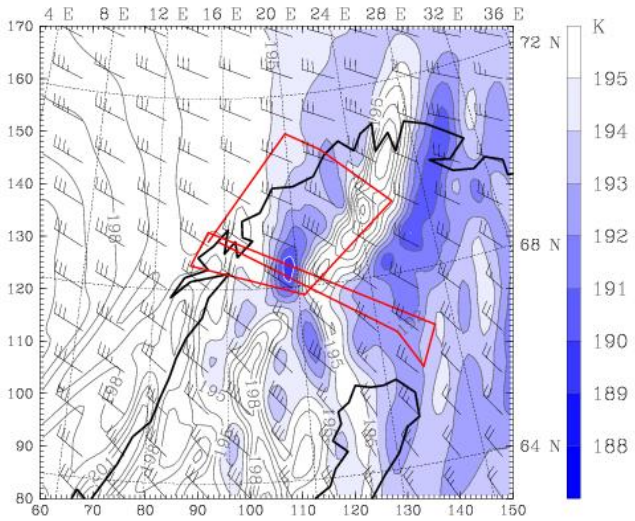


**Fig. 6.8 Temperature field at 55 hPa on 8th February 2003, 16.00 UT, analysed with the mesoscale MM5 model, together with the flight path of the Geophysica.**

In the northern flight leg, the Geophysica penetrated a mountain-wave PSC, as demonstrated from the chemical and optical measurements. Fig. 6.9 shows the simultaneous in-situ and remote sensing measurements during the PSC encounter. Correlated increases in particle NOy measured by DLR as well as backscatter ratios detected with the Lidar systems of CNR-ISAC and ON show the presence of a liquid ternary solution PSC. These observations are further supported by the simultaneous detection of liquid PSCs with the OLEX Lidar onboard the Falcon. Interestingly, the OLEX measurements also showed a slight depolarization in the perpendicular channel, indicating that a few solid particles could be mixed in the STS cloud.

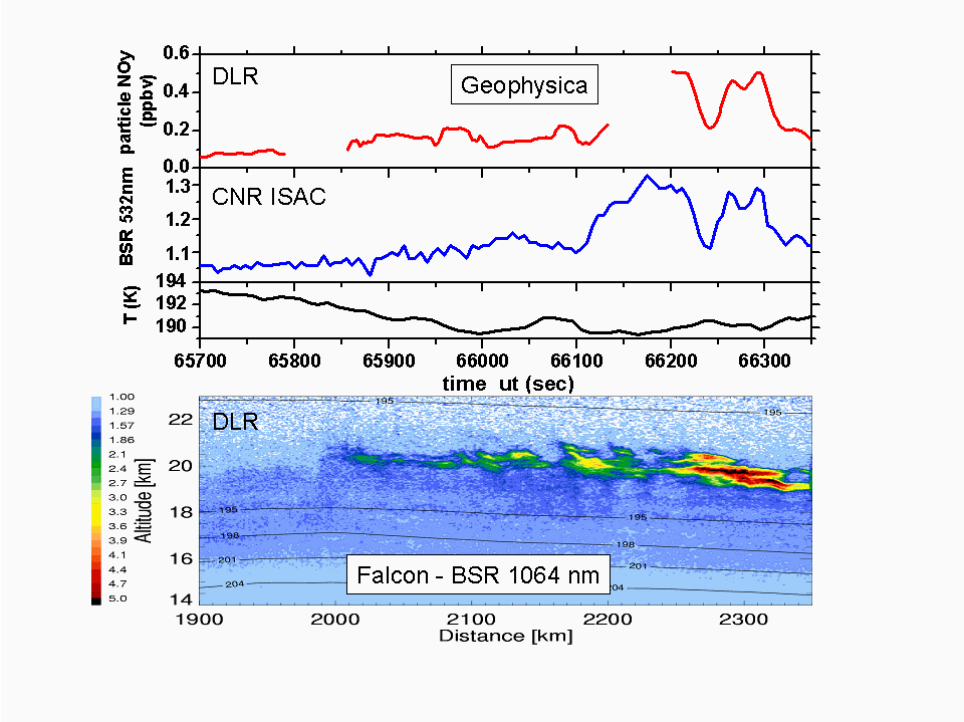


**Fig. 6.9 Coordinated in-situ and remote sensing measurements of a mountain-wave PSC on 8th Feb 03 (Upper panel: Particle NOy (DLR) and backscatter ratio at 532 nm (CNR-ISAC) from Geophysica measurements. Lower panel: Backscatter ratio at 1064 nm from OLEX (DLR) measured from the Falcon in the same region.**

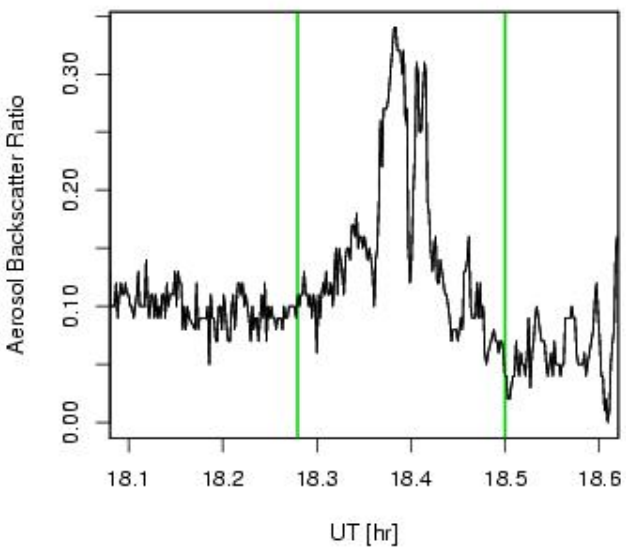


**Fig. 6.10 Aerosol backscatter ratios measured by the MAS instrument. The green lines denote the edges of the region of PSC.**

Measurements taken by the MAS instrument are shown in Fig. 6.10. This shows an increase in backscatter within the mountain-wave event, shown by the green lines, indicating an increase in the mass of the aerosol phase due to $HNO_3$ and water uptake and confirming the analysis of the SIUX data.

The section of the Geophysica flight that passes through the PSC shown in Fig. 6.9 and Fig. 6.10 was in the direction of, and practically parallel to, the local wind; this allows us to use the flight to construct a quasi-lagrangian trajectory. Just how lagrangian the flight path was, can be gauged from the isentropes derived from MTP measurements. These are shown, along with the Geophysica flight path, in Fig. 6.11.

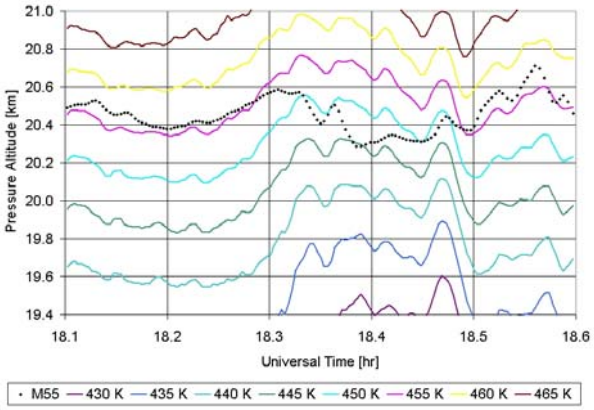


**Fig. 6.11 Pressure altitude of the Geophysica during the flight on the 8th February 2003 (black diamonds) with the pressure altitudes of isentropic surfaces (coloured solid lines) at 5K intervals.**

To generate trajectories for our models, we have combined a 6-hour MM5 back trajectory with temperature and pressure measurements from the Geophysica aircraft. We then model the evolution of aerosol along the trajectory using equilibrium aerosol-growth equations, or using MADVEC, a model that describes the dynamics of condensational growth of liquid PSC particles. MADVEC uses the advection of mass components in radius-space, driven by differences be-

tween ambient partial pressures and the equilibrium vapour pressures (see Lowe et al., 2003, for more details).

In Fig. 6.12, we compare the model particle-phase $NO_y$ content with SIOUX and MAS measurements. The dynamic model is markedly better than the equilibrium calculation (grey line) at capturing the magnitude of the measurements.

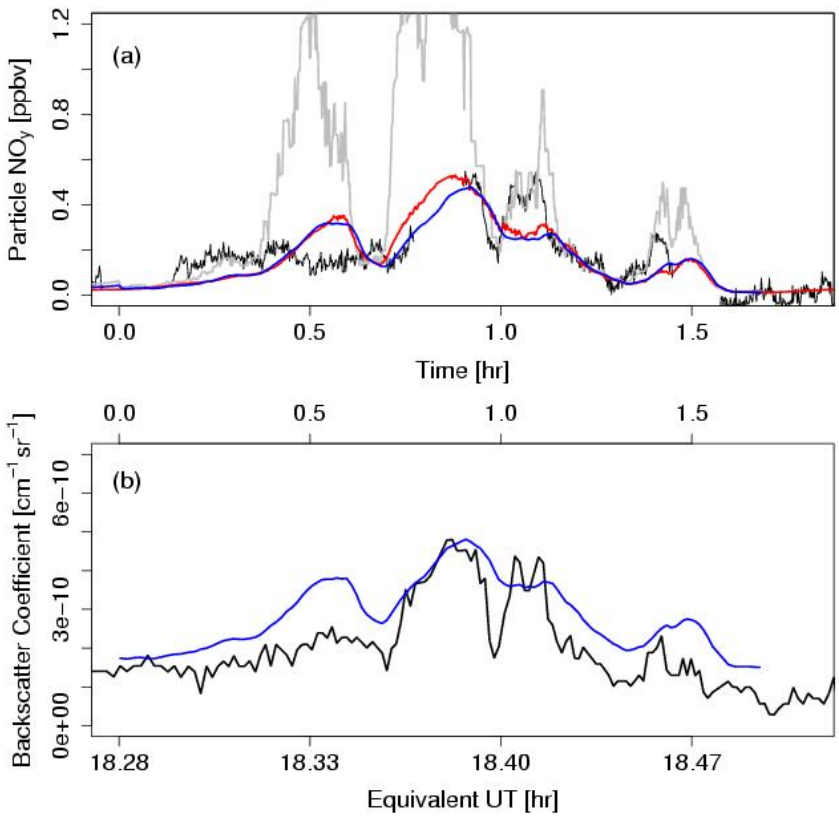


**Fig. 6.12 (a) NOy content of the condensed phase for the dynamical model (blue & red lines) and equilibrium calculations (grey line) along quasi-lagrangian trajectories, compared with those measured by the SIOUX instrument (black line). (b) Backscatter coefficients calculated from the MAS data (black line) and the dynamical model (blue line).**

This study demonstrates the maturity of PSC models for data analysis, and also the importance of multiple measurements of physical and chemical parameters that are important in determining the evolution of PSCs. Deployments of high-altitude aircraft, such as the Geophysica, and very large balloon payloads, are the only way to collect multi-instrument datasets of this kind. Associated activities of individual groups are described briefly, below.

*IPA-UMZ*

These are described in WP6, see below.

*IFA-CNR: Multiwavelength Aerosol Scatterometer (MAS)*

The participant CNR_ISAC section of Rome has deployed during the EUPLEX field campaign the Multiwavelength Aerosol Scatterometer (MAS — see above). Also, an optical model has been developed, in conjunction with partner 11, to simulate the optical properties of the sounded PSC discussed above. This model is based on a T-matrix computation of scattering efficiencies to estimate the optical properties of particles. The code allows for modeling over a wide range of particle compositions (i.e. refractive index) and asphericities. Results from MADVEC microphysical modelling (partner 10) served as input for the optical model (see above). Particular care was posed in the study of the dependence of optical properties from the refractive index. An optimal value of the refractive index has been determined, either from direct comparison between

modelled-observed backscattering, and from theoretical calculations based on the presumed particle composition. The two methods give very good accordance.

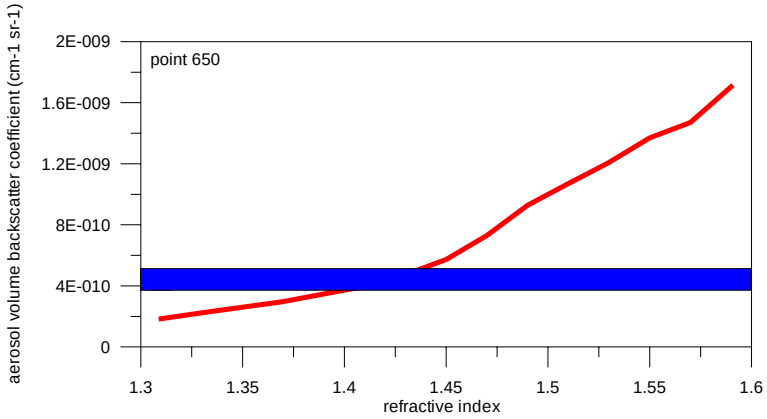


**Fig. 6.13 For a simulated particle size distribution, the red line shows the variation of the computed aerosol scattering coefficient versus the index of refraction. The blue bar show the experimental uncertainty associated with the observed backscatter coefficient from MAS observations. The intersection between the two lines indicates the range of refractive index values for which observations and simulations are compatible.**

An extensive dataset of observations of cirrus clouds at or below the polar tropopause has also been acquired. Cirrus clouds have been measured on ascent and descent on the 26$^{th}$ of January, and on the 2$^{nd}$, the 8$^{th}$, the 11$^{th}$, 15$^{th}$ of February. Analysis of mid-cloud height and temperature, cloud top and bottom and the optical and microphysical parameters have been carried out, and comparison with the particle and CCN counter is under way, to assess the role of those cloud in the polar upper tropospheric water balance.

*INOA:*

These are described in WP5.

*CAO: FLASH (Fluorescent Airborne Stratospheric Hygrometer)*

FLASH participated in the field campaign of VINTERSOL-EUPLEX project in Kiruna (Sweden) in January-February 2003 on board of high altitude aircraft M55 Geophysica, as reported previously. All obtained valid data have been presented in NASA-AMES format and put on the EUPLEX and NILU servers.

*ULANC: trajectory modelling of aerosol composition*

The group at Lancaster continues to develop their model of stratospheric aerosol — see the application discussed above (Lowe et al., 2004).

*ETH: microphysical modelling of aerosol growth and freezing*

These are described in WP1.

### 6.2.3 Socio-economic relevance and policy implication

Knowledge about the state of the ozone layer constitutes the basis for negotiations and decisions on the political level concerning the phase-out of ozone depleting substances. WP2 demonstrates the world-leading position of EU science in the provision of data and model interpretation of processes leading to ozone depletion. WP2 aims to deliver an objective that will inform calculations of future ozone depletion, by providing information necessary for the improvement of PSC parameterisations in global climate models.

### 6.2.4 Discussion and conclusion

The EuPLEx field campaign, like all field campaigns, was at the mercy of the weather and, in the end, provided only a relatively small number of mountain-wave events for study. However, the state of readiness of the group meant that these events were probed closely, in new ways, and with new instrumentation. The outlook for achieving our objective is therefore good.

### 6.2.5 Publications from the project

Bogdan, A., M. Kulmala, A. R. MacKenzie, A. Laaksonen, M. J. Molina, and A. Avramenko, The study of finely divided aqueous systems as a clue to understanding the formation mechanisms of polar stratospheric clouds: 1. $HNO_3/H_2O$ and $H_2SO_4/H_2O$ systems, *J. Geophys. Res.*, **108** (D10), 4302, doi:10.1029/2002JD002605.

Bogdan, A., M. Kulmala, A. R. MacKenzie, A. Laaksonen, M. J. Molina, and A. Avramenko, The study of finely divided aqueous systems as a clue to understanding the formation mechanisms of polar stratospheric clouds: 2. $HCl/H_2O$ and $HNO_3/HCl/H_2O$ systems, *J. Geophys. Res.*, **108** (D10), 4303, doi:10.1029/2002JD002606.

Lowe, D., and A. R. MacKenzie, Modelling Liquid particle Composition in Polar Stratospheric Clouds, *Abstracts of Presentations and Posters, Sixth European Symposium on Stratospheric Ozone,* Göteborg, Sweden, 2nd to 6th September 2002.

Lowe, D., A. R. MacKenzie, N. Nikiforakis, and J. Kettleborough, A condensed-mass advection based model of liquid polar stratospheric clouds, *Atmos. Chem. Phys.*, **3**, 29-38, 2003.

Lowe, D., A. R. MacKenzie, H. Schlager, C. Voigt, A. Dörnbrack, M. J. Mahoney, and F. Cairo, Liquid particle composition and heterogeneous reactions in a mountain-wave Polar Stratospheric Cloud, *Atmos. Chem. Phys. Discuss.*, submitted November 2004.

MacKenzie, A. R., Recent advances in the study of polar stratospheric and tropical tropopause clouds, *Recent Res. Developments in Geophysics*, **4**, 439-462, 2002.

### 6.2.6 Extended abstracts

Lowe, D., A. R. MacKenzie, H. Schlager, and C. Voigt, Liquid Particle Composition and Heterogeneous Reactions in a Lee-Wave Polar Stratospheric Cloud, in *Nucleation and Atmospheric Aerosols 2004,* M. Kasahara and M. Kulmala (eds.), Kyoto Univ. Press, pp371-374, 2004.

### 6.2.7 Talks:

D. Lowe (Speaker): Liquid Particle Composition and Heterogeneous Reactions in a Lee-Wave Polar Stratospheric Cloud, ICNAA, Kyoto, 26-30 July, 2004

D. Lowe (Speaker): Liquid Particle Composition and Heterogeneous Reactions in a Lee-Wave Polar Stratospheric Cloud, UGAMP, Oxford, 8-10 September, 2004

## 6.3 WP3: PSC Optical Properties

### 6.3.1 Objectives

Coordinated measurements of remote optical (lidars and aerosols scatterometers on both aircraft) and in-situ micro-physical properties of synoptic scale and mountain-wave PSCs. Use lidar information for path finding and real time PSC identification (including NAT rocks), and provide input for post-campaign modelling within WP1 (synoptic PSCs and denitrification) and WP2 (local PSCs and mountain waves). Determination of PSC particle size/shape as functions of time and space. Test and improve optical and micro-physical PSC models.

### 6.3.2 Methodology and scientific achievements

Owing to minor warmings in late December 2002 and mid January 2003, the vortex was strongly disturbed during the EUPLEX campaign and temperatures only occasionally fell below $T_{NAT}$ at the very beginning an near the end of the campaign. In spite of sufficiently low temperatures however, no NAT particles were observed by the OLEX lidar and other remote optical instruments during the entire campaign (see below). While these marginal PSC conditions gave little opportunity to measure PSCs remotely using optical instruments, they offered a great chance for a search for young NAT particles at extremely low number densities by in situ instrumentation. Thus, while main achievements have been established in WP1, results from WP3 presented here are mainly collateral evidence.

### 6.3.3 Measurements of small scale PSCs

During the EUPLEX campaign 9 Falcon and Geophysica flights have been performed with nearly 30 hours of lidar measurement onboard of the Falcon and lidar and in-situ measurements on Geophysica. PSCs were observed by the Falcon lidar during both transfers and during three regional flights, two of which were co-ordinated with the Geophysica. Geophysica was equipped with both in-situ (FSSP, MAS) and remote sensing (MAL) instrumentation for the investigation of particle optical and microphysical properties. As an example, the compact airborne aerosol backscatter/depolarisation lidars (MAL-up and MAL-down, probing the atmosphere in zenith and nadir respectively) from Observatory of Neuchâtel, Switzerland, are shown in Fig. 6.14.

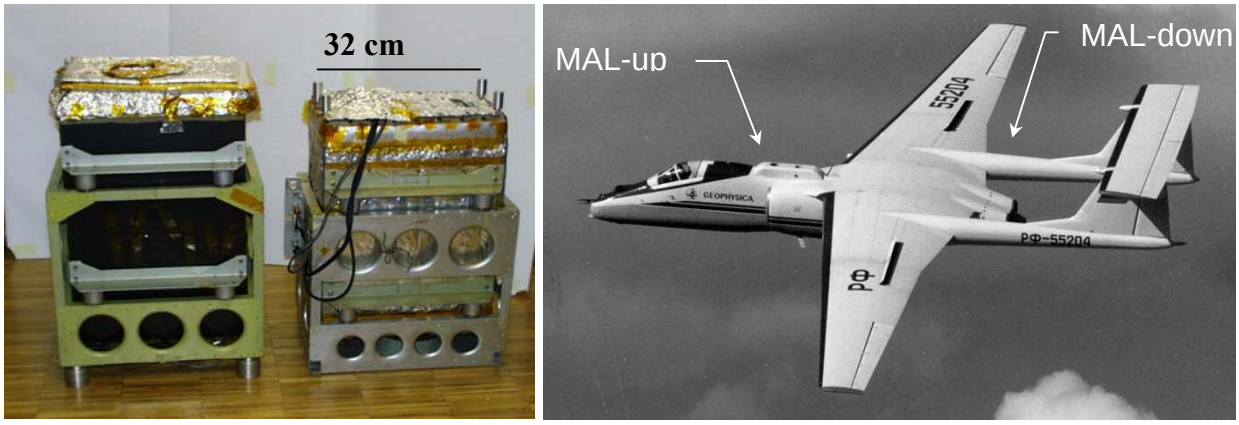


**Fig. 6.14 .Left panel: instruments MAL-up (zenith) and MAL2 (MAL-down /right one) ready for installation on the M-55. Right panel: M55 with indications for the location of MAL 1 and MAL2.**

Another optical instrument from the partner CNR-ISAC of Rome has been deployed during the EUPLEX field campaign: the Multiwavelength Aerosol Scatterometer (MAS), an instrument capable of performing measurements of the optical properties of micron size particles present in the atmosphere in close proximity of the mounting platform, ranging from 3 to 30 metres from it. The instrument emits laser light at 532 and 1064 nm and collects the light backscattered by molecules and particulate present in the atmosphere close to it.

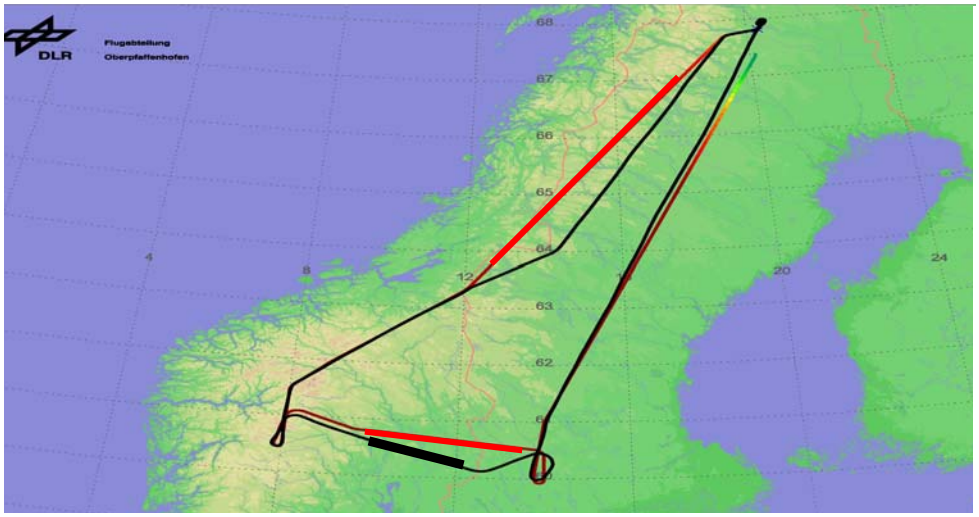


**Fig. 6.15 Flight path of the DLR Falcon (in red) and Geophysica (in black) on 15 January 2003. The ice PSC event observed Geophysica is marked by the thick black line. The thick red lines show the STS cloud observed by Falcon.**

The first coordinated flight was performed on 15 January over the Scandinavian Mountains as shown by Fig. 6.15. STS PSCs were observed over the southern Scandinavian mountains on 15 January (Fig. 6.16, red-coloured regions). Indeed, the temperature from ECWMF analyses was as low as 189 K (contours in Fig. 6.16), reaching the STS temperature.

The STS clouds on 15 January were too high (≈ 20.5 km) to be reached by the Geophysica in-situ instruments (Fig. 6.16). The MAL instrument on board detected an ice cloud around 10ºE, 60.6ºN. This ice cloud was not detected by the Falcon, which flew parallel to the Geophysica but ~ 20 km more to the North, suggesting a small horizontal extent of the ice clouds. The liquid clouds remained thin and could be hardly detected by the MAL instruments due to their detection limits.

The second coordinated PSC flight was performed on 8 February 2003. Relatively small mountain-wave-induced PSC patches reached down to about 19 km and were measured by both the in-situ instruments and the remote sensing instruments on Geophysica (Fig. 6.17). A more detailed analysis of this case is described in WP2. There, it is also shown that the depolarization of the observed particles is at the detection limit (≈ 1 %) of the OLEX lidar and thus not a significant indication for the existence of solid particles. Rather, the lidar signal is dominated by the signal stemming from liquid particles. NAT particles with sufficiently high number density ($> 0.01$ cm$^{-3}$) or sufficiently large radius (large $> 5$ µm) can thus be excluded. The same is valid for the even thinner and smaller PSCs observed over northern Scandinavia one day later (i.e. on 9 February 2003, see below).

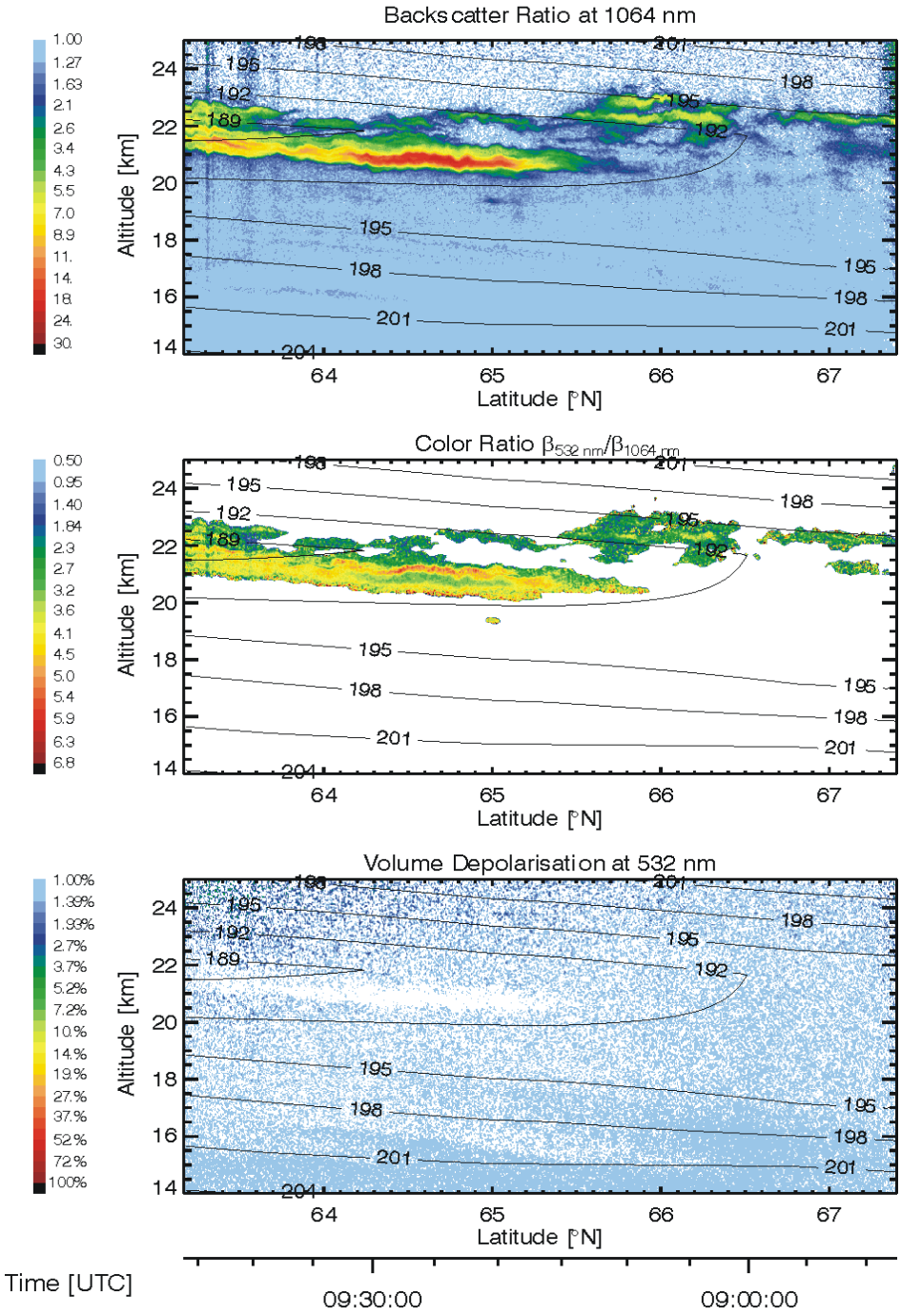


**Fig. 6.16 Measurements by OLEX onboard of the Falcon on 15 January 2003. (a) Backscatter ratio at 1064 nm. (b) Colour ratio $\beta_{532nm}/\beta_{1064nm}$, which is a measure of particle size. (c) Volume depolarization at 532 nm, which is a measure of particle shape. The STS clouds were above the flight level of the Geophysica (20 km).**

The Falcon with its lidar directed the Geophysica aircraft into the liquid cloud marked in Fig. 6.17. This cloud was probed by in-situ and remote sensing instruments on Geophysica.

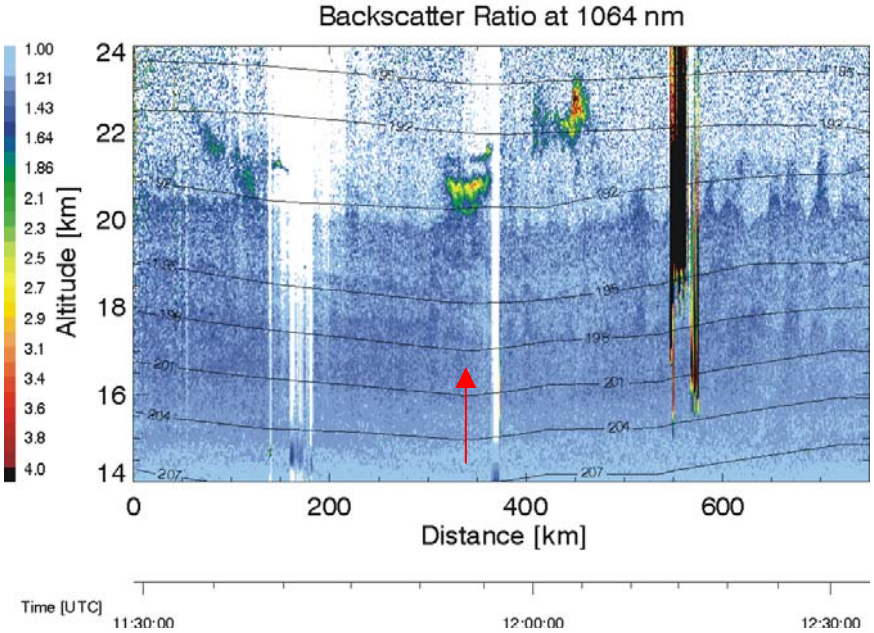


**Fig. 6.17 Particle backscatter ratio at 1064 nm along the flight on 8 February 2003. Gravity waves are evident at the upper edge of distinct aerosol layers. The arrow shows the signal of a gravity-wave-induced PSC.**

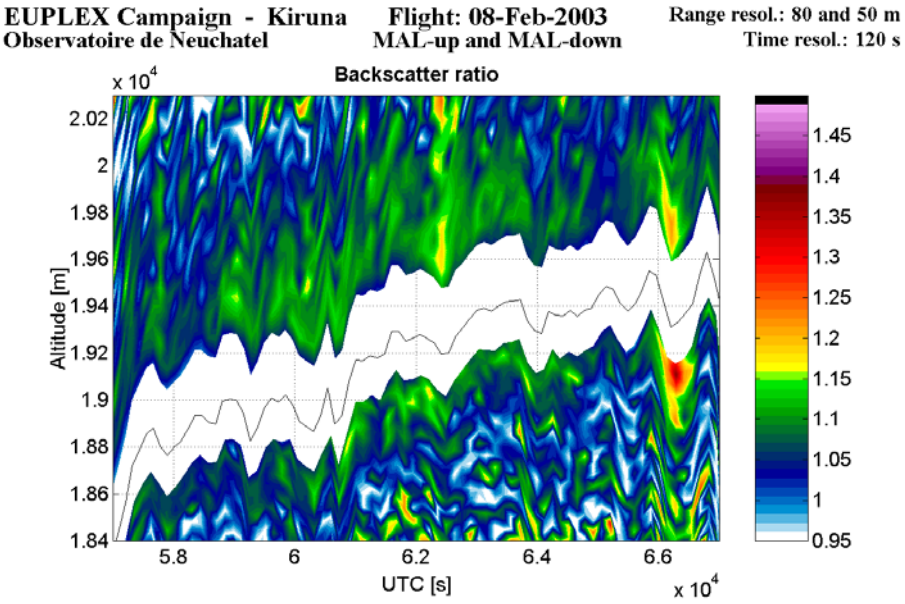


**Fig. 6.18 PSCs as detected by MAL-up and MAL-down during the flight on 8 February 2003. The abscissa is the UTC time in seconds. The ordinate is the altitude (asl). In colour code is the measured backscatter ratio. The thin black line is the Geophysica flight path. The white band indicates the region without measurements.**

In the time interval 59'000 s-67'000 s, a layer with backscatter ratio around 1.10-1.15 is present, though this value is near the instrument sensitivity threshold. The simultaneous measurement by MAS is shown in Fig. 6.19 Analysis of the state of polarization of the scattered light allows classifying this PSC as type-Ib, i.e. STS particles. In the subsequent data processing and case study, comparisons with the NOy content of the PSC particles, as inferred from SIOUX data (partner 2) have been carried out (Fig. 6.20).

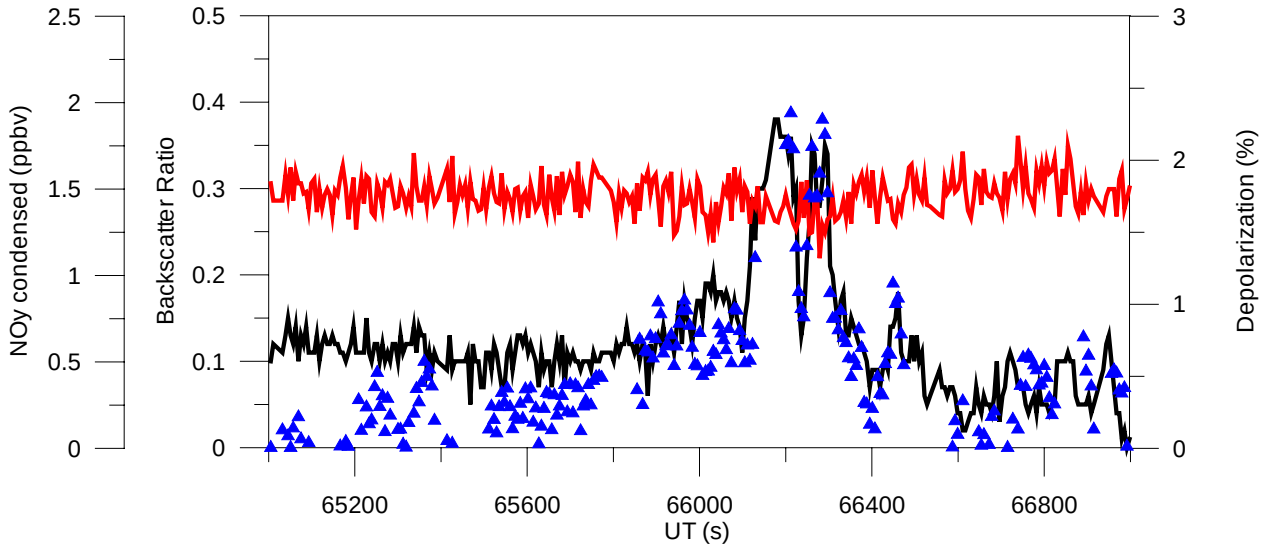


**Fig. 6.20 PSC event detected during the flight on 8 February 2003. The red line shows the depolarization, while the black line shows backscatter ratio, the blue triangles shows NOy in condensed phase, as revealed by SIOUX data from partner 2.**

### 6.3.4 Microphysical and optical modelling of STS clouds

Optical models have been developed to simulate the optical properties of the measured PSCs. They are based on a T-matrix computation of scattering efficiencies to estimate the optical properties of particles. The code allows for modelling a wide range of particle compositions (i.e. refractive indices) and asphericities. Combined with the microphysical model which takes into count of the $HNO_3$ and $H_2O$ uptake of background sulphuric aerosol particles, the optical properties can be calculated using the output of the microphysical modelling (Fig. 6.21). The observed backscattering ratios by MAS and condensed phase $HNO_3$ by SIOUX shown in Figure 3.6 are indicated in Fig. 6.21. The model result shows good agreement with the observed value, indicating a liquid cloud.

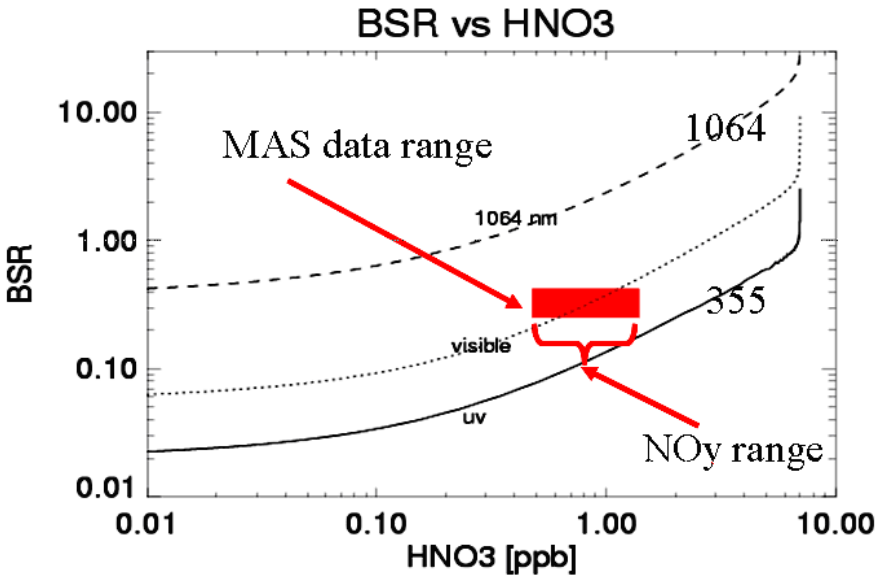


**Fig. 6.21 Backscatter signal of STS particles as a function of the $HNO_3$ amount in the aerosol particles. The $HNO_3$ mixing ratio and size of the particles has been calculated by Partner 11.**

The optical signal was also calculated using the results from microphysical modelling using MADVEC by partner 10, which served as input for the optical model. From the simulated size distributions the PSC optical properties have been computed, which have been compared with those observed by instrument MAS (see Fig. 6.22).

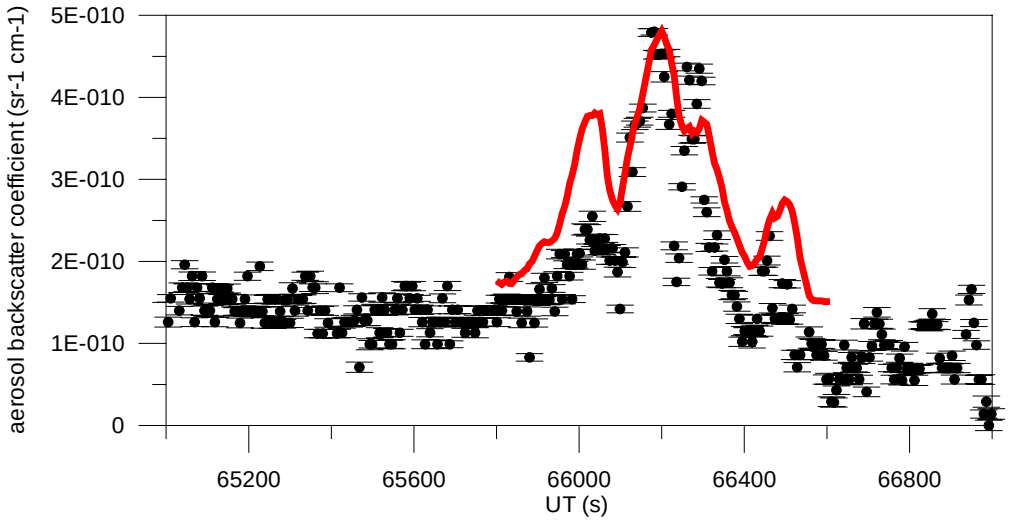


**Fig. 6.22 The black dots shows the aerosol volume backscatter coefficient as computed from MAS measurements, the red line shows the aerosol volume backscatter coefficient as computed by means of a Mie optical model from the aerosol size distributions given by the MADVEC model microphysical simulation of partner 10.**

Particular care was given in this study to the dependence of the optical properties on the refractive index. An optimal value of the refractive index has been determined directly from comparison between modelled and observed backscattering, or from theoretical calculations based on the presumed particle composition (Fig. 6.23). The two methods are in good accordance.

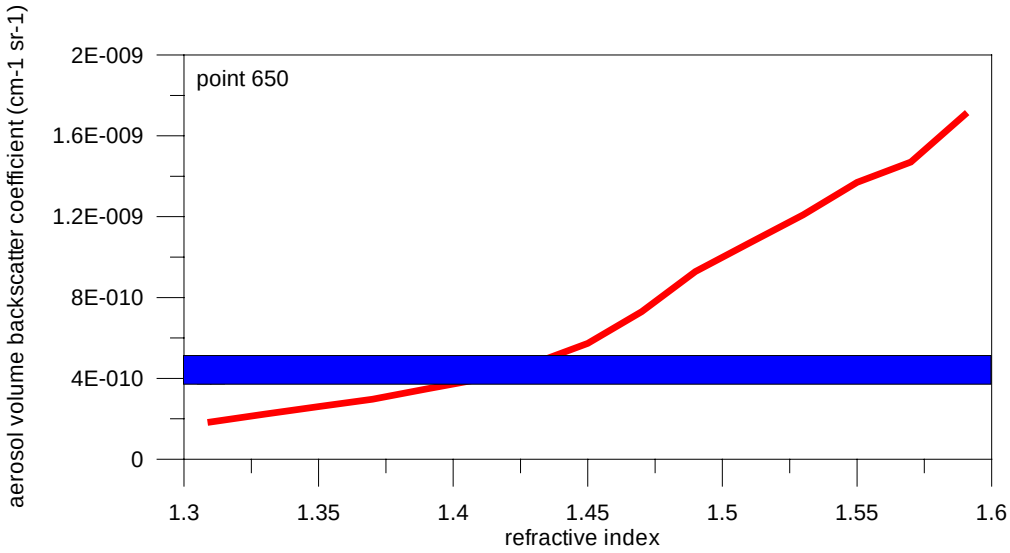


**Fig. 6.23 For a simulated particle size distribution, the red line displays the variation of the computed aerosol scattering coefficient versus the index of refraction. The blue bar show the experimental uncertainty associated with the observed backscatter coefficient from measurements by MAS. The intersection between the two select a range of refractive index values for which observations and simulations are compatible.**

While during the timeframe of the campaign in situ PSC measurements have been carried out only on a single event, an extensive dataset of observations of cirrus clouds at or below the polar tropopause has been acquired. Cirrus clouds have been measured on ascent and descent on the 26 January and on 2, 8, 11, and 15 February 2003. Analysis of mid-cloud height and temperature, cloud top and bottom and the optical and microphysical parameters have been carried out, and comparison with the particle and CCN counter is presently underway, to assess the role of these cloud in the polar upper tropospheric water budget.

### 6.3.5 Optical Measurement on the Synoptic-Scale PSCs

Owing to the warming in late December 2002 and mid-January 2003, the temperature was only occasionally below the NAT equilibrium temperature during the campaign period. Several flights were performed probing air masses in which the temperature had only recently dropped from very high temperatures ($T$ > 210 K) to NAT equilibrium temperature. Indeed, NAT particles were found by means on 6 February 2003 of the chemical measurement using the NOy instrument. Number densities were ~ $10^{-4}$ $cm^{-3}$ with radii of ~ 1 μm. These tenuous particle veils could not have detected by the optical FSSP-300 measurements by themselves, however the optical measurements can be shown to be compatible with the chemical measurements, corroborating their finding. More importantly, the size distribution of these particles can be derived by simultaneously exploiting the chemical measurements from the NOy instrument and the optical measurement from the FSSP-300 (for the details see WP2). Backward trajectory calculations show that the temperature was for only ~ 20 h at most 3 K below $T_{NAT}$ and remained clearly above the frost point $T_{ice}$. The nucleation of these particles above the frost point is the big new finding of EUPLEX. It indicates a higher nucleation rate of NAT at background condition than suggested previously, and proves for the first time conclusively the existence of such a nucleation pathway. The size distribution of NAT particles shown by the thick black line in Fig. 6.24 is used as input for the optical model to simulate the optical signal. We obtained a backscattering ratio of 0.001 at a wave length of 532 nm and of 0.03 at 1064 nm, which is far below the detection limit of OLEX, MAL and MAS. Therefore, we were not able to draw conclusions from the remote optical measurements on the NAT clouds during this campaign.

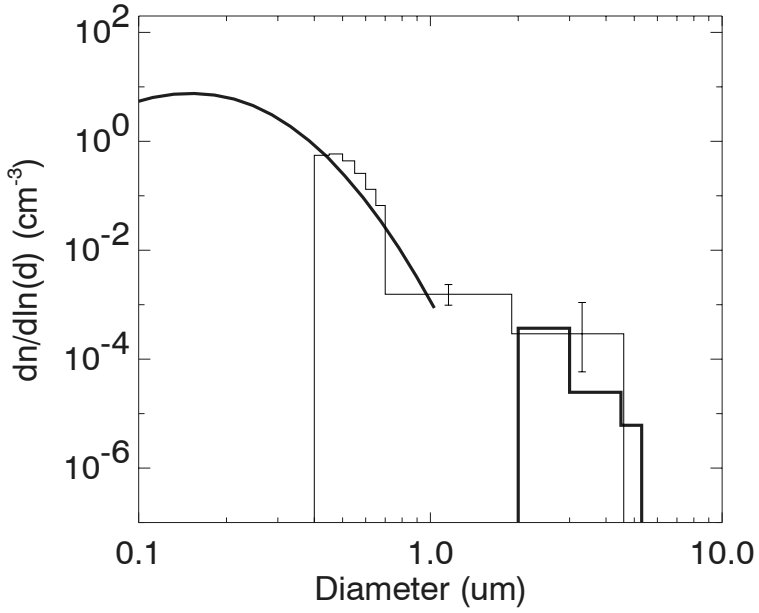


**Fig. 6.24 Particle size distribution at 18.3 km altitude derived from a Monte Carlo simulation of the $NO_y$ data (thick histogram line) and the measurement by the FSSP-300 (thin histogram line). The large particle mode within the size distribution shows the tenuous, young NAT rock particles, containing about 50 pptv $HNO_3$. The small particle mode is the ternary background aerosol distribution with a median diameter of 0.17 μm containing about 30 pptv $HNO_3$.**

### 6.3.6 Measurement on background aerosol layers

An interesting feature observed during several flights is the distinct layering with stepwise decrease of the particle backscatter ratio between 15 and 21 km, modulated by a pronounced mountain wave signature (Fig. 6.16 and Fig. 6.17).

In the warmer PSC free period, cross sections of background aerosol and ozone were measured up to more than 30 km altitude, mirroring the dynamical activity, particularly at levels below 500 K. Generally, the stratosphere during the campaign period was too disturbed to cool sufficiently long to allow for a detectable gradual formation of large NAT particles.

Several sections with background aerosol have been measured between northern Sweden and Spitsbergen which exhibit a considerable signature of dynamical processes and intruding mid-latitude air-masses inside the polar vortex. On 23 January a flight from Kiruna to Spitsbergen and back probed a large segment of the polar vortex marked by the purple rectangular in the upper panel of Fig. 6.25. The background aerosol inside the vortex reaches to only about 19 km (500 K) with clean upper stratospheric air aloft. The top of this layer continues across the vortex edge. Outside the vortex a high-reaching aerosol layer of non-depolarizing droplets, presumably volcanic sulfuric acid, appears above 22 km and reaches to 32 km with infrared backscatter ratios near 1.5. The spectral dependence indicates particles radii near 60 nm, trajectories originate from sub-tropical latitudes.

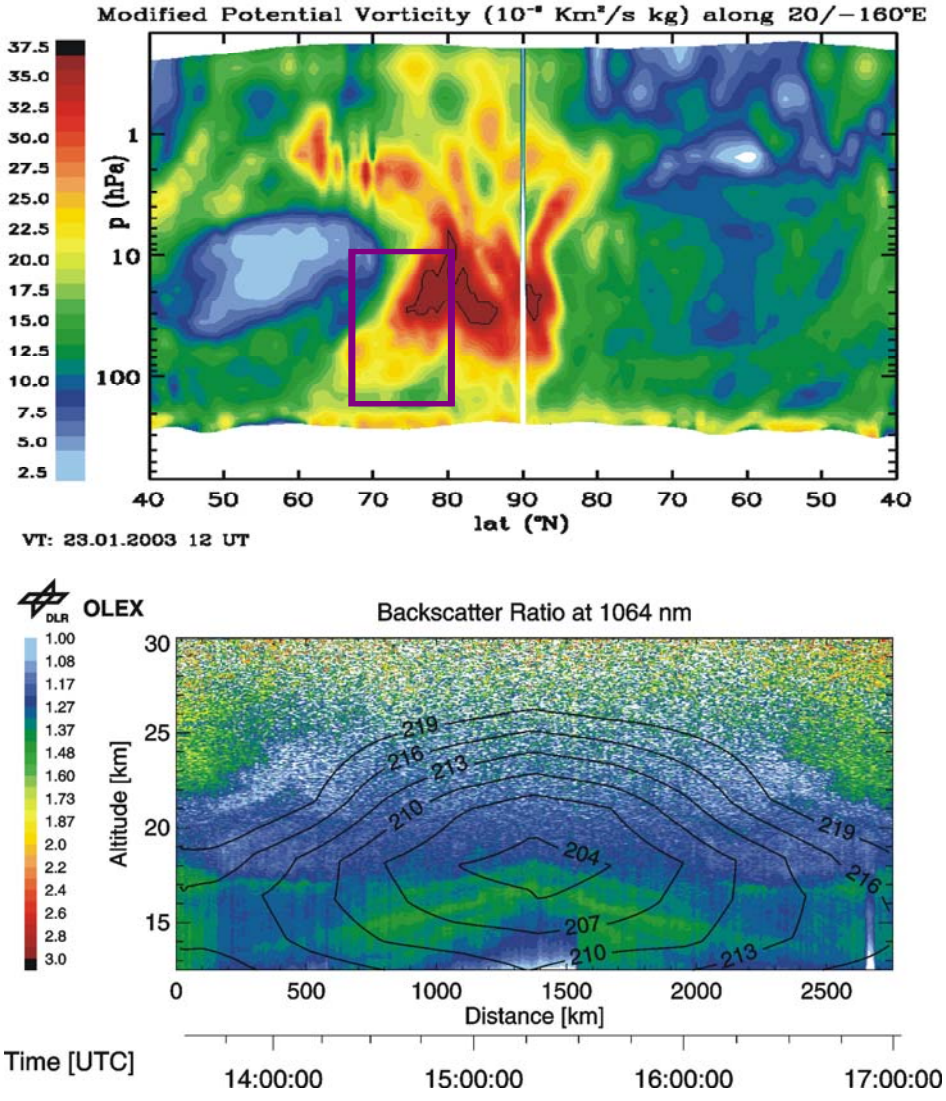


**Fig. 6.25 Upper panel: Vertical section of modified PV across the polar vortex along the 20°E/160°W meridian. Lower panel: Cross section of backscatter ratio at 1064 nm from Kiruna to Spitsbergen and back on 23 Jan 2003. Black lines indicate temperature from ECMWF.**

### 6.3.7 Socio-economic relevance and policy implication

The improved understanding of the formation of liquid and NAT PSCs increases the reliabilities about future development of ozone and other trace gas species in the polar stratosphere. The transport processes from lower latitude to Polar Regions have an effect on the dynamics of the atmosphere and thus on the climate.

### 6.3.8 Discussion and conclusion

STS clouds were detected by different instrument and model studies consistently. The formation of NAT particles at temperatures (1-3 K) below $T_{NAT}$ with a higher nucleation rate would affect the denitrification potential of the NAT particles and affect the ozone depletion potential of chlorine and bromine species. The active transport of air masses (in particular aerosols) may occur over large distances from the subtropics to Polar Regions.

## 6.4 WP4: Halogen Chemistry and ozone loss rates

### 6.4.1 Objectives

The objectives of WP 4 of the EuPLEx project were: Derive the rate of change of the chemical composition in individual air-masses; in particular the rate of chemical ozone loss for a well characterised chemical environment. Test in how far the stratospheric halogen chemistry is quantitatively understood.

### 6.4.2 Methodology and scientific achivements

The activities of WP 4 in the EuPLEx project have focussed on exploiting the data obtained in the project for deducing ozone loss and, in particular, for conducting model simulations with the objective to gain a deeper insight into the underlying chemical and physical mechanisms of polar ozone loss. The success of the WP 4 activities becomes particularly evident in the fact that by now several papers including WP 4 results have been published in ACPD within the special issue in Atmos. Chem. Phys. on the EuPLEx project.

*The Lagrangian model CLaMS as a tool for flight planning*

The Lagrangian model CLaMS is a chemical transport model that is normally driven by meteorological analyses such as they are available from ECMWF or UKMO. However, it is of course also possible to use the model in a mode where it is driven by *forecasted* rather than by observed winds. For the EuPLEx campaign, the model was run in this mode during the campaingn and high resolution forecasts of chemical and potential vorticity fields were provided in real time during the campaign so that they could be used for flight planning.

*Three-dimesional CLaMS simulation of the winter 2002/03*

Within the EuPLEx project, a module for the 3-d version of CLaMS was developed that simulates sedimentation of NAT particles and the corresponding redistribution of total inorganic nitrogen (NOy) in a Lagrangian way. The mechanism is described in the section of WP5 of this report and details of the CLaMS sedimentation module are published elsewhere (Grooß et al., 2004).

This enhanced , three-dimensional version of CLaMS has been employed for a simulation of the Arctic vortex in winter 2002/2003 has been conducted. The results of these simulations will be discussed below.

*Ozone loss*

For the CLaMS simulation for the winter 2002/2003, chemical ozone depletion was investigated. The simulation was initialized using ozone mixing ratios derived from ENVISAT-MIPAS data on 17 November 2002. To verify that CLaMS is simulating ozone mixing ratios correctly the simulated ozone mixing ratios were compared to observations in March. One example is the comparison with the observations by FOX on the Geophysica that are displayed in Fig. 6.26. These observations were made during the EnviSat validation campaign between 28 February and 16 March. The average difference of the ozone mixing ratios (CLaMS-FOX) is very low –0.06 ppm ± 0.18 ppm (1 sigma). The remaining differences may be explained by small-scale structures below the resolution of CLaMS.

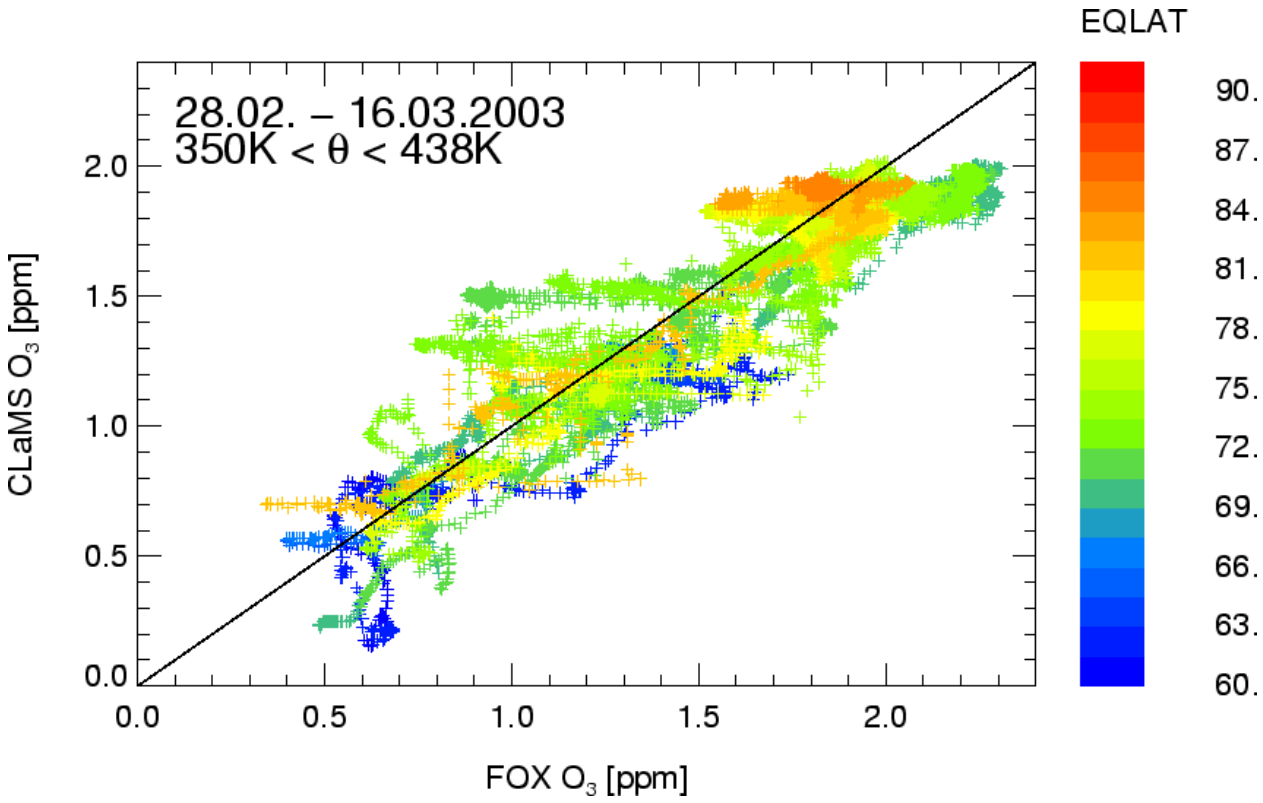


**Fig. 6.26 Comparison of ozone mixing ratios simulated by CLaMS and observed by FOX on Geophysica between 28 February and 16 March 2003. The colour of the symbols denotes the equivalent latitude of the observation location.**

Similar results have been obtained by comparisons with MIPAS-EnviSat and ozone sonde observations. This indicates that all significant ozone loss processes in the vortex have been covered by the simulation.

Similar as for the denitrification, the chemical ozone depletion was determined by taking the difference between model ozone and a passive ozone tracer that was initialized on 17 December identically as ozone and that is advected and mixed without chemical change. The simulated ozone depletion averaged over the vortex as defined by Nash et al. (1996) as function of time and potential temperature is shown in Fig. 6.27. The simulations indicate that vortex average ozone depletion reaches about 1.1 ppm in mid-March around the 460K level. The simulated vortex average ozone column loss on 13 March between 380 K and 500 K was 46 Dobson units (21% of the partial ozone column), and between 350 K and 900 K it was 67 Dobson units (18%).

Further, the impact of denitrification on the simulated ozone depletion was investigated through an additional simulation in which the sedimentation scheme was deactivated. In general, the simulated ozone depletion is very similar to the reference simulation. The largest effect of the denitrification was found towards the end of the simulation in mid-March when the deactivation of active chlorine species is hindered by the denitrification. The maximum of the ozone depletion due to denitrification averaged over the vortex as defined by Nash et al. (1996) was determined to be 100 ppb at 460 K potential temperature corresponding to 10% of the ozone depletion of the reference simulation.

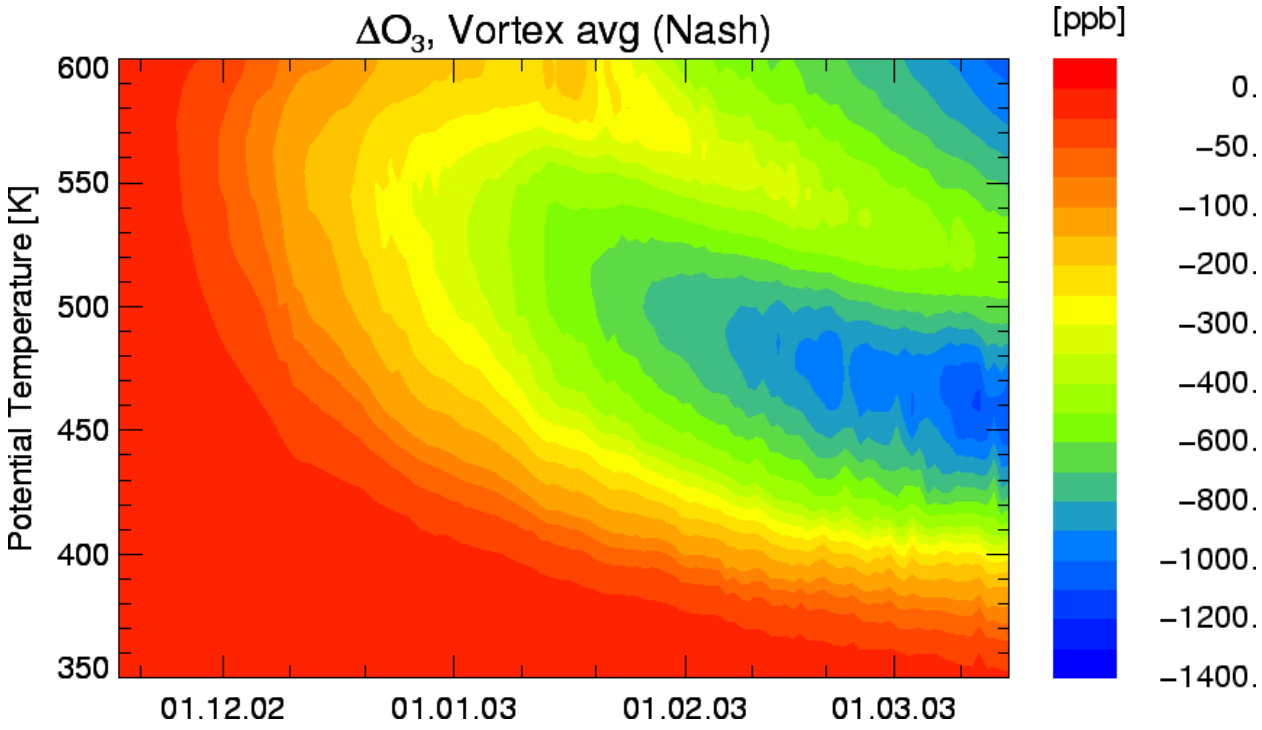


**Fig. 6.27 Simulated ozone loss as function of time and potential temperature. Shown is the vortex average using the vortex definition of Nash et al. (1996) for the period 17 November 2002 to 16 March 2003.**

### *Chlorine activation*

During the EUPLEX campaign, measurements of ClO, $Cl_2O_2$, and $ClONO_2$ were made by the HALOX experiment on board the Geophysica aircraft. We performed simulations with the Chemical Lagrangian Model of the Stratosphere (CLaMS) that aim to reproduce the observed chlorine compounds. Simulations for the observed airmasses on the flight track were done by running the chemistry code on 1-day back-trajectories from the exact flight path position initialized from the CLaMS output one day earlier. For the flights on February 6 and February 9, the simulations indicate significant chlorine activation within the last day before the observation. We investigated the simulated chlorine activation under different assumptions for the underlying PSC microphysics and heterogeneous chemistry (STS/NAT, dependence on particle number density) and compare the results with the HALOX observations. The observations and simulations agree within their uncertainties.

An update of these simulations initializing the considered air masses from the CLaMS 3-d simulation showed similar results. However, it is clear from these simulations that the initial chlorine activation introduces a large uncertainty as the air masses are not directly observed prior to the chlorine activation.

*Study of the ClO/$Cl_2O_2$ Equilibrium .*

ClO and its dimer ($Cl_2O_2$) are the key species involved in the most important ozone destruction cycle in the cold polar winter stratosphere (Molina and Molina, 1987):

$$ClO + ClO + M \leftrightarrow Cl_2O_2 + M$$
$$Cl_2O_2 + h\nu \rightarrow Cl + ClOO$$
$$ClOO + M \rightarrow Cl + O_2 + M$$
$$2\,(Cl + O_3) \rightarrow 2\,(ClO + O_2)$$

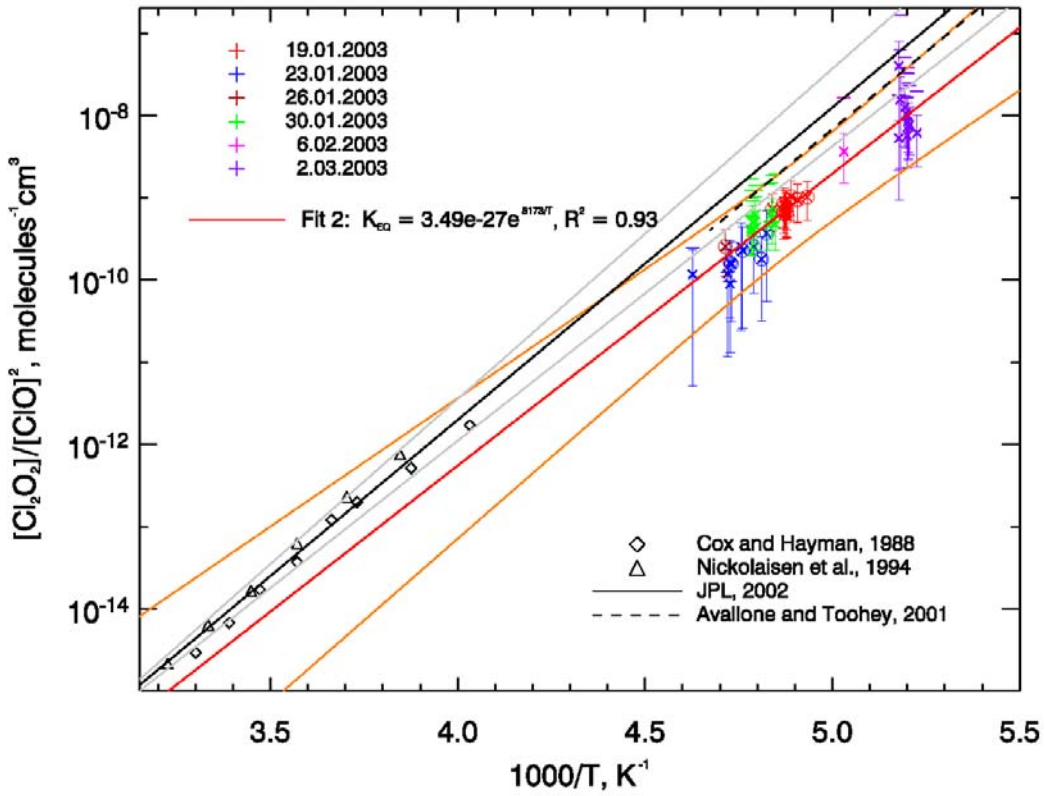


**Fig. 6.28 Van't Hoff plot of EUPLEX data for which thermal equilibrium can be assumed.**

During the SOLVE II/VINTERSOL-EUPLEX and ENVISAT Validation campaigns in the Arctic winter 2003, simultaneous in-situ measurements of ClO and its dimer were carried out with the HALOX instrument. These were only the second simultaneous $ClO/Cl_2O_2$ measurements (the first were made by Stimpfle et al., 2004).

The results suggest that the thermal equilibrium between the dimer formation and dissociation is shifted significantly towards the monomer compared to the current JPL 2002 recommendation (Sander et al., 2003) which extrapolates laboratory studies to stratospheric temperatures. Detailed analysis of observations made in darkness was used to re-evaluate the magnitude and temperature dependence of the equilibrium constant. A fit of the JPL format for equilibrium constants yields $K_{EQ} = 3.49 \times 10^{-27} \exp(8174/T)$, a factor of 4 to 8 smaller than JPL 2002 (Fig. 6.28).

Fig. 6.29 shows how changing $K_{EQ}$ from the JPL 2002 recommendation to the new value greatly increases predicted night-time ClO concentrations. However, calculations using the CLaMS model (McKenna et al., 2002) do not predict the adjustment of the equilibrium constant to have a large impact on simulated ozone loss. Solely at large zenith angles after sunrise, a small decrease of the ozone loss rate due to the ClO dimer cycle and an increase due to the ClO-BrO cycle (attributed to the enhanced equilibrium ClO concentrations) is observed, the net effect being a slightly stronger ozone loss rate.

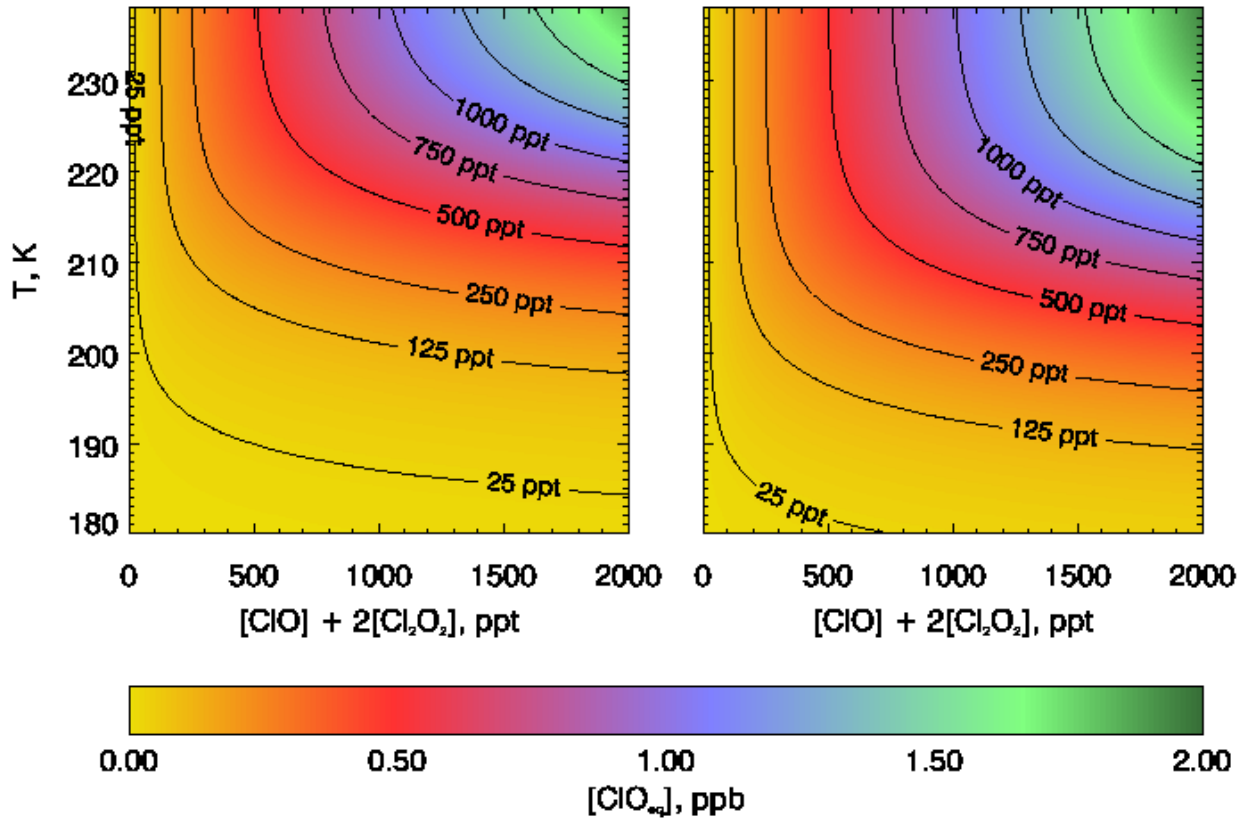


**Fig. 6.29 Equilibrium ClO concentration as a function of temperature and $ClO_X$ for the JPL 2002 equilibrium constant (left panel) and the equilibrium constant inferred from fit 2 in this study (right panel).**

*Evaluation of the Geophysica self-match flight of January 30, 2003.*

During the "self-match flight" on Jan 30 2003 the Geophysica measured the same air parcels first in sunlight (SZA < 87deg) and then in darkness (SZA > 95deg).

The flight trace is shown in white in Fig. 6.30. Flight path 1-> 2 is matched again between 4->5 with a time distance of about 2 h; 2->3 is matched again between 3-> 4 with time distances between some minutes and 1 h.

We started trajectories at 54 different points (between 1 and 3) when the air parcels were measured for the first time. From these points the trajectories are calculated 24h backwards to and 3h forwards (which includes the second measurement). The match radius (distance between the predicted and the real position) is between 0 and 20 km for most of the pairs. The offset in potential temperature is generally in the range +/-2 K.

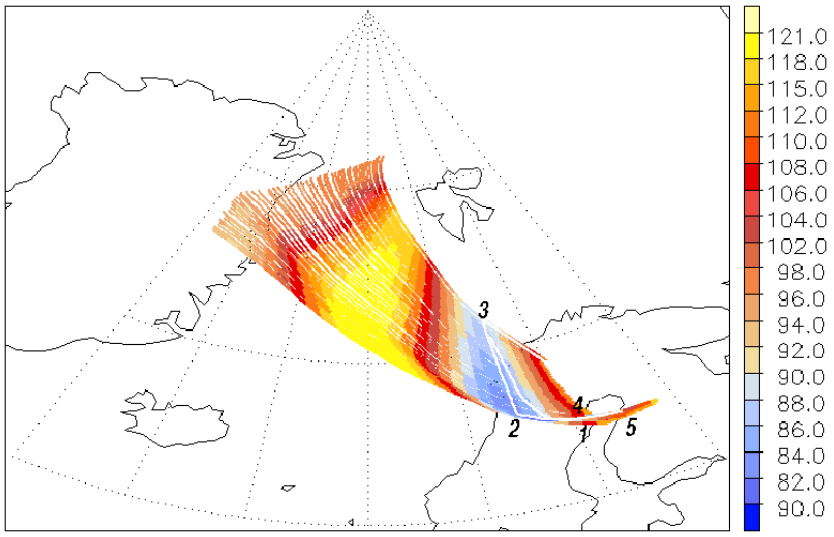


**Fig. 6.30 Path of the M55 aircraft for the MATCH flight on 30 Jan 2003 (white): 1 -> 2 -> 3 -> 4 -> 5. The colors indicate the Solar Zenith Angle for the trajectories started at 54 points between 1 and 3 and calculated 24h backwards and 3h forwards.**

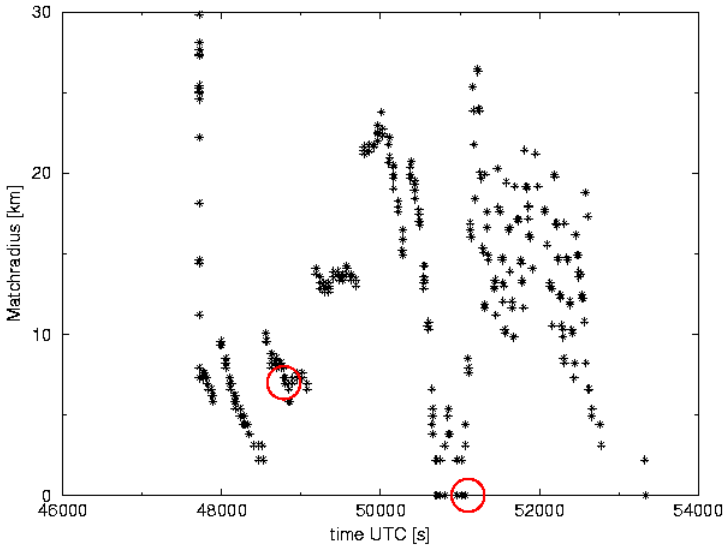


**Fig. 6.31 Distance between the location of the remeasured air parcel and the calculated location for the aircraft MATCH flight on 30.01.2003. The red circles indicate the peaks recorded by the COPAS instrument.**

There are two periods of near zero match radii: at 48500UTC sec, which should be the same air parcel as at 46520sec, and the pair at 50900sec/44095sec. these two periods perfectly match two of the three peaks in COPAS' particle concentration (seen at 48500sec, 50900sec, 52200sec), which means that the contrail has probably been measured again. With the Mainz photochemical box model we calculates the temporal evolution of the most important chemical species in a ``box'' moving along a given trajectory. The model is initialised 24h before the first measurement to match the total ClOx.

ClO and $Cl_2O_2$ concentrations have been measured by the HalOx instrument of FZJ. These measured concentrations and their temporal evolution are compared with concentrations calculated with the Mainz photo-chemical box-model run along trajectories tracing the twice measured air parcels. The JPL equilibrium constant K for the partitioning of ClO and $Cl_2O_2$ will be referred to as $K_{jpl}$ and is

$K/ (cm^3 molecule^{-1}) = A \exp(B/T)$ for $[200K < T < 300K]$ with

$A/(cm^3 molecule^{-1}) = 1.27\ 10^{-27}$ and

$(B +/- \Delta B)/K = 8744 +/- 500.$

Fig. 6.32 shows the results from the model runs using different equilibrium constants (changing only B). Obviously, for this case the best value of $K_{eq}$ lies between K-ΔB and K-2ΔB. Fig. 6.33 shows the calculated ClO and $Cl_2O_2$ using $K_{eq}$ =1.27 10-27 exp(7900/T) =: $K_{euplex}$ Sensitivity studies have been performed and indicate that the impact of small inaccuracies in the position of the air parcels and thus the solar zenith angle do not lead to fundamental changes for the equilibrium constant.

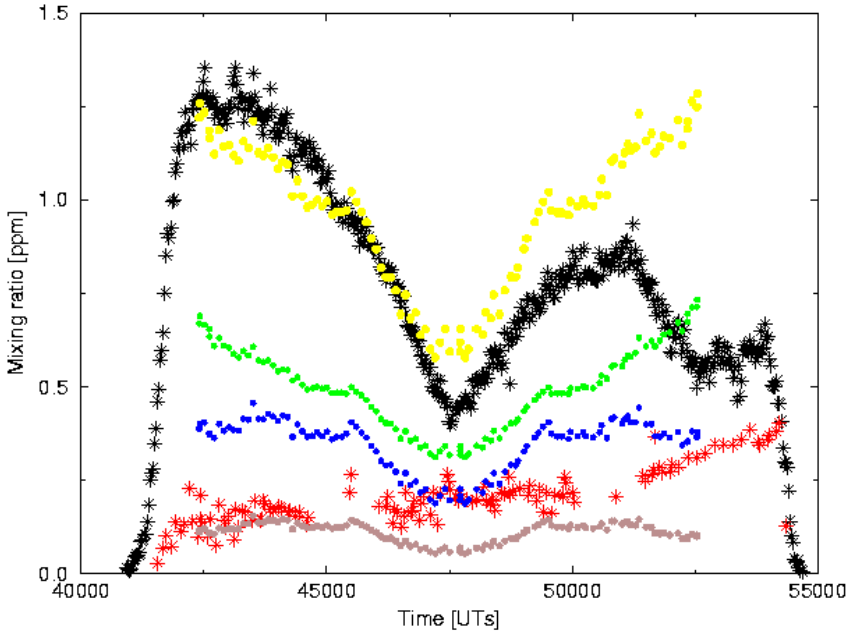


**Fig. 6.32 ClO (black) and $Cl_2O_2$ (red) concentrations along the flight path. Calculated values are for ClO green: - ΔB, yellow: -2ΔB and for $Cl_2O_2$ blue: -ΔB, brown: -2ΔB.**

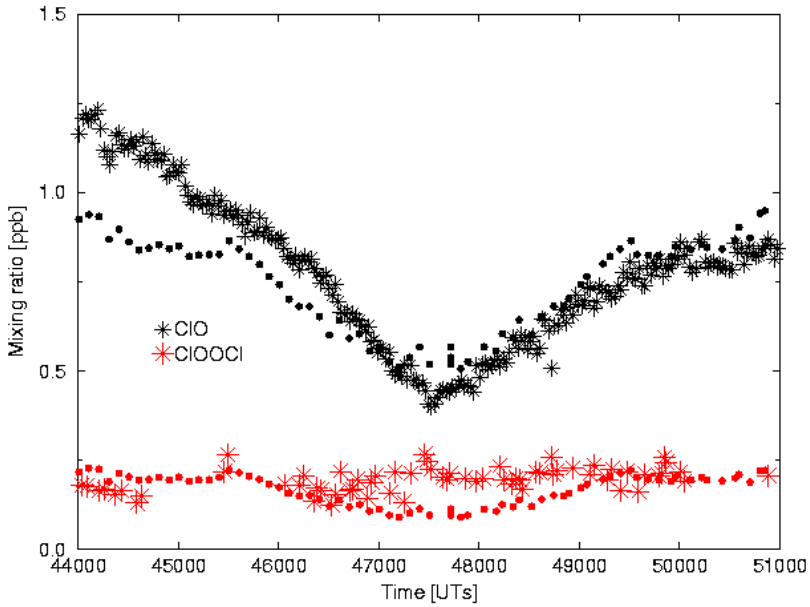


**Fig. 6.33 Calculated (dotted) and measured (stars) concentrations for ClO (black) and $Cl_2O_2$ (red) with $K_{euplex} = 1.27\ 10^{-27}\ exp(7900/T)$.**

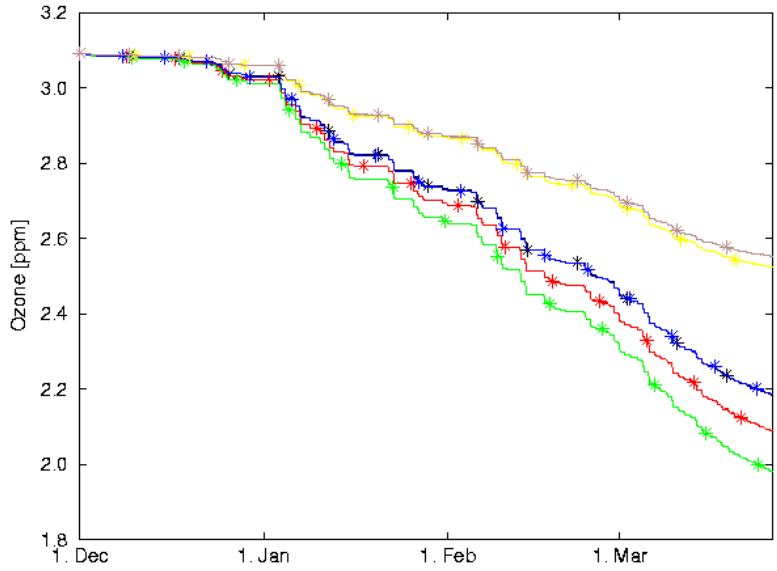


**Fig. 6.34 Plotted along a trajectory starting on 1 Dec 1999 on 590K: a) $K_{jpl}$ equilibrium constant and "old" BrO concentrations (black). b) $K_{euplex}$ and "old" BrO concentrations (blue). c) $K_{jpl}$ equilibrium constant and "new" BrO concentrations (red). d) $K_{euplex}$ and "new" BrO concentrations (green). e) $K_{jpl}$ equilibrium constant without any bromine (yellow). f) $K_{euplex}$ equilibrium constant without any bromine (brown)**

The impact of this new equilibrium constant on ozone seems unimportant on first sight. An example trajectory (see Fig. 6.34) started on 590K on 1 Dec 1999 and calculated onwards until end of March 2000 shows hardly any differences in ozone depletion for the "old" ($K_{jpl}$ and the "new" ($K_{euplex}$) equilibrium constant (black and blue stars in Fig. 6.34), which is 30% for this case.

This changes when higher amounts of BrO ($10 \cdot 10^{-12}$) (Pundt et al., 2002) are assumed. Ozone depletion is 33% during the winter assuming this higher amount of BrO and $K_{jpl}$(red line in Fig.

6.34), but further increases to 36% (green line in Fig. 6.34) using the "new" equilibrium constant $K_{euplex}$.

In summary, the Match radii and the correlation between nearly zero match radius and peaks in COPAS allow a comparison between the twice measured air parcels. Box-model calculations suggest that the actual JPL equilibrium constant for the partitioning of ClO and its dimer is shifted towards the monomer with $K_{Euplex}=1.27\ 10^{-27}\ \exp(7900/T)$.

*Observation of Enhanced ClO Mixing Ratios in the Arctic Polar UTLS.*

During the VINTERSOL-EUPLEX campaign in late winter/early spring 2002/2003 enhancements of ClO mixing ratios in the altitude regime below 14km were observed in-situ by the HALOX instrument onboard the high-flying research aircraft M55-Geophysica flying out of Kiruna, Sweden. Elaborate data analysis for the respective flight segments taking into account effects of higher air density and humidity as compared to the stratospheric environment are still in progress but preliminary data with an accuracy of around 40% are available.

Mostly these enhancements were observed as shallow layers during ascent and descent of the aircraft. Fig. shows one out of three pronounced examples where the enhancement was detected on ascent as well as on descent slightly above the thermal tropopause. On 11. Feb. 2003 when flying level at around 10km slightly below the tropopause within a cirrus cloud enhanced ClO was observed correlated with the appearance of cirrus particles as shown in Fig.. . First studies in order to identify the origin of the ClO enhancements by means of airmass back trajectories are underways. A forthcoming publication of these results (Stroh et al.) is envisaged for the end of 2005.

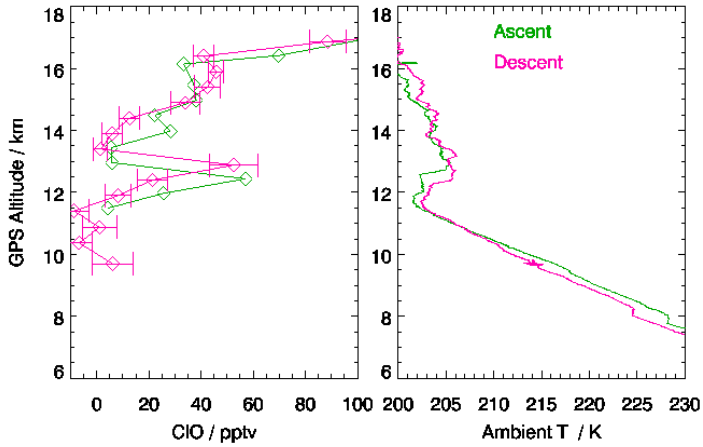


**Fig. 6.35 Profiles of ClO (left panel) and temperature (right panel) as observed by the HALOX instrument on the flight on 28. Feb. 2003. Note the clear enhancements peaking at about 12.5km altitude. Error bars on the ClO data represent 1 sigma standard deviation of the averaged data points (500m averaging intervals). The accuracy of the preliminary data is around 40%.**

*Measurements of Ozone, Chlorine and Nitorgen Compunds by the ASUR SubMM Radiometer*

The Airborne SUbmillimeter Radiometer ASUR on board the FALCON aircraft took numerous measurements of HCl, ClO, $O_3$, $HNO_3$, and $N_2O$ inside the Arctic vortex and in its edge region. The quality of the measured spectra is reasonable. Data analysis were performed and vertical profiles of volume mixing ratio of the aforementioned species were submitted to the NILU data server.

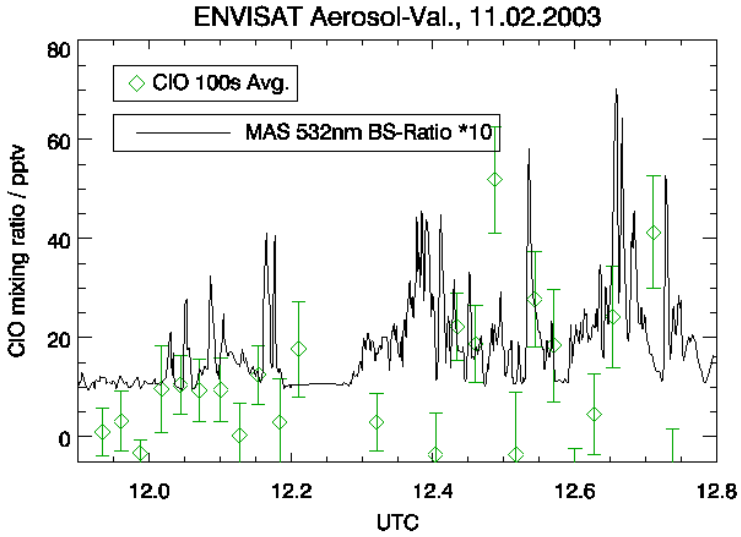


**Fig. 6.36 ClO time series (green trace) observed on a level flight segment at around 10km altitude. The black trace is aerosol backscatter ratio observed by the CNR-IFA backscatter sonde MAS indicating the presence of cirrus particles. Note the slight enhancements in ClO correlated with the detection of cirrus particles. Error bars on the ClO data points denote standard deviation (1 sigma) of the 100s time average.**

Analyses of ASUR $N_2O$ measurements in mid-January 2003 reveal comparable values to January 2000 inside the Arctic vortex, indicating that significant diabatic descent the of airmasses had taken place. An interesting observation was made on 23 and 26 January 2003 in the meteorological situation of a major stratospheric warming, where unusually high values of $N_2O$ and ozone were measured in the Arctic. Maximum values of ~190 ppb $N_2O$ and ~10 ppm ozone were observed at middle stratospheric altitudes. ASUR observations during the SCIAMACHY validation campaign early March 2003 in the tropics suggest that the observed Arctic airmasses were transported from the tropics to the Arctic by rapid meridional transport on a time scale of days (Kleinboehl el al., 2004).

ASUR $HNO_3$ measurements in mid-January 2003 showed maximum mixing ratios of typically ~9.9 ppb inside the vortex in the lower stratosphere. These values were generally higher than observed in January 2000. However, the retrieved peak altitudes of 16-18 km (rather than ~20 km as expected from the descent of airmasses) suggest some denitrification in the Arctic vortex. This is supported by comparisons with modeled $HNO_3$ from the SLIMCAT model, which reproduced the overall $HNO_3$ mixing ratios measured by ASUR in mid-January reasonably well (Kleinboehl et al., 2003).

ASUR observations of HCl and ClO show that chlorine activation had taken place in the Arctic vortex in January 2003. However, comparisons with HCl measurements in January 2000 indicate higher values of HCl in the lower stratosphere in January 2003, so chlorine activation did not seem to be as intense as in January 2000.

*Model calculations of the Match trajectory set for 2002/03.*

The planned aircraft Match could not be conducted in the Geophysica campaingn because of the meteorological conditions. However, data from the classic ozone sonde Match are available. Model simulations have been carried out using the CLaMS model in the boxmodel mode and can be compared to the Match results. Initialisation was obtained from the SLIMCAT model and the exately the same trajectories used in the model that were emplyed in the Match analysis. The results of the model comparison are shown in Fig. 6.37. The results corroborate earlier findings that a problem exits in the simulation of cold January ozone loss rates.

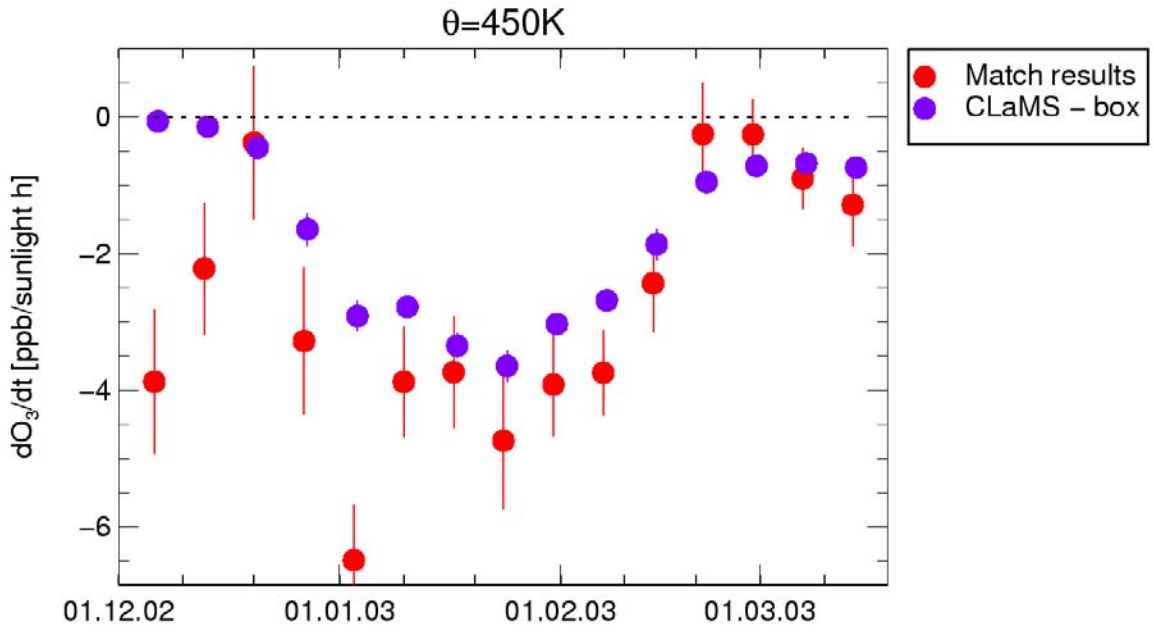


**Fig. 6.37 MATCH Comparison of simulated (purple symbols) and measured (red symbols) ozone loss rates in winter 2002/03. Shown are results for the 450 K isentropic level. The ozone loss rate is expressed in ozone loss per sunlight hour.**

The combination of in-situ observations of ClOx species at low temperatures during SOLVE with observations under relatively warm conditions during EUPLEX provided a perfect observational basis for constraining reaction kinetics of the ClO/ $Cl_2O_2$ system. The in-situ observations suggest that both, the thermal decomposition of the $Cl_2O_2$ molecule and its photolysis appears to be faster than current recommendations in JPL2002.
We have analysed the impact of these changes in reaction kinetics on polar ozone chemistry. The effects of changes in reaction kinetics depend very sensitively and in a non-linear way on the precise meteorological conditions and the solar zenith angle history of the air masses. Therefore, analysing the changes in ozone loss rates for "typical" conditions can be misleading. On the other hand, running a full box model for a large set of real air mass trajectories that realistically reflects the range of conditions inside the polar vortex is numerically expensive and not a good option when many runs are required to test the sensitivity of the reaction system on changes in kinetics. We have used a simplified box model that is based on ClOx, BrOx,and Ox chemistry and that does not attempt to calculate the balance between Cly and ClOx. By specifying ClOx the isolated effect of changes in reaction constants and photolysis cross sections in the ClOx system on ozone loss rates can be studied. The simplified model has been run along all Match trajectories from all winters in the Match data set and the impact of changes in kinetics on calculated ozone loss rates have been studied. While increasing the photolysis rate of $Cl_2O_2$ will always lead to faster ozone loss, particularly during twilight conditions, the effect of increasing the thermal decomposition rate turns out to be more complex. While increasing this rate always reduces ozone loss by the ClO+ClO cycle, it tends to increase ClO concentrations during twilight, which makes the ClO+BrO cycle more efficient. Hence, the net effect of this change depends on the amount of BrOx in the model. For standard levels of BrOx in the model the slow down of ozone loss by the ClO+ClO cycle has pretty much balanced by faster ozone loss due to the ClO+BrO cycle.

But recent balloon-borne observations of BrO suggest that larger levels of BrOx are present in the stratosphere than previously thought. Also, our knowledge about BrOx levels in the stratosphere is completely based on BrO measurements that are combined with photochemical calculation to derive the levels of BrOx that are consistent with the observations of BrO. Recently suggested changes in the reaction kinetics of BrOx species (substantially larger branching ratio of BrO+ClO into BrCl; Canthy et al., submitted) further increase the level of BrOx that would be derived from any observation of BrO. For these higher levels of BrOx the net effect of increasing the thermal decomposition rate is to increase ozone loss rates. This increase in ozone loss rates is particularly effective at high solar zenith angles, when ClO concentrations are relatively small and ClO+BrO is the more effective ozone loss cycle compared to ClO+ClO.

*Ozone loss deduced from the vortex average method*

Results are available for the vortex average ozone loss estimate. A total ozone depletion of 68 Dobson units from 10 December 2002 to 10 March 2003 is derived by the vortex-average method taking into account both diabatic descent of the air masses and transport of air into the vortex. When the vortex is divided into three equal-area regions, the results are 85 DU for the collar region (closest to the edge), 52 DU for the vortex centre and 68 DU for the middle region in between centre and collar.

*Ozone loss estimates from the OLEX Lidar measurements*

Airborne lidar (OLEX) observations from EUPLEX have been investigated with respect to ozone depletion, its temporal development and distribution inside the Arctic vortex. Owing to strong activation of the vortex air by widespread PSCs in December 2002 considerable $O_3$-depletion was observed in late January 2003, inhomogeneously distributed over the vortex:

While the vortex boundary air masses experienced sunlight due to repeated troughing towards illuminated middle latitudes during the strong minor warming in late December, the vortex core remained centred over polar regions and dark till mid-February. Vortex stirring occurred due to a temporary split and incorporation of vortex edge air into the vortex core during re-merging. Correspondingly, around 475 K by 0.5 – 0.7 ppm ($\Delta\ O_3 \approx 15\%$) reduced $O_3$ values were found in several occasions directly neighboured to chemically nearly undisturbed air masses. The amount of $O_3$-depletion and the location was in most cases reproduced by the CLaMS chemical transport model. Strong stirring and more frequent vortex elongation towards illuminated latitudes included ever larger fractions of the vortex in $O_3$ destruction from mid-February onward, resulting in a widespread homogeneous ozone loss of 0.7 - 0.8 ppm ($\Delta\ O_3 \approx 20\%$) between 17 to 23 km altitude in mid-March (observed during a SCIAMACHY validation flight).

The skill of the CLaMS model to simulate realistic ozone loss rates is demonstrated by the comparison with ozone values measured by the OLEX lidar, e.g on 23 January 2003 (Fig. 6.38). The deviation in mixing ratio between both data sets, even in the complex vortex boundary region mostly stays below few 100 ppb. Similarly good agreement has also been observed in other cases with larger scales and off strong dynamical activity.

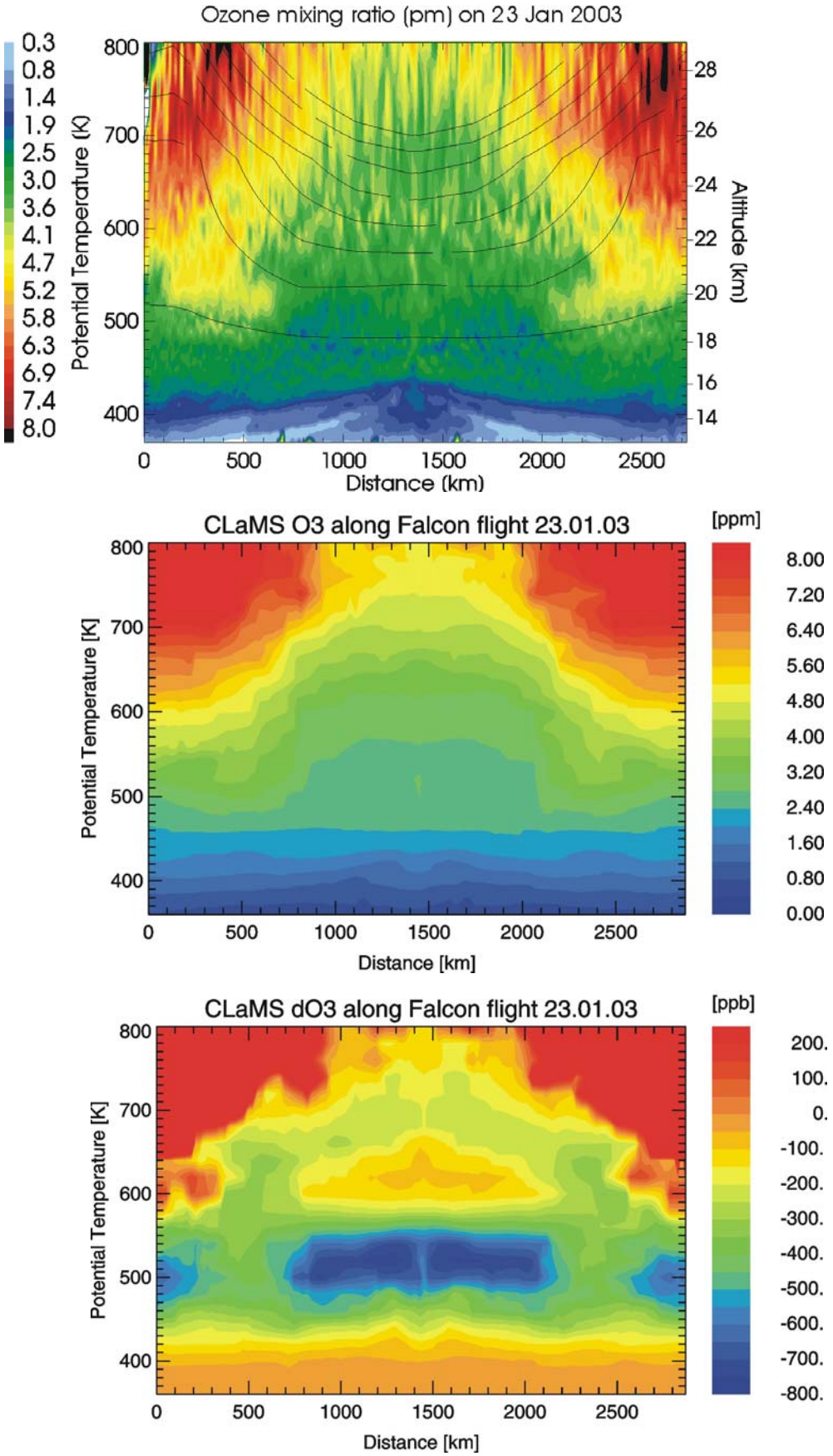


**Fig. 6.38 Sections of Ozone and ozone loss from Kiruna to Spitsbergen and back for 23.01.2003. Upper panel: OLEX with PV contours, middle: CLaMS-$O_3$, lower: CLaMS ozone loss ($dO_3$).**

**References**

Brune, W. H., Anderson, J. G., and Chan, K. R.: Insitu Observations of ClO in the Antarctic - Er-2 Aircraft Results From 54-Degrees-S to 72-Degrees-S Latitude, J. Geophys. Res.-A., 94 (D14), 16649-16663, 1989.

Kleinboehl, A., J. Kuttippurath, M. Sinnhuber, B.-M. Sinnhuber, H. Kuellmann, K. Kuenzi, J. Notholt, Rapid meridional transport of tropical airmasses to the Arctic during the major stratospheric warming in January 2003, Atmos. Chem. Phys. Discuss., 4, 7121-7138, 2004.

Kleinboehl, A., J. Kuttippurath, M. von Koenig, H. Kuellmann, J. Notholt, and K. Kuenzi, Results of stratospheric trace gas measurements by ASUR in Arctic winter and spring 2002/03, Paper presented at the SOLVE II / VINTERSOL Joint Science Team meeting , Orlando, FL, 21-24 October 2003.

McKenna, D. S., Grooß, J. U., Günther, G., Konopka, P., Müller, R., Carver, G., and Sasano, Y.: A new Chemical Lagrangian Model of the Stratosphere (CLaMS) - 2. Formulation of chemistry scheme and initialization, J. Geophys. Res., 107, doi: 10.1029/2000JD000113, 2002.

Molina, L. T., and Molina, M. J.: Production of $Cl_2O_2$ From the Self-Reaction of the ClO Radical, J. Phys. Chem., 91 (2), 433-436, 1987.

Pundt, I., J.-P. Pommereau, M. P. Chipperfield, M. Van Roozendael, and F. Goutail, Climatology of the stratospheric BrO vertical distribution by balloon-borne UV–visible spectrometry, J. Geophys. Res., 107(D24), 4806, doi:10.1029/2002JD002230, 2002.

Sander, S. P., Friedl, R. R., Golden, M. M., Kurylo, M. J., Huie, R. E., Orkin, V. L., Moortgat, G. K., Ravishankara, A. R., Kolb, C. E., Molina, M. J., and Finlayson-Pitts, B. J.: Chemical Kinetics and Photochemical Data for Use in Atmospheric Studies, in Evaluation Number 14, Jet Propulsion Laboratory, Pasadena, 2003.

Stimpfle, R. M., Wilmouth, D. M., Salawitch, R. J., and Anderson, J. G.: First measurements of ClOOCl in the stratosphere: The coupling of ClOOCl and ClO in the Arctic polar vortex, J. Geophys. Res., 109, doi: 10.1029/2003JD003811, 2004.

## 6.5 WP5: Impact of transport on trace gas budgets

### 6.5.1 Objectives

The general objectives of this WP5 are:

1. To assess the effect of transport on the development of the constituent distributions, particularly of ozone and reactive nitrogen, and water vapour.
2. To quantify cumulative chemical ozone loss, denitrification and dehydration from simultaneous aircraft observations (to be used as input to WP1).
3. To determine the total amount of inorganic chlorine, bromine, and available nitrogen along the flight track (to be used as input to WP4)
4. To examine mixing between vortex and extra-vortex air and its effect on tracer relationships.
5.

### 6.5.2 Applied methodology, scientific achievements and main deliverables

The methodologies and scientific achievements are described in the following according to the main deliverables defined in the description of work:

*D5.1 Initial relations for Cly:$N_2O$, Bry:CFC-11 valid for the time of the mission*

Relations for $Cl_y$:$N_2O$ and $Br_y$:F11 valid for the time of the mission were established from airborne ER-2 and balloon measurements (J. Elkins and the ACATS and LACE teams at NOAA/CMDL) and made available to the EUPLEX team. Since the calibration of the HAGAR (JWG-IMG) instrument is based on a standard originating from NOAA/CMDL these relations can be directly applied to the EUPLEX measurements to derive $Cl_y$ and $Br_y$ from $N_2O$ and F11 measurements by HAGAR. Fig. 6.39 shows the established $Cl_y$:$N_2O$ relation which is expected to be universal in the extratropical lower stratosphere and thus valid along the Geophysica flight tracks during EUPLEX.

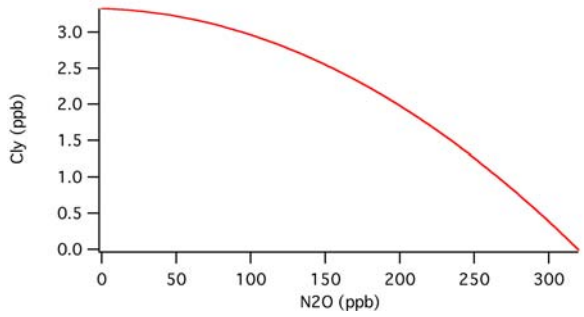


**Fig. 6.39 $Cl_y$:$N_2O$ relation established from ER-2 and balloon measurements and valid for EUPLEX.**

*D5.2 Initial relations for $O_3$:$N_2O$, $O_3$:$CH_4$ and $NO_y$:$N_2O$ in the early vortex*

Initial relations for $O_3$:$N_2O$, $O_3$:$CH_4$ in the early vortex were derived from a balloon flight of the MkIV instrument on December 16, 2002 conducted in the frame of the NASA SOLVE II mission. PV analysis show that all the measurements were indeed inside the vortex, even though the flight path was close to the vortex edge.

An initial NOy:N2O relation could not be derived from the MkIV observations on December 16, 2002, since at that time, denitrification already had occurred. Therefore the relation was established from MkIV observations in December 1999 (NASA SOLVE campaign) that were published by Popp et al. (2001):

$$NOy^* = 17.3 - 0.0222*N_2O - 9.85*10^{-5}*N_2O^2, \quad \text{for } N_2O \text{ and NOy in ppb, } N_2O > 33 \text{ ppb.}$$

The relation was extended to higher altitudes ($N_2O$ mixing ratios below 33 ppb) using the same data set:

$NOy^* = 11.7 + 4.49 \ln(N_2O) - 0.948(\ln(N_2O))^2$, $N_2O$ and NOy in ppb, 1 ppb<$N_2O$<33 ppb.

The validity of this initial relation was verified from NOy and $N_2O$ observations by the SIOUX (DLR) and HAGAR (JWG-IMG) instruments during the Geophysica flight of January 15, 2003 outside the polar vortex. Fig. 6.40 shows the excellent agreement between the observed $NO_y$-$N_2O$ correlation during this flight (at equivalent latitudes < 63°N) and the $NOy^*$-$N_2O$ correlation, whereby $NOy^*$ was calculated from HAGAR $N_20$ using the equations given above. CLaMS calculations of a vortex tracer confirm that these data were sampled well outside the vortex. The above equations derived from observations during the SOLVE campaign can thus indeed be used to infer denitrification and renitrification from the SIOUX and HAGAR data.

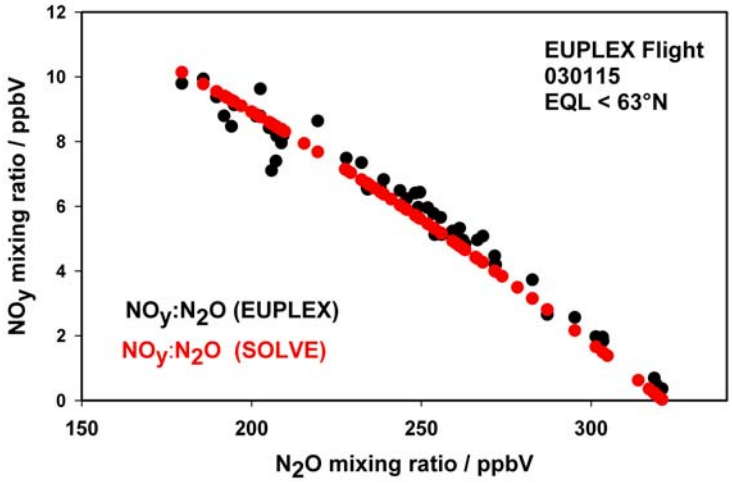


**Fig. 6.40 NOy:$N_2O$ relation established from SIOUX and HAGAR data from the Geophysica flight on January 15, 2003 (black dots) and during the SOLVE campaign from MkIV balloon data (red dots).**

### *D5.3 Total inorganic chlorine and bromine along the Geophysica flight track*

Total inorganic chlorine and bromine along the Geophysica flight track was calculated from HAGAR $N_2O$ and F11 using the relations of $Cl_y$:$N_2O$ and $Br_y$:F11 established above.

### *D5.4 Estimates of integrated ozone loss, denitrification and dehydration*

**Integrated ozone loss**

Chemical ozone destruction and chlorine activation in the lower stratosphere during the Arctic winter 2002/03 was investigated using the tracer-tracer correlation technique using satellite (FZJ) and in situ (Geophysica) observations (JWG-IMG).

The analysis of satellite observations was based mainly on HALOE/UARS data. Consistent with the very low temperatures observed in the Arctic early vortex in December and early January, strong chlorine activation at 520 K potential temperature is noticeable already in mid-December 2002 in balloon-borne observations of the MkIV instrument and in January 2003 at 400-500 K in HALOE observations. Relatively large column ozone loss in the potential temperature range 380-550 K was derived inside the outer vortex in January (23+/-9 DU) and February (26+/-9 DU). Substantially greater losses in February inside the vortex core (51+/-9 DU). Early ozone loss of this extent is a particular feature of the Arctic winter of the EuPLEx campaign. Calculated ozone loss profiles and ozone mixing ratios are very similar in February in the two completely separated parts of the vortex. A small influence of mixing processes was found after the reunification of these vortex parts on February 23-25, 2003, mainly inside the outer vortex. Some ozone

loss possibly occurred in the lower stratosphere below 400 K during late March and April consistent with Polar Stratospheric Clouds detected by MIPAS-ENVISAT towards the end of March. A detailed description of this investigation is published by Tilmes et al. (2003).

Tracer correlation studies were also performed using the $O_3$:$N_2O$ and $O_3$:$CH_4$ relations from ENVISAT-MIPAS data (retrieval from IMK-FZ Karlsruhe/Univ. Karlsruhe). Fig. 6.41 shows the preliminary evaluation for the tracer relation technique for 18 February 2003. It shows about 0.5 ppm ozone depletion for $N_2O$ mixing ratios between 100 and 200 ppb. These results are still preliminary.

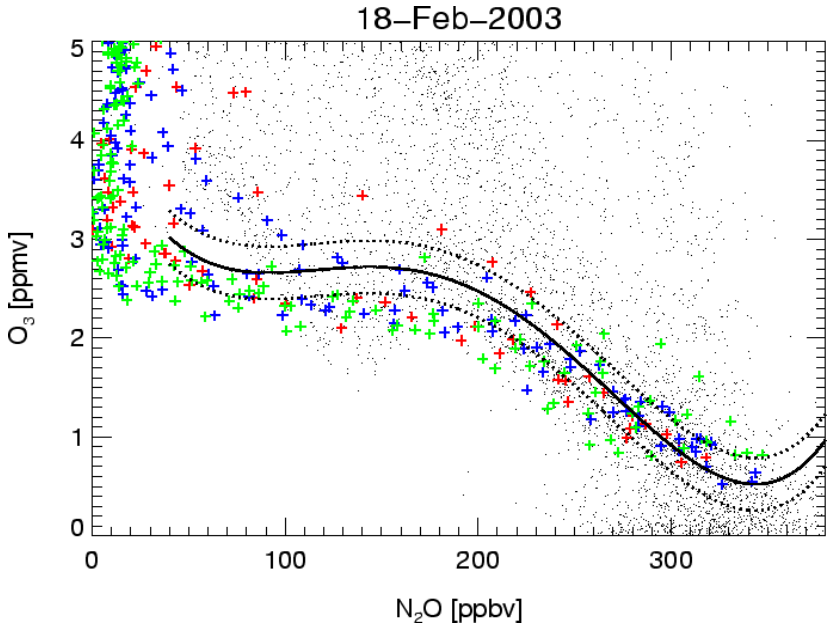


**Fig. 6.41 $O_3$:$N_2O$ relation derived from MIPAS-ENVISAT data. The solid black line indicates the early winter reference relation derived from MIPAS data on 16 November 2002, the dashed lines correspond to a 1-sigma deviation. Different colors denote different parts of the vortex, green crosses: inside the vortex core; blue crosses: outer vortex; red crosses: inside the outer boundary region of the vortex according to the definitions of Nash et al. (1996). Black dots indicate observations outside the polar vortex.**

The tracer-correlation analysis of ozone loss based on Geophysica in situ observations (JWG-IMG) includes ozone measurements of FOZAN (CAO and CNR-ISAC) and FOX (DLR), and $N_2O$ and $CO_2$ measurements of HAGAR (JWG-IMG) obtained during EuPLEx and ENVISAT Arctic chemistry validation between January 15 and March 16, 2003. The agreement between FOX and FOZAN was found to be within about 25%, with FOZAN typically showing higher values (at flight altitude) than FOX. The reasons for the disagreement are still under investigation. In addition to the $O_3$-$N_2O$ correlation, the evolution of the $O_3$-$CO_2$ correlation was analysed, which gives the advantage of a larger data set (as $CO_2$ was measured by HAGAR about 10 times more frequently than $N_2O$). An $O_3$-$N_2O$ reference correlation before substantial ozone loss occurred was inferred from the Mark-IV balloon measurements as described above (cf. D5.2). An $O_3$-$CO_2$ reference was similarly derived from Mark-IV ozone and $N_2O$ data using the $CO_2$-$N_2O$ correlation measured by HAGAR inside the vortex during EUPLEX.

As the majority of the flights encountered not only vortex-air, but also air located or recently mixed from outside the vortex (exhibiting a different $O_3$-tracer reference correlation), an essential first step of this analysis was to find the best criterion for identifying and selecting pure (undiluted) vortex air. Such a criterion was derived directly from the observed $N_2O$ and $CO_2$ vertical distributions whose lowest values (at a given potential temperature) were used to define pure vortex profiles for $N_2O$ and $CO_2$ for each campaign phase. An empirical fraction of vortex air was then defined by assuming positive deviations from these pure vortex profiles to be due to

mixing with extra-vortex air (cf. also D5.5 below). Only data with an empirical vortex fraction larger than 90% were incuded in the analysis of ozone loss. Application of this filtering criterion to the correlation of a passive ozone tracer and $N_2O$ simulated by the CLaMS model confirms that indeed all data follow the reference $O_3$-$N_2O$ correlation from January to March without any changes due to mixing, such that any changes in the observed $O_3$-$N_2O$ correlation from the reference must be due to chemical loss.

Cumulative ozone loss was finally derived from the $O_3$-$N_2O$ and $O_3$-$CO_2$ relations as a function of the respective tracer mixing ratio, which can be converted to the "spring equivalent" potential temperature. Fig. 6.42 shows that deduced ozone loss between mid January and mid February amounts to roughly 800 ppb between spring equivalent potential temperatures of 415 K and 435 K (similarly at 435 to 460 K, not shown), and 600 ppb between 400 K and 415 K (with no detectable loss below 400 K, not shown). Thereafter slower ozone loss, about 200 ppb until mid March, was observed above 400 K, with an apparent increase of ozone for three flights in late February/early March found only by the FOZAN instrument. The total ozone loss throughout the winter until mid March is estimated to be 1200 ppb for equivalent spring potential temperatures between 415 K and 460 K.

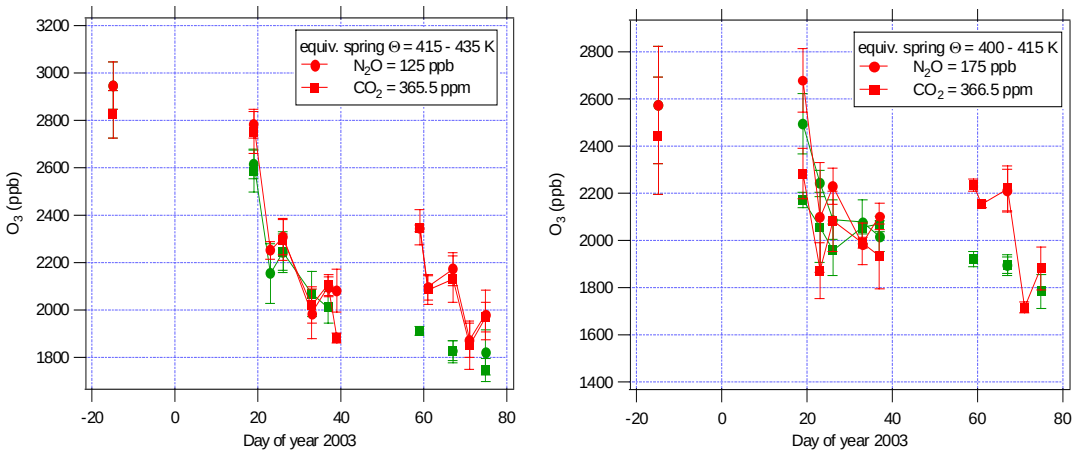


**Fig. 6.42 Evolution of ozone on $N_2O$ and $CO_2$ surfaces as measured inside the Arctic vortex from the Geophysica aircraft during the EUPLEX and Arctic validation campaigns. Data shown are flight averages and standard deviations (error bars) of ozone as measured by FOZAN (red) and FOX (green) for each $N_2O$ and $CO_2$ range (measured by HAGAR), corresponding to ranges of spring equivalent potential temperature as indicated.**

**Observed Denitrification**

Survey flights into the polar vortex to study the redistribution of $NO_y$ were performed during EuPLEx on January 19, 23, 26, 30, and on Feburary 02 and 06, 2003. The flights in January 2003 were conducted during conditions with temperatures well above the threshold temperatures for the formation of PSCs. Hence, sampling of denitrified air masses indicates irreversible removal of $NO_y$ by the sedimentation of particles during previous PSC events. Denitrification/renitrification is quantified by comparing measured gas-phase $NO_y$ (from SIOUX) with reference values ($NO_y^*$) inferred from $N_2O$ (from HAGAR) using the initial $NO_y$:$N_2O$ correlation (see D5.2). Fig. 6.43 shows time series and vertical profiles of measured $NO_y$ and inferred $NO_y^*$ during the Geophysica flight on 19 January 2003 and $NO_y^*$. The flight pattern included a northbound flight leg at 430 K, a dive near Spitzbergen, and a southbound flight leg at 460 K. The data show severe renitrification and denitrification during the northbound (at lower altitude) and southbound (at higher altitude) flight legs, respectively.

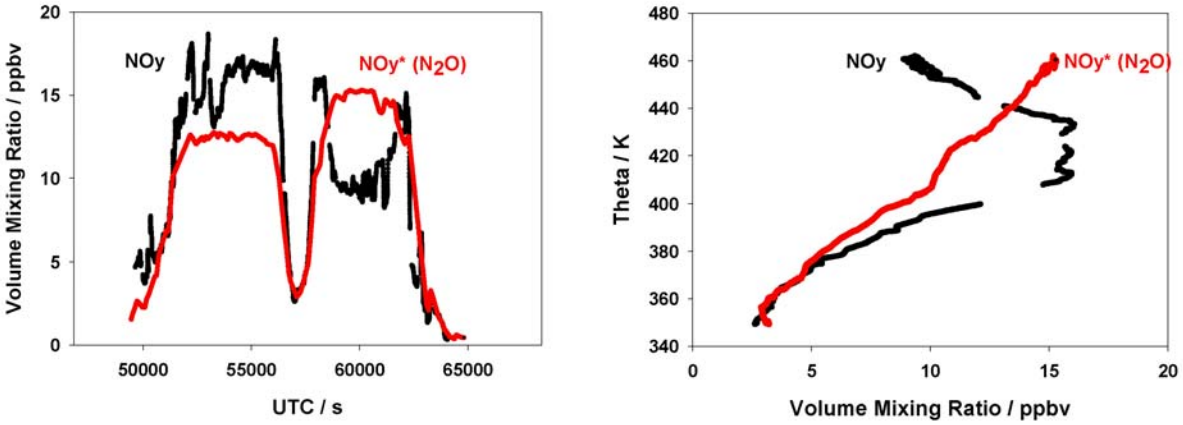


**Fig. 6.43 Left panel: Time series of gas-phase $NO_y$ (SIOUX) and $NO_y$* (HAGAR) for the EuPLEx Geophysica flight on 19 January 2003 into the polar vortex. Right panel: Profiles of $NO_y$ and $NO_y$* measured during the dive of the Geophysica during this flight near Spitzbergen.**

Fig. 6.44 shows measured NOy and inferred NOy* versus $N_2O$ for five EUPLEX survey flights into the vortex. A substantial denitrification and renitrification of up to 50% was observed in the vortex during January/February 2003. The turnover from denitrification to renitrification was observed at about 440 K (17.5 km).

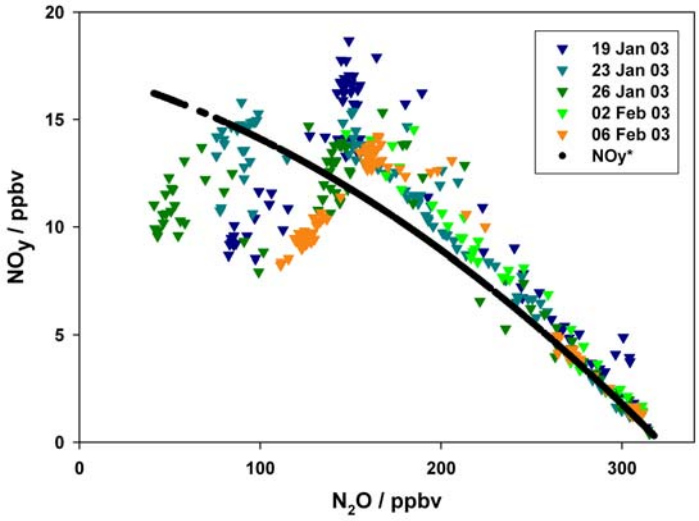


**Fig. 6.44 NOy:$N_2O$ scatter plot for SIOUX and HAGAR measurements during 5 Geophysica flights during EUPLEX. The NOy* reference (black line) is derived frm SOLVE MkIV balloon observations before onset of denitrification in the polar vortex (cf. D5.2).**

**CLaMS simulation of denitrification**

Within the EuPLEx project, a module for CLaMS was developed that simulates sedimentation of NAT particles and the corresponding redistribution of total inorganic nitrogen (NOy) in a Lagrangian way. Single particle boxes that are representative for a larger number of particles are advected, using the horizontal wind from the meteorological analyses and their vertical settling velocity calculated from the particle size. This scheme calculates the growth and evaporation of the particles and with that, the vertical NOy redistribution, i.e. denitrification where the particles uptake HNO3 from the gas phase and re-nitrification where they evaporate.

With this sedimentation scheme, CLaMS simulations were performed for the Arctic winter 2002/2003. Details of the CLaMS simulation are published by Grooß et al. (2004). Fig. 6.45

shows the simulated NOy change due to the sedimentation of the large NAT particles averaged over equivalent latitude range 65-90N for the reference CLaMS simulation. The unperturbed NOy* was simulated by a passive tracer that was initialized identically as NOy and that was then advected and mixed without chemistry and denitrification. The maximum denitrification of over 5 ppb between 500 and 550 K is reached in early January. After that, no significant additional denitrification was simulated and the denitrified air masses were only advected further. Also clearly visible in Fig. 6.45 is the re-nitrification at lower levels caused by the evaporation of the NAT particles corresponding to a NOy increase of over 2 ppb below about 450 K. The diabatic descent within the polar vortex causes the downward motion of the denitrification peak.

The simulated vertical redistribution of NOy was compared with balloon observations by MkIV and in-situ observations obtained during the EuPLEx campaign from the HAGAR and SIOUX instruments on board Geophysica. The MkIV data observed on December 16, 2002 indicated already significant denitrification at this early time. Fig. 6.46 shows the observations of NOy (green line) and NOy* derived from $N_2O$ (green dotted line) using the correlation mentioned above. The deviation between NOy and $NOy^*$ from MkIV between about 500 and 650 K is very likely caused by denitrification. The colored lines show the corresponding CLaMS NOy mixing ratios for different chosen NAT nucleation rates. These results show clearly that an increase of the nucleation rate yields larger denitrification. For the reference simulation (blue line) the assumption of a globally uniform NAT particle nucleation rate the nucleation rate of $J=3.4*10^{-6}$ $cm^{-3}h^{-1}$ yields the best agreement with observed NOy, the use of a larger nucleation rate overestimates the denitrification in early winter.

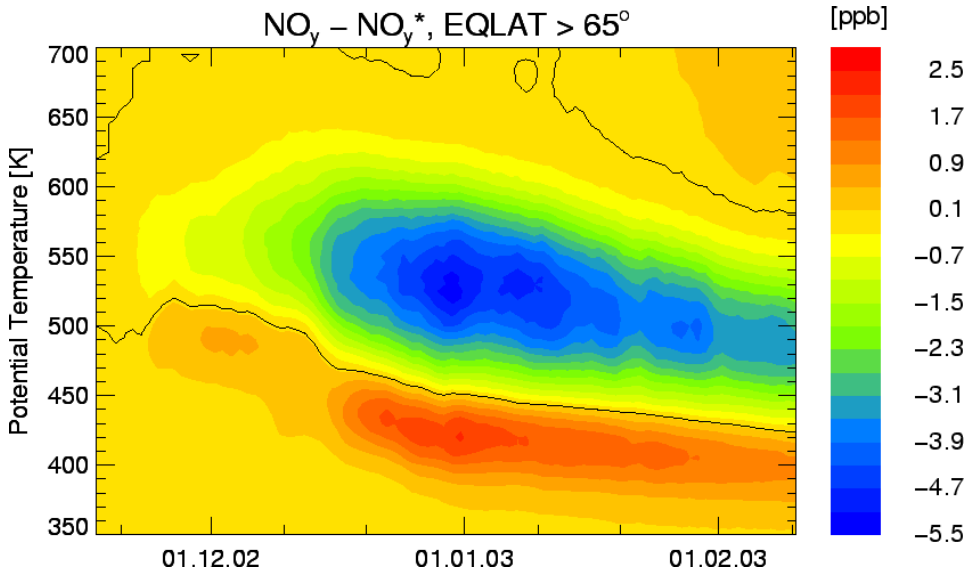


**Fig. 6.45 Simulated redistribution of NOy as function of time and potential temperature. Shown is the average over equivalent latitude range 65-90N for the period 17 November 2002 to 10 February 2003. The zero contour is displayed as a black line.**

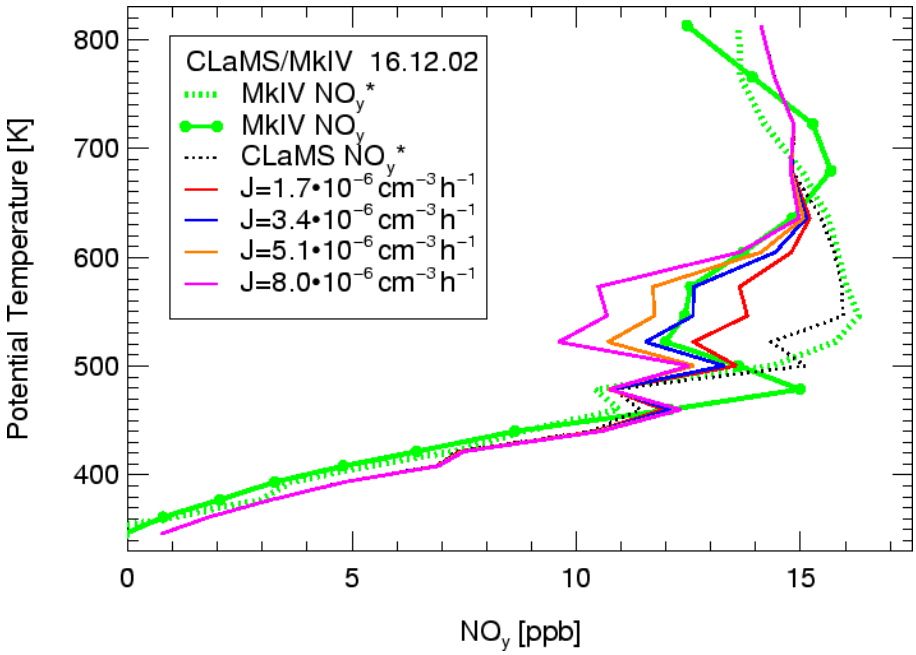


**Fig. 6.46 NOy observation and simulations. Shown are MkIV observation of NOy (green line) and NOy* derived from N2O (dotted green line) as well as CLaMS simulations for NOy* (black dotted line) and NOy (colored lines) with different nucleation rates J as indicated in the legend.**

The sensitivity simulations have shown that for the period from the onset of PSCs until mid-December the simulated denitrification is most sensitive to the nucleation rate of the NAT particles. Later in the winter in mid-January to early February during the time of the Geophysica flights, the simulated denitrification does not significantly depend on the nucleation rate due to saturation effects.

Fig. 6.47 shows the altitude dependence of vertical NOy redistribution for the parts of the flight of 19 January within the polar vortex (equivalent latitude>70N) and 2 choices of NAT nucleation rate. The shape of the denitrification and re-nitrification profile is reproduced well. The absolute values are slightly under-estimated for $J=3.4*10^{-6}$ $cm^{-3}h^{-1}$ and agree better for $J=8.0*10^{-6}$ $cm^{-3}h^{-1}$. The larger nucleation rate produces slightly higher denitrification and renitrification and the results may agree slightly better with the observations, but from the comparison cannot be judged which choice is better. Both, observations and the simulation do show the turnover level from denitrification to re-nitrification at about 440 K at that time. The northward part of the flight on 19 January was flown around the 440 K level. At this level CLaMS underestimates the re-nitrification. This may be caused by a too coarse vertical model resolution since a small deviation in altitude corresponds to a large deviation of NOy-NOy* at this level.

The higher NAT nucleation rate of $J=8.0*10^{-6}$ $cm^{-3}h^{-1}$ is about consistent with estimates derived from the observations on the Geophysica flight on 6 February and back-trajectories while in early winter it would produce too much denitrification.

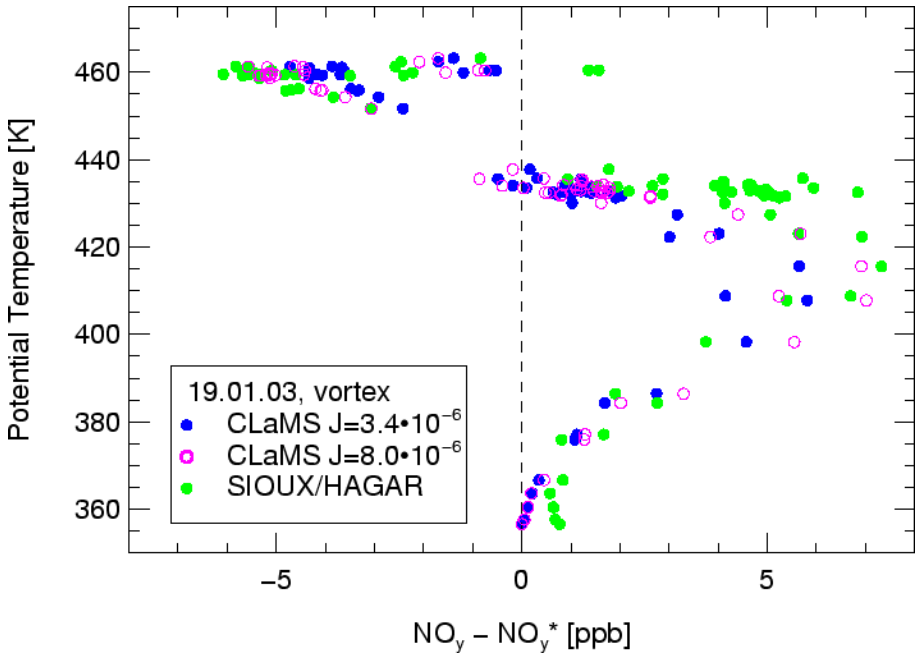


**Fig. 6.47 Comparison of denitrification from CLaMS simulation with that derived from SIOUX and HAGAR observations. The top panel shows the altitude profile within the polar vortex core (equivalent latitude >70N). Only the CLaMS data directly corresponding to the observations are shown. Blue circles correspond to the reference simulation with nucleation rate J=3.4*10$^{-6}$ cm$^{-3}$ h$^{-1}$ and the pink open circles the simulation with nucleation rate J=8.0*10$^{-6}$ cm$^{-3}$h$^{-1}$.**

**Dehydration**

Total hydrogen, i.e. the sum 2 $CH_4$ + $H_2O$, has been determined for 11 Geophysica flights in the period January to March 2003, based on FISH $H_2O$-measurements of FZ Jülich and HAGAR $CH_4$-measurements of U. Frankfurt. At flight altitudes in the stratospheric overworld, where this quantity is expected to be constant in the absence of dehydration processes, no significantly reduced observations of total hydrogen have been made during this period (an example is shown in Fig. 6.48). Since the polar vortex of the EUPLEX winter in this period was characterised by temperatures above the ice threshold, one might not have expected a major recent dehydration of the vortex air masses. The measurements however imply, that no persistent dehydration occurred in the earlier colder period of that winter.

The average value of 2*$CH_4$ + $H_2O$ determined from all 11 flights in this winter is 6.9 ± 0.2 ppmv. Comparing this value to balloon-borne measurements of our and the Frankfurt group carried out since 1995 in various projects (including the EU programmes WAVE, THESEO etc.), this quantity did not change in the lower stratosphere over the last 8 years. This finding is consistent with other observations e.g. from the HALOE satellite experiment, that the long-term increase of stratospheric water vapour might have slowed-down or even stopped during the last years.

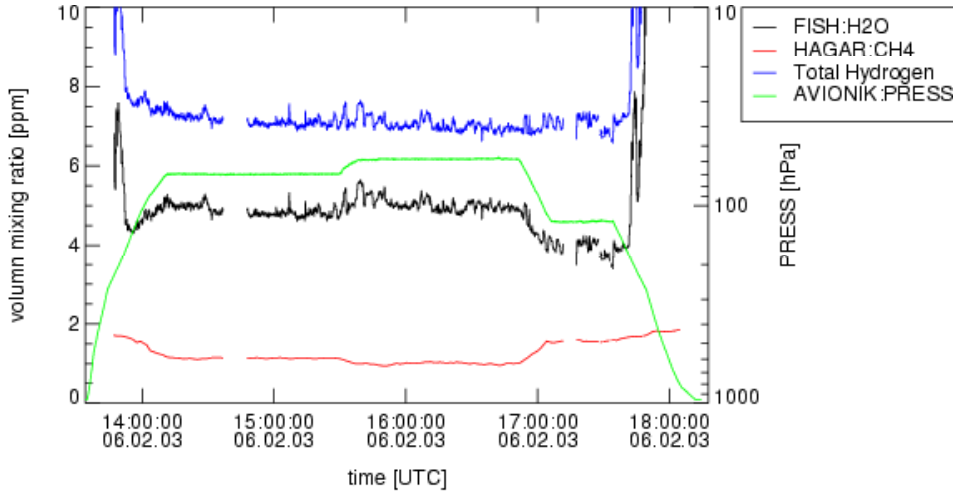


**Fig. 6.48 Time series of $H_2O$, $CH_4$, and 2 $CH_4$ + $H_2O$ and the flight profile of the Geophysica flight on 030206 during the EUPLEX mission.**

## *D5.5 Estimates of the amount and character of mixing across the vortex edge*

**Observed mixing and vortex dilution**

The 2002/2003 winter was dynamically very active with intrusions of extra-vortex air into the vortex occurring after minor warming events in mid January and mid February. A pronounced change in the observed F11-$N_2O$ correlation, particularly after mid-February (Fig. 6.49) immediately suggests that subsequent irreversible mixing of this intruded air affected the chemical composition of the vortex on the larger scale.

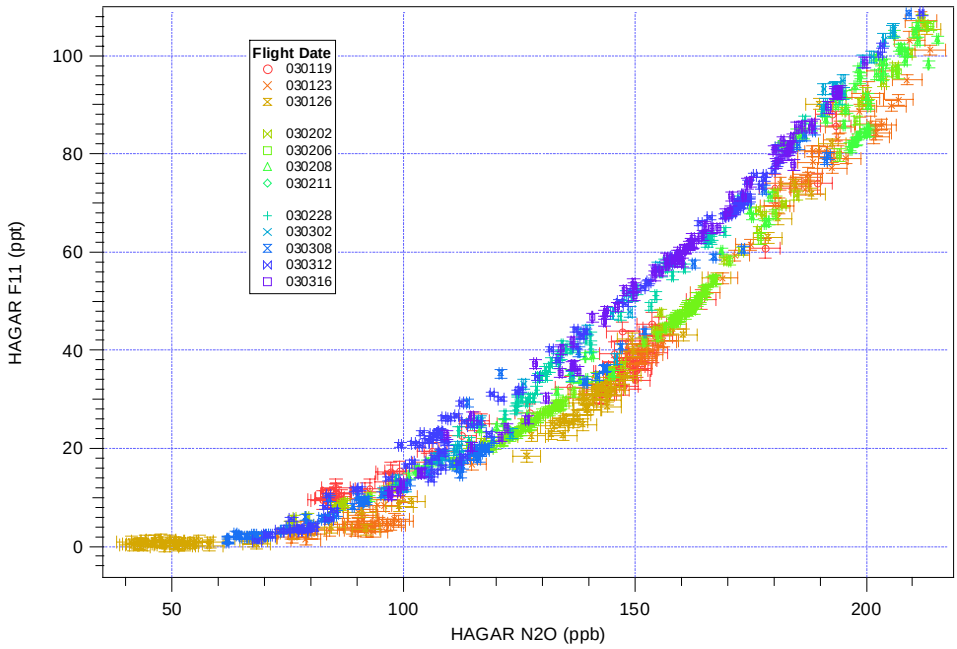


**Fig. 6.49 Evolution of the F11-$N_2O$ correlation (shown for $N_2O$<215 ppb) measured by HAGAR for 12 flights between January 19 and March 16, 2003. Error bars correspond to the 1-sigma precision uncertainty.**

In order to quantify the degree of mixing from observations, an empirical fraction of vortex air for each sampled air parcel was defined from HAGAR $N_2O$ observations as follows: vertical profiles of $N_2O$ representative of unmixed vortex air and extra-vortex air were established (as functions of potential temperature) by fits to the observations furthest inside and outside the vor-

tex (selected by appropriate equivalent latitude criteria). Assuming air to generally be a mixture of these pure vortex and extra-vortex air masses, the observed $N_2O$ mixing ratio gives a measure of their fractions and can thus be translated into an empirical fraction of vortex air (ranging from 0 for extra-vortex air to 1 for pure vortex air). The empirical vortex air fraction was "validated" by calculating it for $N_2O$ data simulated by the CLaMS model and comparing it to a true tracer for vortex air calculated in CLaMS (also ranging from 0 to 1). There is good agreement in CLaMS between the two quantities, suggesting that this simple procedure succeeds in quantifying the degree of mixing in an individual air parcel directly from the $N_2O$ observations. Fig. 6.50 shows the distribution of empirical vortex air fractions in equivalent latitude – potential temperature space. Thus, according to this analysis, some extra-vortex air had already mixed into the vortex before mid-February, but did not penetrate very deep. Pronounced mixing partly affecting the vortex core, however, occurred after the vortex split in mid February. A closer examination of the F11-$N_2O$ correlation with respect to vortex air fraction confirms that the changed parts of the correlation during the March flights (blue symbols in Fig. 6.49) consist indeed of mixed air with vortex air fractions between 0.3 and 0.8, while air parcels with higher vortex air fractions still largely follow the original correlation of the January/February flights.

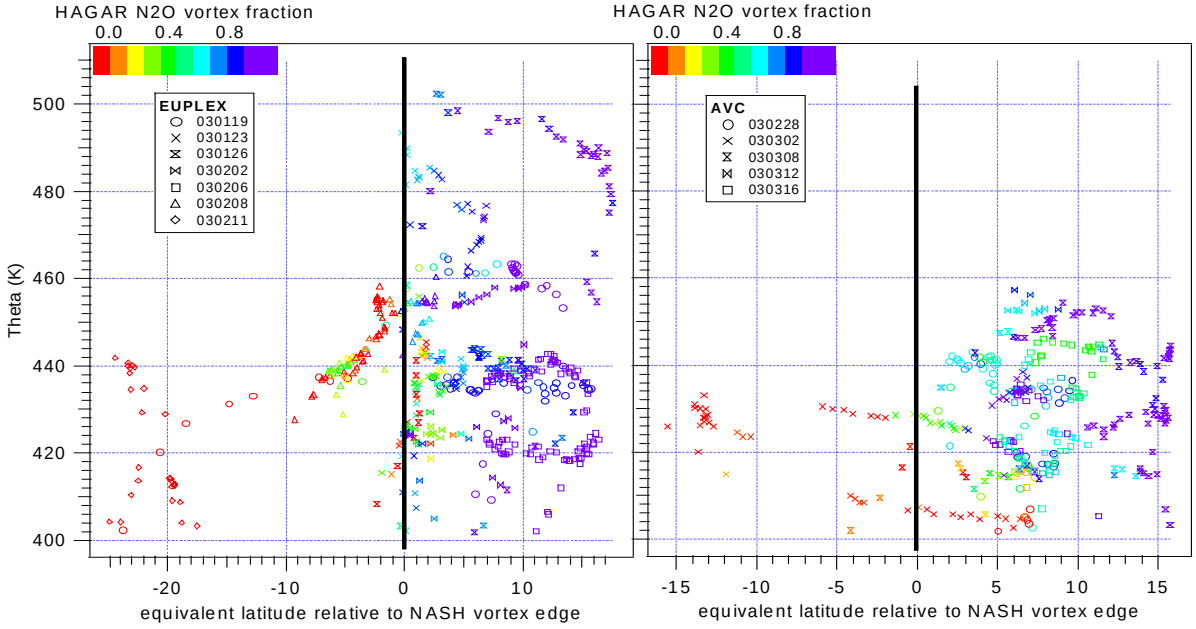


**Fig. 6.50 Spatial distribution of observed empirical fractions of vortex air (ranging from 0 for pure extra-vortex air to 1 for pure vortex air) during EUPLEX (left) and the Arctic validation campaign (right). The vortex edge (black line) was defined by the Nash-criterion (Nash et al., 1996).**

**CLaMS simulation of transport and mixing**

High-resolution tracer transport studies of $CH_4$, $N_2O$, and CFC-11 were carried out using the CLaMS model (McKenna et al., 2002a; Konopka et al., 2004), with Lagrangian air parcels (APs) covering the northern hemisphere in the potential temperature ($\theta$) range between 350 and 1400 K. The mean horizontal separation between the APs is given by 50 km and 100 km pole- and equatorward of 30°, respectively. The mean vertical separation between the APs results from a prescribed constant aspect ratio $\alpha$=250 and is given by 200 and 500 m in the high and low resolution regime, respectively. The mixing parameters are chosen as discussed by (Konopka et al., 2004).

Transport in CLaMS was validated by comparing tracer distributions with HAGAR measurements on-board of the Geophysica (Fig. 6.51), balloon flights (MkIV, Triple) and HALOE observations with a good agreement, similar to the results obtained for the winter 1999/00 (Ko-

nopka et al., 2004). In Fig. 6.51, observed $N_2O$ time series and $CH_4$/CFC-11 correlations are compared with CLaMS simulations for January 19 (a), 26 (b), February 6 (c) and March 8 (d). The upper left part of each of the four panels depicts the time series of $N_2O$ observed by HAGAR instrument (black crosses) and simulated with CLaMS model (filled circles) along the Geophysica flight track with colours denoting the percentage of the vortex tracer (CLaMS) in the sampled air masses. The lower left part of each panel shows the potential temperature θ (black), equivalent latitude (red) and the equivalent latitude of the vortex edge calculated with the Nash-criterion (Nash et al., 1996) for each θ-value along the flight track. Thus, the deviation of the red from the green line measures how deep the Geophysica flight penetrated the Arctic vortex. The left part of each panel illustrates the observed (black crosses) and simulated (circles) $CH_4$/CFC-11 correlations in comparison to the correlations used to initialize the model (black, gray and yellow solid lines). The filled gray circles denote $CH_4$/CFC-11 CLaMS correlation calculated approximately every 2 seconds along the flight, the open circles correspond to the observation times and are colored, in the same way as the time series, with the vortex tracer.

Both the time series and the correlations show that CLaMS reproduces fairly well the observed features of tracer distributions. In particular, low $N_2O$ values within the vortex caused by diabatic descent of the vortex air masses during the winter are well reproduced, even if slightly underestimating the diabatic descent above 500 K in January by about 10 K. Furthermore, the model reproduces the profiles of $N_2O$ measured during the descents, ascents, and dives of the Geophysica, $N_2O$ gradients across the vortex edge, fine scale structures as filaments (gray dashed areas) and curvature of the $CH_4$/$N_2O$ correlations. The ongoing dilution of the vortex air due to intrusions of the mid-latitude air manifests in a gradual decrease of the vortex tracer values within the air masses sampled in the vortex and by flattening of the curvature of the $CH_4$/$N_2O$ correlation if compared with the initial vortex correlation (black line), with the strongest difference between February 6 and March 8.

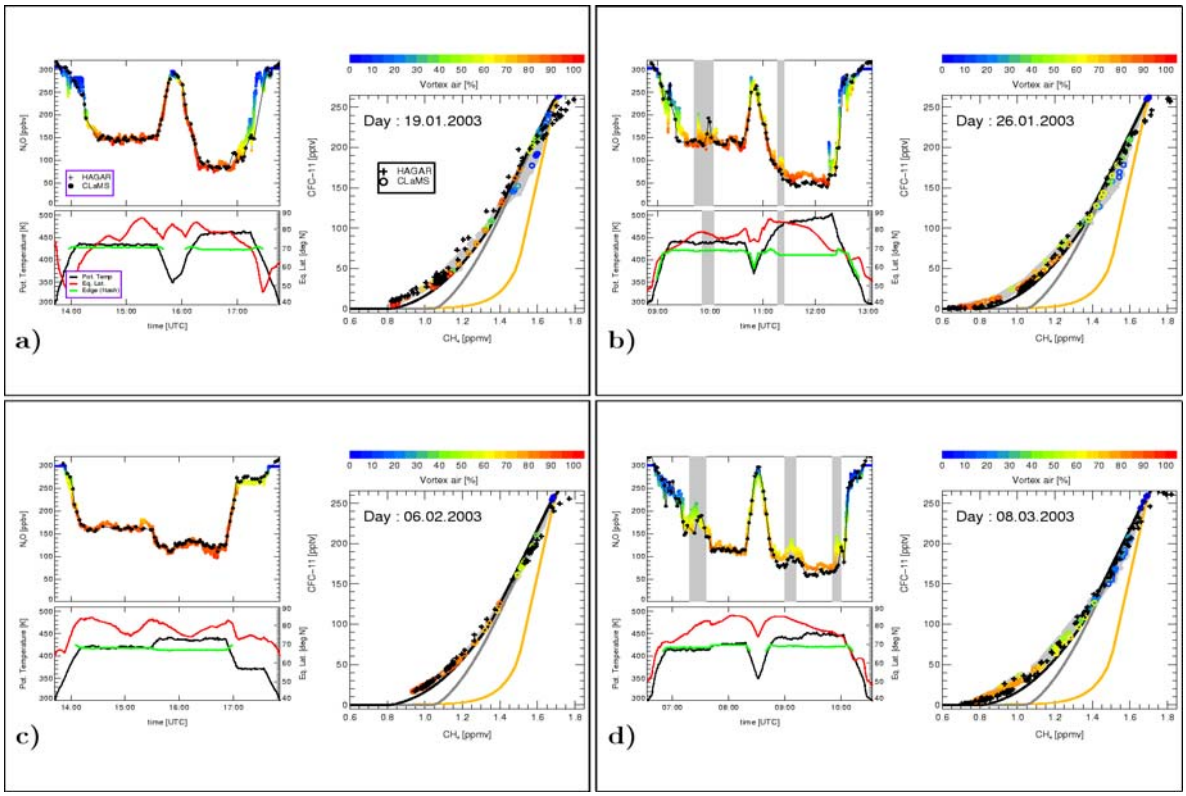


**Fig. 6.51 $N_2O$ time series and $CH_4$/CFC-11 correlations calculated with CLaMS versus HAGAR observations for 4 representative days between January and March 2003. Furthermore, the potential temperature, equivalent latitude and the equivalent latitude of the vortex edge are plotted along the flight track. For more explanations see text.**

The winter 2002/03 was characterized by a very early (mid of November) onset of cold temperatures in the polar vortex over a large altitude range in the lower and middle stratosphere (Spang et al., 2004). A first minor warming (mW, see Fig. 6.53) occurred in the upper stratosphere in late December and, according to the analysis of planetary waves (not shown), was accompanied by a strong wave number 1 activity. Around mid of January, the activity of wave number 2 increased, leading to a major warming event (MW). After that the upper (above 700 K) and lower (below 550 K) parts of the vortex first split around January 20 into two centres and than reunified to a circumpolar vortex. Two similar "split and merge" periods of vortex evolution were induced by a minor warming around mid of February and begin of March. Both events could be assigned to a high activity of wave number 1. The vortex decayed slowly until the final warming (FW) around April 20 (Naujokat and Grunow, 2003).

Based on frequency distributions of the mean zonal wind and statistics of wave number 1 heights, Pierce and Fairlie (1993) and Pawson and Kubitz (1996) defined 3 preferred flow types which characterize the wave activity of the winter Arctic stratosphere. Without describing their methods in detail, here solely the principal characteristics of the flow regimes are mentioned:

- large-amplitude mode which occurs most frequently and is characteristic for normal mid-winter conditions (mode 2)
- small-amplitude mode with strong zonal winds associated with a deep, cold polar vortex that is typical for cold, undisturbed conditions (mode 1B)
- small-amplitude mode with weak zonal winds associated with a weak vortex and generally weak gradients of geopotential heights, typically forming major warmings (mode 1A).

Following the categories of Pierce and Fairlie (1993), the analysis of the mean zonal wind and geopotential heights at 10 hPa and 60_N for December 2002 to February 2003 yields about 79% mode 2 days, about 8% mode 1A days and only 1% 1B days. The missing 12% do not belong to any category. Using the categories defined by Pawson and Kubitz (1996) leads to about 71% mode 2 days, 13% mode 1A and 16% mode 1B days. Remarkable for winter 2002/03 is the relatively high percentage of mode 1A days associated with warming events and indicating a polar vortex disturbed by a strong planetary wave activity. For comparison, in a relatively undisturbed 1999/2000 winter about 70% mode 2 days, 13% mode 1B days and no 1A mode days were clasified (Steinhorst et al., 2004) (17% day do not belong to any category).

To quantify mixing into the vortex, we calculate in Fig. 6.52 the mean dilution of the vortex by averaging every day the vortex tracer over all APs northward of 70_N equivalent latitude. From December to the final warming (FW) in late April, the vortex edge shrunk from about 60 to 70_N. Thus, the mean vortex tracer averaged over APs with equivalent latitude>70_N quantifies the dilution of the vortex core rather than of the entire vortex. The 50% contour line (black line) approximately confines the well-isolated part of the vortex. The dashed (dotted) line is the 50% contour resulting from the averaging over APs with equivalent latitude> 65 (75)_N shows an earlier (later) onset of the mean vortex dilution due to a stronger (weaker) contribution of the extra-vortex air in the vicinity of the vortex edge. The white line is a measure of the permeability of the vortex edge and is defined as the maximum of the gradient of modified potential vorticity (Lait, 1994) at the vortex edge determined by the Nash et al. (1996) criterion. The isoline of 1.5 modified PV units per degree eq. latitude ( PVU deg_1) was determined empirical by Steinhorst et al. (2004), i.e. air masses within (without) this region are well-isolated (permeable) with respect to the transport across the vortex edge.

The pattern of the mean dilution in Fig. 6.51 that is partially correlated with the increase of the vortex permeability indicates the top-down vortex decay until the vortex breakup. In particular, a strong vortex dilution around 800 K is triggered by the major warming at the end of January and a slow dilution of the vortex bottom can be seen, slightly accelerated after February 1 and after March 1. In the potential temperature region between 500 and 600 K, the vortex persisted until the final warming in April 2003. Balloon measurements in June 2003 (Triple flight on June 9) confirm the existence of moderately mixed but clearly distinguishable vortex air masses in this

altitude region. Thus, the correlation between the warming events (wave activities), vortex permeability and the intensity of vortex dilution indicates that the dilution of the Arctic vortex can be roughly regarded as the result of planetary wave activity.

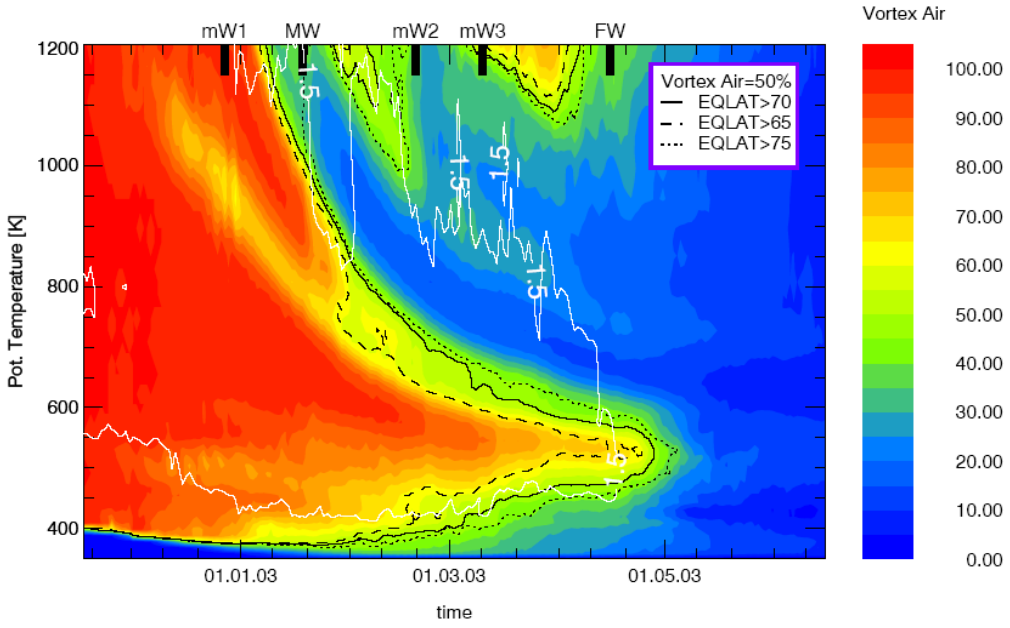


**Fig. 6.52 Mean vortex dilution in winter 2002/03 derived from the CLaMS vortex tracer averaged every day over all APs with eq. latitude>70_N. The black contours (solid, dashed and dotted) are the 50% isolines of the mean vortex tracer calculated for APs with eq. latitude>70, 65, 75_N, respectively. Thus, the black line separates approximately the well-isolated vortex from the mid-latitude air. Dates of the minor (mW) major (MW) and final (FW) warmings are marked by thick solid lines.**

Simulations with CLaMS already have shown that the polar vortex during the winter 2002/2003 was eroded by planetary waves. As usual the height range of maximal erosion was moving downward during the course of the winter, leading to a final breakdown of the vortex in May, 2003. The lowest part of the vortex between 400 K and 650 K was likewise affected by the stirring of planetary scale waves. To investigate the effects of transport and mixing of air masses from outside the vortex across the border another study with CLaMS was performed, utilizing a whole suite of inert tracers. These tracers where initialized mutually exclusive according to their initial mPV conditions, thus giving the 2 opportunity to distinguish between air originating from the vortex core, the inner and outer edge, the mid latitudes and the tropics.

Investigating the budget of these tracers makes it possible to quantify the amount of air mass, which enters or leaves the polar vortex in the lower stratosphere during the winter. Fig. 6.53 shows the temporal evolution of the fluxes across the vortex boundary as estimated from the above mentioned simulation. Positive and negative signs correspond to net inward and outward fluxes, respectively.

The strongest peaks in the net inward fluxes can be observed around mid January and the beginning of February. This corresponds very well to the enhanced planetary wave activity found on these days. During these events the lower stratosphere vortex was almost split and remerged afterwards, incorporating air from the mid latitudes into the re-formed vortex. Strongest outflows can be observed during mid January, shortly after the first re-merging event, and in mid February. The outflow events are mainly due to the interaction between anticyclonic structures built up near the vortex edge and the vortex itself. These processes usually lead to vortex erosion.

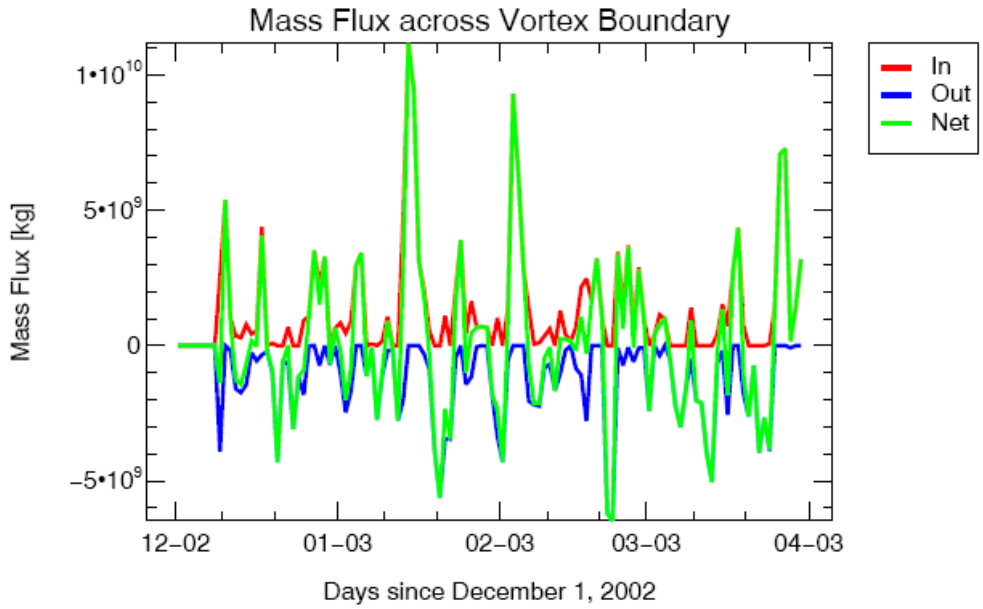


**Fig. 6.53 Temporal evolution of the in, out and net fluxes across the vortex boundary from the beginning of December, 2003, to the end of March, 2004. The vortex edge was defined by the 21 mPVU contour line.**

### 6.5.3 References

Grooß, J.-U., G. Günther, R. Müller, P. Konopka, S. Bausch, H. Schlager, C.M. Volk, and G.C. Toon, Simulation of denitrification and ozone loss for the Arctic winter 2002/03, Atmos. Chem. Phys. Discuss., 4, 8069–8101, 2004.

Konopka, P., H.-M. Steinhorst, J.-U. Grooß, G. G¨unther, R. M¨uller, J. W. Elkins, H.-J. Jost, E. Richard, U. Schmidt, G. Toon and D. S. McKenna, 2004: Mixing and ozone loss in the 1999-2000 arctic vortex: Simulations with the 3-dimensional Chemical Lagrangian Model of the Stratosphere (CLaMS). *J. Geophys. Res.*, **109**(D2), doi:10.1029/2003JD003792.

Lait, L. R., 1994: An alternative form for potential vorticity. *J. Atmos. Sci.*, **51**, 1754–1759.

McKenna, D. S., P. Konopka, J.-U. Grooß, G. G¨unther, R. M¨uller, R. Spang, D. Offermann and Y. Orsolini, 2002: A new Chemical Lagrangian Model of the Stratosphere (CLaMS): Part I Formulation of advection and mixing. *J. Geophys. Res.*, **107**(D16), 4309, doi:10.1029/2000JD000114.

Nash, E. R., P. A. Newman, J. E. Rosenfield and M. R. Schoeberl, 1996: An objective determination of the polar vortex using Ertel's potential vorticity. *J. Geophys. Res.*, **101**, 9471–9478.

Naujokat, B. and K. Grunow, 2003: The stratospheric arctic winter 2002/03: Balloon flight planning by trajectory calculation. in *Proceedings of the 16th ESA Symposium on European Rocket and Balloon Programmes and Related Research*, no. ESA SP-530, pp. 421–425, St.Gallen.

Pawson, S. and T. Kubitz, 1996: Climatology of planetary waves in the northern stratosphere. *J. Geophys. Res.*, **101**, 16,987–16,996.

Pierce, R. B. and T. D. Fairlie, 1993: Observational Evidence of Preferred Flow Regimes in the Northern Hemisphere Winter Stratosphere. *J. Atmos. Sci.*, **50**, 1936–1949. Spang, R., J. J. Remedios, L. J. Kramer, L. R. Poole, M. D. Fromm, M. M¨uller, G. Baumgarten and P. Konopka, 2004: Polar stratospheric cloud observations by MIPAS on ENVISAT: Detection method, validataion and analysis of the Northern hemisphere winter 2002/2003. *Atmos. Chem. Phys. Discuss.*, **4**, 6283–6319.

Steinhorst, H.-M., P. Konopka, G. G¨unther and R. M¨uller, 2004: How permeable is the edge of the Arctic vortex - Model studies of winter 1999-2000. *J. Geophys. Res.*, accepted.

Tilmes, S., R. Müller, J.-U. Grooß, M. Höpfner, G. C. Toon, and J. M. Russell III, Very early chlorine activation and ozone loss in the Arctic winter 2002 – 2003, Geophys. Res. Lett., 30(23), 2201, doi:10.1029/2003GL018079, 2003.

## 6.6 WP6: Aircraft In-Situ Measurements

### 6.6.1 Objectives

The in-situ aircraft measurements of WP 6 were the basis of the data pool for the various scientific fields of interest discussed in detail by WP1-WP5 in this section. Here we report on the completion of the proposed deliverables and milestones and on the final data status of the Geophysica in-situ instruments.

*D6.1 2-D Quick-look data from all instruments within 24 hr after flight for strategy identification.*

Quick-look meetings were held within 24 hours after each of the ten EuPLEx measurement flights. Data from all in-situ instruments (SIOUX, HALOX, HAGAR, FISH, FLASH, FOZAN, ECOC, FOX, CVI-$N_2O$, ALTO, COPAS, FSSP, MAS, and TDC) were presented during all quick-look meetings.

*D6.2 Validated time series of concentration of ClO, BrO, ClOOCL and $ClONO_2$*

The HALOX instrument employs the chemical conversion resonance fluorescence (CCRF) technique described by Brune et al. (1989) for measuring ClO in two parallel measurement ducts, A and B. In measurement duct B, which is pumped to decrease the pressure inside by about 40 %, the sum of ClO and $Cl_2O_2$ is measured after thermal dissociation of the dimer in a heated inlet nozzle depicted in Fig. 6.54. To extract the $Cl_2O_2$ concentration, the ClO background measured in duct A is subtracted. The conversion efficiency of the inlet heater with respect to $Cl_2O_2$ has been tested in the laboratory: a stream of nitrogen gas with ClO added is passed through the HALOX measurement duct B. When the gas is cooled to below –50° C, the fluorescence signal produced by the ClO decreases; when the inlet heater is turned to 100 °C, the fluorescence signal returns quantitatively as illustrated in Fig. 6.55 We ascribe this to formation of $Cl_2O_2$ upon cooling, and dissociation in the heated inlet. However, a small proportion of ClO may be removed by wall loss, especially at low pressures and flow rates. The laboratory studies do not suggest any problems with incomplete dimer conversion in the heated inlet. A lower limit for the conversion efficiency is estimated to 80 % based on the accuracy and precision of the laboratory measurements. This laboratory calibration constitutes the first such measurement for the ClO dimer. Earlier dimer measurements (Stimpfle et al., 2004) have relied on a 100% thermal conversion efficiency.

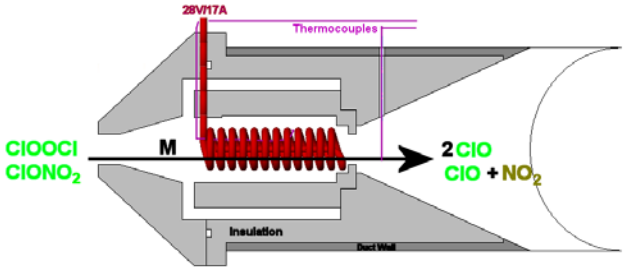


**Fig. 6.54 Schematic of HALOX heated inlet.**

Calibration for ClO and BrO has been completed. The final ClO data for all 10 flights have been delivered to the EuPLEx data base. Observed BrO levels remained around the HALOX detection limit throughout the EuPLEx campaign. ClO dimer (ClOOCl) and $ClONO_2$ were observed during most EuPLEx flights. The ClO dimer data has been submitted to the data base. The quantification of the $ClONO_2$ data suffers from large error bars due to outgassing of some unknown compound from the heated nozzle at high temperatures. This problem has been solved but can hardly be accounted for for the EUPLEX flights.

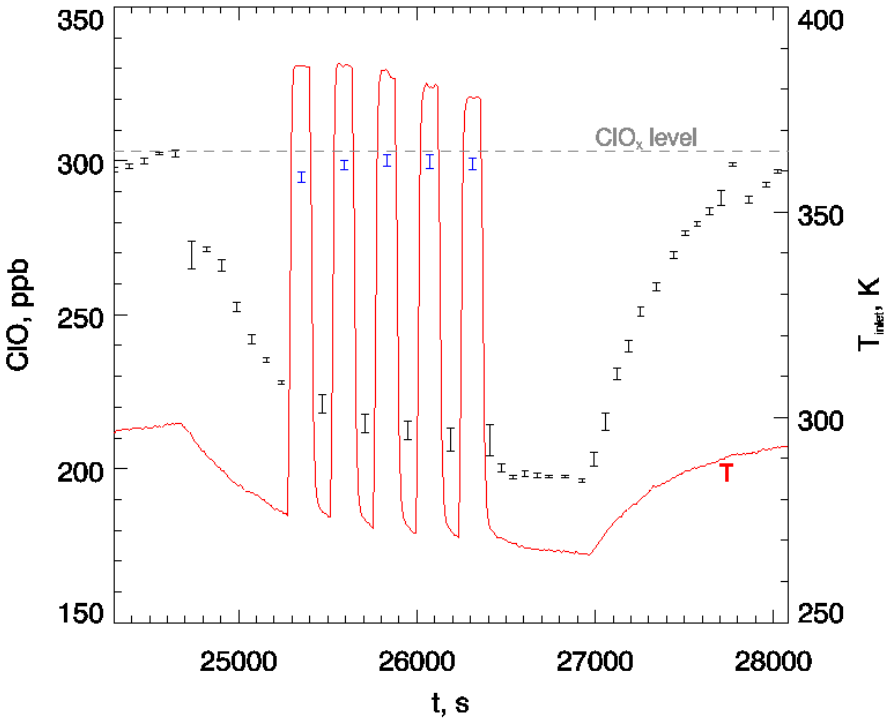


**Fig. 6.55 Laboratory test ($P_{duct}$ = 80 hPa) of dimer conversion efficiency of the heated inlet. Error bars represent the standard error of the mean for one minute averages (equivalent to six NO addition cycles), blue colour indicates that the temperature (red line) of the inlet heater was at the dimer dissociation temperature (363 K < *T* < 383 K). The dashed line indicates the reference ClO concentration measured without cooling or heating.**

### *D6.3 Validated time series of the tracer species $N_2O$, $CH_4$, $O_3$, $H_2O$, $CO_2$, F11 and F12*

Final data for $N_2O$, $CH_4$, F11, F12, H-1211, $SF_6$, $H_2$, and $CO_2$ from HAGAR were delivered to the EuPLEx data base. Correlations of species measured by HAGAR with each other were examined and compared with respective correlations measured during previous campaigns by HAGAR and the NOAA ACATS instrument. The agreement was generally within the error bars, although for several flights a significant high bias for F12 was identified and attributed to shortcomings in the integration algorithm. Also, a variable bias (up to 1%) was identified for all species due to drift of the in-flight calibration gas. These problems have been corrected for as far as possible by laboratory calibrations and re-analysis of the data.

Data from the CVI-TDL for $N_2O$ and from ALTO for $CH_4$ (three flights) were delivered to the EuPLEx data base. TDL $N_2O$ data are in general agreement, within errors, with those of HAGAR and other instruments or related gases. $CH_4$ data from HAGAR and ALTO have been inter-compared. The data quality of the ALTO $CH_4$ measurements proved to be poorer than expected. Only a qualitative agreement with HAGAR data can be found.

Ozone data from FOZAN, ECOC, and FOX were delivered to the EuPLEx data base. Data of the instruments have been inter-compared. FOX (uv-absorption photometer) was used for the first time during EuPLEx and provided already very useful data for most of the flights. Pressure and temperature sensors of FOX were recalibrated and final data was supplied to the data base. The inter-comparison of the FOZAN and FOX data with other tracers and with ozone sonde data revealed some problematic time-dependent drift in the FOZAN data at high altitudes.

The Fast In-situ Stratospheric Hygrometer (FISH) was used during all EuPLEx flights to measure total water, i.e. the sum of condensed and gas phase $H_2O$. These measurements are complemented by gas-phase measurements of $H_2O$ by FLASH. Flight parts inside clouds close to the tropopause clearly show the different sampling characteristics of both hygrometers. FISH was

calibrated before each flight using the laboratory calibration bench of FZJ. Final data of the campaign have been subbmitted to the NILU data base. In 2002, FZJ calibrated also the CAO FLASH instrument in the Jülich laboratories in order to achieve best agreement and characterisation of both hygrometers. Though the agreement of FISH and FLASH is very good during most of the flight parts of the EuPLEx mission, some discrepancies occurred during rapid changes of cruise altitude. Preliminary FLASH data for all flights have been placed on the data server.

### *D6.4 Validated time series of reactive nitrogen species $NO_y$*

Final $NO_y$ data were delivered to the EuPLEx data base. Several papers have been submitted to ACPD or are currently in the final stages before submission. For details see sections 6.1 and 6.2 of this report.

### *D6.5 Validated time series of cloud particle size distributions with optical particle counter*

Final data of cloud particle concentrations > 0.4 μm measured by the FSSP instrument were delivered to the EuPLEx data base. A manuscript analysing this data is close to submission for ACPD.

### *D6.6 Validated time series of background aerosol particle number density*

Final data of total and non-volatile aerosol number densities were delivered to the EuPLEx data base. For Flights 6-10 two independent dual channel COPAS CN-Counters were operated onboard Geophysica. The inter-comparison of the two instruments shows excellent agreement. Post-flight calibrations to determine exact pressure-dependent lower cut-off diameters of the counters have been performed. A manuscript analysing this data is close to submission for ACPD.

### *D6.7 Validated time series of cloud backscatter and depolarization data*

The Multiwavelength Aerosol Scatterometer (MAS) instrument of CNR-IFA acquired data on all flights performed during the campaign with satisfying performance. Two wavelengths of laser light (532 and 1064 nm) scattered back by aerosol particles in close proximity to the Geophysica aircraft (3-30 m) have been analysed. The two wavelength capability of the instrument - in daylight conditions - was demonstrated, although the new 1064 nm channel suffered from inaccuracies that degraded the measurements when the highest altitudes were achieved. Time series were delivered to the EuPLEx data base.

### *D6.8 Validated time series of meteorological base parameters*

Time series of meteorological base parameters were delivered to each instrument during flight (UCSE data). This data was also placed on the EuPLEx data base. There are three temperature measurements on the M55-Geophysica, which are provided by:

1. the aircraft navigational data system (UCSE)
2. the CAO Thermo Dynamic Complex (TDC) instrument (Rosemount sensor),
3. the Microwave Temperature Profiler (MTP) of JPL, USA.

The temperatures by the different systems have been inter-compared. By comprehensive re-analysis several discrepancies in the data were resolved. Final data by UCSE, TDC and MTP has been submitted to the data base.

*M6.1 Modifications of in-situ $NO_y$ instrument for detection of particle $NO_y$ completed*

The in-situ $NO_y$ instrument on the Geophysica (SIOUX) has been modified for the detection of $NO_y$ contained in particles. It was equipped with a second converter unit to sample both particle and gas-phase $NO_y$ via reduction to NO and subsequent detection using chemiluminescence technique. Specific for the modified instrument is a new inlet configuration optimised for the detection of solid and liquid nitric acid containing PSCs. In a forward facing inlet particles with radii >2µm are highly oversampled (enhancement factor 16 at 70 hPa), whereas particles are discriminated by the rear inlet with a cut-off size of <0.1µm. Particle $NO_y$ is derived by subtracting the data sampled through the rear and front inlets. At particle number densities $<10^{-4}$ $cm^{-3}$ this configuration enabled the detection and sizing of nitric acid containing particles with radii >1.5 µm by single particle analysis. At higher particle number densities as prevalent in liquid STS PSCs, the total particle $NO_y$ content is measured. The optimised instrument has been calibrated, integrated in the wingpod of the Geophysica and operated continuously without any malfunction during all EuPLEx flights.

| instrument | F1 150103 | F2 190103 | F3 230103 | F4 260103 | F5 300103 | F6 020203 | F7 060203 | F8 080203 | F9 090203 | F10 110203 |
|---|---|---|---|---|---|---|---|---|---|---|
| SIOUX | final | final | final | final | final | final | final | final | final | final |
| HALOX | final | final | final | final | final | final | final | final | final | final |
| HAGAR | final | final | final | final | no data | final | final | final | no data | final |
| FISH | final | final | final | final | no data | no data | final | final | final | final |
| FLASH | final | final | final | final | final | final | final | final | final | final |
| FOZAN/ ECOC | (final) | (final) | (final) | (final) | (final) | (final) | (final) | (final) | no data | (final) |
| FOX | final | final | final | (final) | (final) | (final) | final | (final) | (final) | (final) |
| ALTO | no data | (final) | (final) | (final) | (final) | no data | (final) | (final) | (final) | no data |
| CVI-TDL | final | final | final | final | final | final | no data | (final) | final | final |
| FSSP | final | final | final | final | final | final | final | (final) | (final) | final |
| COPAS | final | no data | final | no data | final | final | final | final | (final) | final |
| MAS | prelim | prelim | prelim | prelim | prelim | prelim | prelim | prelim | prelim | prelim |
| TDC/ UCSE | (final) | (final) | final | final | final | final | final | final | final | final |
| MTP | (final) | final | final | final | final | final | final | final | final | final |
| WAS | (final) | (final) | (final) | final | final | final | final | final | final | final |

**Tab. 6.1: Data status for all in-situ measurements during Geophysica flights. WAS = whole air sampler, not funded by EUPLEX. Legend:**

**final:** **data ok, final data set on server.**

**(final):** **instrumental failure in part of the flight, or poor data quality, partial or best available data on server**

**prelim:** **preliminary data on server**

**no data:** **instrumental failure in all of the flight**

*M6.2 Calibrated instruments ready for aircraft measurement campaign*

In addition to the standard instrument preparation and calibration numerous instrumental improvements and upgrades were implemented, i.e. the HALOX upgrade to measure ClO dimer and $ClONO_2$.

*M6.3 Preliminary data ready 12 hours after flight*

Preliminary data from all Geophysica in-situ measurements were placed on the common campaign data server within 12 hr after each flight.

*M6.4 Final data ready on data base*

Final data sets have been submitted to the data base (see report on Deliverables 6.2-6.8). The table shows the detailed data status for all in-situ measurements for all EUPLEx flights.

### 6.6.2 Discussion and conclusion

WP6 reached all milestones and fulfilled all its deliverables. Final data of high quality has been submitted to the data base for almost all instruments. Several manuscripts on the data have been published, submitted or are close to being submitted. Completion of WP 6 of EUPLEX was very successful.

## 6.7 WP7: Overall Co-ordination, Flight Planning, and Logistics

### 6.7.1 Objectives

The main objectives for WP7 within the EUPLEX project have been:

1. Project Co-ordination
2. Campaign Organization
3. Data base management and supply of meteorological (ECMWF) data
4. Web-site support

### 6.7.2 Methodology and Achievements

*Coordination tasks*

General tasks of the co-ordinator are to ensure that within EUPLEX all mechanisms are in place to guarantee the project progress and achievement of the results, envisaged in this proposal. The coordinator represented the project towards the EC and other organisations. Major tasks were:

1. Set-up of project coordination, organization, and communication tools
2. Set-up and organization of co-operations with other projects and groups
3. Organization of the field campaign and data interpretation work
4. Representation of the project at meetings
5. Initiation and planning of project meetings and assembly of project reports
6. Organization of publications

The major tool for the exchange of information within the EUPLEX project was email. Therefore the mailing lists:

- euplex_all@nilu.no (all people involved in the EUPLEX project) and
- euplex_cg@nilu.no (EUPLEX core group)

were set-up and have been updated regularly in order to have easy access to all project participants or just the core group.

In order to ensure the proper flow of information between the partners and to readily initiate project tasks within the different work packages project meetings were planned and held as scheduled in the Description of Work and detailed in Table 6.2. Minutes of the project meetings are available from the EUPLEX web site.

Very interesting data was gathered during the Arctic campaign also in the UTLS region enabling new stufies into NOy partitioning in the presence of ice particles in the form of cirrus clouds and also on their potential for halogen activation. These subjects have not been primary scientific objectives of EUPLEX but alternate objectives in case of unfavourable meteorological conditions. However, since these data are available anyway, the consortium will keep working on their exploitation. The further plans for the analysis and interpretation of this data and first studies were discussed on 10. Jan. 2005 at a dedicated meeting at DLR, Oberpfaffenhofen.

Several overview presentations on the project have been given by the coordinator at scientific meetings (EGU 2003, Science Meeting Orlando 2003, and AGU 2003) An abstract for an overview presentation of the EUPLEX project results and the implications for the Arctic ozone problem has been submitted to the Polar ozone session for the EGU meeting 2005 in Vienna. The

possibility of an overview paper in the peer reviewed literature (Atmos. Chem. Phys.) is currently being investigated.

| Date | Meeting (Attendees) | Agenda |
|---|---|---|
| **06/07. May 2002 FZJ** | Kick-Off Meeting (all partners, invited representatives of SOLVE-II and ENVIVAL) | Presentation and review of project timetable and scientific priorities for flight plan, discussion of campaign location, and flight strategies, Synergies and cooperation planning with other campaign activities, Integration of additional instrument and modelling groups. |
| **13. Oct 2002 Forli** | Campaign Group Meeting | Decision on campaign location, presentation of infrastructural requirements, campaign planning, status of instruments, models, and flight planning tools |
| **Jan/Feb 2003 Kiruna** | Science Meetings (all, during and end of campaign) | Review of preliminary results, discussion of further flight plan, review/decision on interpretational strategies, discuss mid-term report |
| **06/07. May 2003 ETH** | Data Interpretation Workshop (all) | Summarise experimental results, review first interpretational results, discuss open questions and further work, discuss publications |
| **21-24. Oct. 2003 Orlando USA** | SOLVE II / VINTERSOL Joint Science Team meeting (selected persons) | Presentation and discussion of results. Status of the project work flow discussed in dedicated project meeting. |
| **14.-15- Sept. 2004 Leeds, UK** | Final Project Meeting | Presentation and discussion of results, coordination of publications, Preparation of the final report |
| **16. Jan. 2005, Oberpfaffenhofen, Germany** | EUPLEX Cirrus Meeting (not a project meeting planned initially) | Presentation and discussion of results with respect to NOy and halogen partitioning within cirrus clouds observed in the UTLS region during the EUPLEX and ENVISAT Arctic field campaigns in 2003. |

**Tab. 6.2 Project meetings held within and after the EUPLEX project (Minutes are available from the restricted area of the EUPLEX web site). The last meeting indicates the wealth of unique data gathered during the field campaign and its potential for further research and upcoming publications dealing with objectives not directly addressed by the EUPLEX project.**

Currently a broad press release on the EUPLEX project results and the implications for the Arctic ozone problem is discussed within the consortium. The activity will be lead by the coordinator even so the official project period is finished.

An article on the EUPLEX campaign and the results with emphasis on the ones obtained at FZJ was recently pulished in the Yearly Report of the HGF (Helmhotz-Gemeinschaft Deutscher Großforschungszentren).

All project reports are available from the restricted part of the project web site. The preferred journal for publications was naturally the SOLVEII/VINTERSOL special issue of Atmso. Chem. Phys. but also other journals have been chosen for publications. Up to now 18 publications are accepted or submitted.

*Campaign Organization*

For the proper organization of the campaign responsibilities were assigned as shown in Table 6.3. Communication with other projects involved:

- co-operation with the parallel American SOLVE-II campaign,
- co-operation with the activities within the ESA-led ENVISAT validation,
- organization of the addition of (new) instruments to the Geophysica and Falcon payloads (WAS, MTP, TDC, ASUR),
- co-operation with an additional American theory group (JPL), and
- co-operation with the APE-INFRA EU-Project.

| Task | Responsible | Assistant |
|---|---|---|
| Coordinator | Fred Stroh | |
| Campaign Scientist (Kiruna) | Hans Schlager | Tasos Kentarchos |
| Campaign Scientist (off-site) | Rob MacKenzie | |
| Logistics | Stefano Balestri | |
| Falcon readiness | Heinz Finkenzeller | |
| Falcon instrument readiness | Harald Flentje | |
| Geophysica instrument readiness | Stephan Borrmann | Piero Mazzinghi |
| Geophysica readiness | Boris Lepouchov | |
| Stratospheric meteorology and ground-based measurements | Andreas Dörnbrack | Thomas Birner |
| Satellite data | Rolf Müller | Jens-Uwe Grooβ |

**Tab. 6.2 Summary of responsibilities during the EuPLEx field campaign.**

Two locations were selected for in-depth investigation of their suitability as EuPLEx campaign basis: Kiruna (Sweden) and Longyearbyen – Svalbard (Norway). A survey visit of both locations was carried out at the beginning of February 2002 by a team comprising Stefano Balestri from ERS-Srl. The report of this survey has been published on the EuPLEx web site. Longyearbyen was perfectly geographically located but had no sufficient facilities available for the project, therefore Kiruna was selected as mission base.

In March 2002 ERS-Srl started the preparation of the campaign. The logistical needs in the airport (office distribution, general facilities and services needed, etc.) were defined and in evaluating the lodging and car rental possibilities in Kiruna for the EuPLEx participants. Based on the requests from the groups, on the availability of the facilities and their costs, the hangar and office layout shown in Fig. 6.56 was chosen, considering also the presence of the NASA–SOLVE II campaign in the same period. The distribution of the hangar and the office space between EuPLEx and SOLVE II was agreed in year 2002 by Stefano Balestri (ERS-Srl) and Mike Craig (NASA). Due to the long period of staying in Kiruna, self-catering accommodation was requested practically by all participants. The Ripan Hotel & Camping and the Gullriset were selected to host the mission participants (approx. 70 persons). A special agreement was also negotiated with Hertz for car rental. During the campaign, ERS-Srl was responsible for the set up of all the facilities in the Arena Arctica, just before the arrival of all the participants.

Basis for the flight planning during the EuPLEx campaign was the Campaign Preparation Document (or "White Book", available from EuPLEx web site). Meetings of the Campaign Group were held daily in the early afternoon to define the specific objectives of the next sortie and to prepare the suitable flight patterns. A multitude of forecast products were used as input for

the flight planning including ECMWF and MM5 forecasts, global and mesoscale air mass trajectory forecasts, and chemical and PSC forecasts.

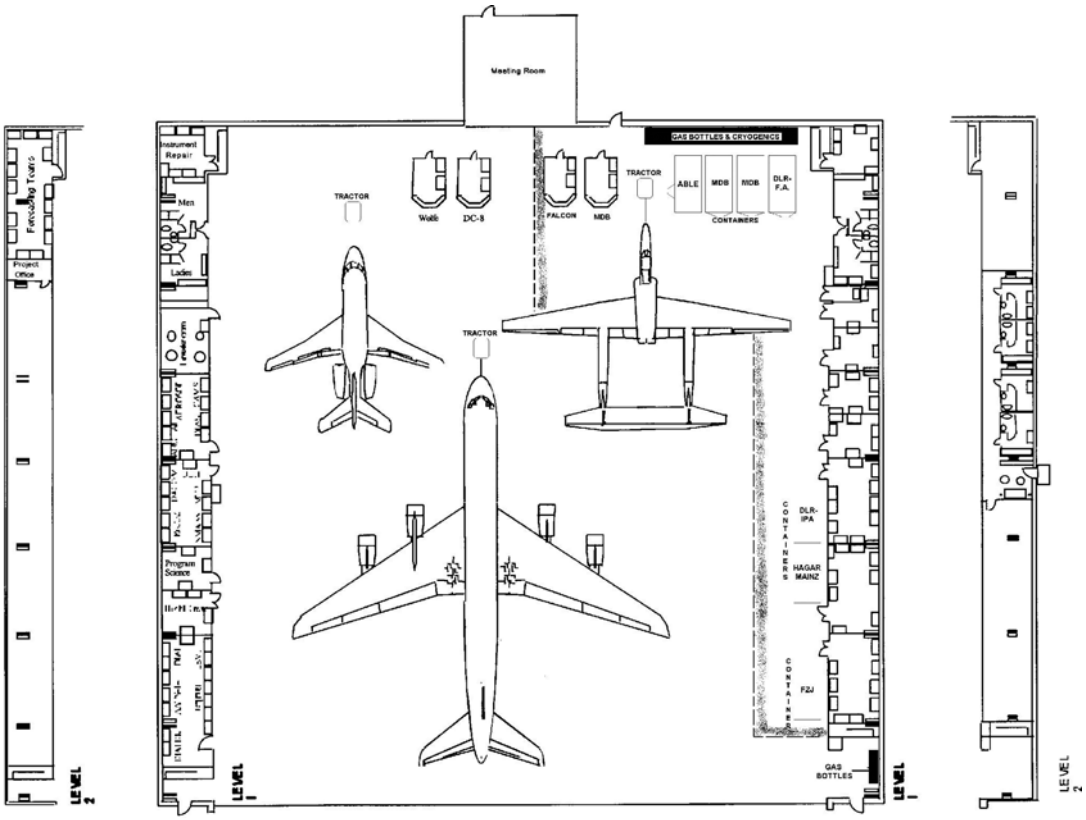


**Fig. 6.56 Hangar layout. The aircraft are: top right: M55, top left: Falcon, below: DC-8.**

The preliminary flight plans were discussed by the project co-ordinator and campaign scientist with the pilots of the Geophysica and Falcon and with the SOLVE-2 co-ordination team. The final flight plans were presented to all campaign participants during regular briefings in the evening.

The ground operations of both aircraft participating in the EuPLEx campaign (M55 and Falcon) as well as of the NASA aircraft DC-8 were co-ordinated, on the EuPLEx side, by Stefano Balestri. The flight co-ordination with the involved air traffic control centres (Sundsvall, Bodø, Stockholm, Rovaniemi, Tampere ACCs) was shared between DLR and ERS-Srl. Stefano Balestri liased with the airport personnel in case a special opening of the airport was required, and was also responsible for the distribution of the badges and office keys and for the preparation of the daily schedule.

The flights performed are summarized in the Management Report. All sorties were performed as joint Geophysica / Falcon flights with the exception of the 6./7. Feb. 2003.

The sorties on 19. and 26. Jan. were co-ordinated with SOLVE-2 including joint measurements of the Geophysica, Falcon and NASA DC-8 in selected regions of interest. Within the EuPLEx campaign period also two Geophysica flights for the validation of ENVISAT aerosol and cloud products were performed on 2. and 11. Feb 2003.

Flight reports detailing the science objectives, meteorological conditions, flight times, profiles, and routes, and preliminary results have been prepared by Tasos Kentarchos within 3 days after each flight. These reports are available on the EUPLEX data base and web site.

*EUPLEX data base and web page*

- A VINTERSOL-EUPLEX database was be set up under NADIR at NILU (zardoz.nilu.no path: /nadir/projects/vintersol/data/euplex/) for acquisition and storage of all experimental and theoretical data sets. Common data format is the NASA-Ames format widely used in the stratospheric scientific community. A project web page (http://www.nilu.no/euplex) was also established at NILU in order to communicate non-urgent information to all project members through a restricted access area. In addition a public access section was maintained to supply information on the objectives, progress, and first results to the interested public. A data CD ROM is in preparation and will become available within the next three months. It is planned to have it ready for the EGU meeting in Vienna in April in order to promote and distribute it there to interested scientists. Meteorological data (analyses and forecasts) have been provided also through NILU for the 2002-03 winter.

## 6.8 Socio-economic Relevance and Policy Implication

Proper co-ordination of research projects is a key pre-requisite for the successful completion of the scientific objectives. These in turn deliver reliable results where policy decisions can be soundly based on. Reliable operation of the instruments, perfect co-ordination and smooth and fast evaluating and publishing of preliminary results form the basis of an economic execution of a multi-partner measurement campaign and an effective use of the available workspace and the limited flight opportunities. Also the careful choice of the suitable campaign basis and modification and improvement of several instruments in order to enable the execution of simultaneous measurements of different species serve this purpose. The execution of the EuPLEx campaign simultaneously with the SOLVE II (NASA) and the ENVISAT Arctic validation campaign enabled the bundling of the results in order to enhance the period and density of measurement points in time and space.

The key objective of EUPLEX namely the thinning of the ozone layer is a global problem and therefore affects all of Europe. The substantial ozone loss that has been observed in the Arctic has affected Europe more than other regions of the Northern Hemisphere. This is due to the fact that the polar vortex often is shifted towards the European sector of the Arctic because of the Aleutian high (a high pressure system over Alaska and Easter Siberia). Therefore it is of strategic importance to Europe to obtain a better understanding of the ozone layer problem in order to enable reliable predictions of its future state. GCM calculations [Shindell et al., Nature, 392, 589 (1998)] predict that the coupling of ozone and climate may lead to far more dramatic ozone loss during the decade from 2010 to 2020 than has been observed during the 1990s. Especially in the Northern hemisphere, the potential for increasing ozone losses exist [Waibel et al., Science, 283, 2064 (1998)]. Thinning of the ozone layer leads to increased levels of UV-B radiation on the ground that has adverse effects on human health, the marine environment, as well as agriculture. The crucial uncertainties for predicting the future development of the Arctic winter ozone layer are those addressed by EUPLEX.

The results obtained within the EuPLEx project improve our understanding of the processes of PSC formation, denitrification, halogen activation, and ozone loss in the Arctic polar winter and spring. The results provide major improvements in the representation of the related processes in our models of the Arctic polar winter and spring stratospheric ozone column. This means a significantly improvement of our capability to predict short term (weeks to months) evolutions of the northern hemisphere ozone layer and consequently UV exposure on ground and therefore may enable policy decisions for mitigation in case of severe events. This is a major contribution to the actions quality of life and health and security.

## 6.9 Discussion and conclusion

WP7 had to ensure the proper organization and logistics for a smooth conduction of the field campaign, a proper flow of information between partners as well as work packages, and the timely availability of all deliverables logistic or scientific in nature. Additionally several available additional measurements were enabled onboard the EUPLEX aircraft through close cooperation with additional groups from Europe and also the US. Synergies with several other parallel activities were utilized in order to maximize the outcome of the projects. Effective flight planning was enabled by employing up to date models in forecast mode.

All these activities combined with an impressive performance of the instrument, modelling, and aircraft teams have lead to a rather complete data set on the January/February 2003 Arctic lower stratosphere. This data set combined with an unique suite of state of the art models of atmospheric chemistry and dynamics which were considerably improved over the course of the project has enabled a suite of unique interpretational studies. At the end of the project several very relevant new results have been worked out which enable a more reliable short term prediction of key processes governing Arctic stratospheric ozone depletion.

## 6.10 Main Literature produced

### 6.10.1 List of peer reviewed and submitted publicatons from the project

Bogdan, A., M. Kulmala, A. R. MacKenzie, A. Laaksonen, M. J. Molina, and A. Avramenko, The study of finely divided aqueous systems as a clue to understanding the formation mechanisms of polar stratospheric clouds: 1. $HNO_3/H_2O$ and $H_2SO_4/H_2O$ systems, *J. Geophys. Res.*, **108** (D10), 4302, doi:10.1029/2002JD002605.

Bogdan, A., M. Kulmala, A. R. MacKenzie, A. Laaksonen, M. J. Molina, and A. Avramenko, The study of finely divided aqueous systems as a clue to understanding the formation mechanisms of polar stratospheric clouds: 2. $HCl/H_2O$ and $HNO_3/HCl/H_2O$ systems, *J. Geophys. Res.*, **108** (D10), 4303, doi:10.1029/2002JD002606.

Curtius, J., R. Weigel, H.-J. V?ssing, C.-M. Volk, A. Werner, H. Schlager, A. Roiger, C. Schiller, H. Wernli, V. Dreiling, and S. Borrmann, In-situ aerosol measurements covering the 10 nm to 30 microm size range in the Arctic lower stratosphere during winter 2003 onboard the high altitude research aircraft Geophysica, submitted to Atmos. Chem. Phys, 2004.

Davies, S., G. W. Mann, K. S. Carslaw, M. P. Chipperfield, J.A. Kettleborough, M.L. Santee, H. Oelhaf, G. Wetzel, Y. Sasano, T. Sugita, 3-D microphysical model studies of Arctic denitrification: Comparison with observations, submitted to Atmos. Chem. Phys. Disc., 2004.

Feng, W., , M.P. Chipperfield, S. Davies, B. Sen, G. Toon, J.F. Blavier, C.R. Webster, C.M. Volk, A. Ulanovsky, F. Ravegnani, P. von der Gathen, H. Jost, E.C. Richard, H. Claude, Three-Dimensional Model Study of the Arctic Ozone Loss in 2002/03 and Comparison with 1999/2000 and 2003/04, Atmos. Chem. Phys. Discuss, 4, 5045-5074, 2004.

Grooß J.-U., G. Günther, R. Müller, P. Konopka, S. Bausch, H. Schlager, C. Voigt, C. M. Volk, G. C. Toon, Simulation of denitrification and ozone loss for the Arctic winter 2002/2003, Atmos. Chem. Phys. Discuss., 4, 8069-8101, 2004.

Hobe, M. von, J.-U. Grooß, R. Müller, S. Hrechanyy, U. Winkler, F. Stroh, A re-evaluation of the ClO/ $Cl_2O_2$ equilibrium constant based on stratospheric in-situ observations, , Atmos. Chem. Phys. Discuss., 4, 5075-5102, 2004

Mann, G.W., K.S. Carslaw, M.P. Chipperfield, S.D. Eckermann, Large NAT particles and denitrification caused by mountain waves in the Arctic stratosphere, accepted for publication in J. Geophys. Res., 2005.

Davies, S., G. W. Mann, K. S. Carslaw, M. P. Chipperfield, J.A. Kettleborough, M.L. Santee, H. Oelhaf, G. Wetzel, Y. Sasano, T. Sugita, 3-D microphysical model studies of Arctic denitrification: Comparison with observations, submitted to Atmos. Chem. Phys. Disc., 2004.

Kleinboehl, A., J. Kuttippurath, M. Sinnhuber, B.-M. Sinnhuber, H. Kuellmann, K. Kuenzi, J. Notholt, Rapid meridional transport of tropical airmasses to the Arctic during the major stratospheric warming in January 2003, Atmos. Chem. Phys. Discuss., 4, 7121-7138, 2004.

Konopka, P., H.-M. Steinhorst, J.-U. Grooß, G. G¨unther, R. M¨uller, J. W. Elkins, H.-J. Jost, E. Richard, U. Schmidt, G. Toon and D. S. McKenna, 2004: Mixing and ozone loss in the 1999-

2000 arctic vortex: Simulations with the 3-dimensional Chemical Lagrangian Model of the Stratosphere (CLaMS). *J. Geophys. Res.*, **109**(D2), doi:10.1029/2003JD003792.

Lowe, D., A. R. MacKenzie, N. Nikiforakis, and J. Kettleborough, A condensed-mass advection based model of liquid polar stratospheric clouds, *Atmos. Chem. Phys.*, **3**, 29-38, 2003.

Lowe, D., A. R. MacKenzie, H. Schlager, C. Voigt, A. Dörnbrack, M. J. Mahoney, and F. Cairo, Liquid particle composition and heterogeneous reactions in a mountain-wave Polar Stratospheric Cloud, *Atmos. Chem. Phys. Discuss.*, submitted November 2004.

MacKenzie, A. R., Recent advances in the study of polar stratospheric and tropical tropopause clouds, *Recent Res. Developments in Geophysics*, **4**, 439-462, 2002.

Steinhorst, H.-M., P. Konopka, G. G¨unther and R. M¨uller, 2004: How permeable is the edge of the Arctic vortex - Model studies of winter 1999-2000. *J. Geophys. Res.*, accepted.

Tilmes, S., R. Müller, J.-U. Grooß, M. Ho¨pfner, G. C. Toon, and J. M. Russell III, Very early chlorine activation and ozone loss in the Arctic winter 2002 – 2003, Geophys. Res. Lett., 30(23), 2201, doi:10.1029/2003GL018079, 2003.

Voigt, C., H. Schlager, B. Luo, A. Dörnbrack, A. Roiger, P. Stock, J. Curtius, H. Vössing, S. Borrmann, S. Davies, P. Konopka, C. Schiller, G. Shur, T. Peter, NAT formation of low Nat supersaturations, Atmos. Chem. Phys. Discuss., 4, 8579-8607, 2004.

### 6.10.2 List of publicatons from the project in preparation

Davies, S., G. W. Mann, K. S. Carslaw, M. P. Chipperfield, J. J. Remedios, A. M. Waterfall, Arctic denitrification during winter 2002/03: using satellite observations to interpret a 3-D microphysical model, manuscript in preparation.

Grooß, J.U., Rolf Müller, Fred Stroh, Marc von Hobe, Observation and simulation of air with recent chlorine activation, in preparation for Atmos. Chem. Phys, 2005.

Günther, G., R. Müller, P. Konopka, F. Stroh, C. M. Volk, Quantification of Mixing and Transport across the Boundary of the Lower Vortex during the Winter 2002/03, in preparation for Atmos. Chem. Phys., 2005.

Remedios, J.J. Remedios, A.M. Waterfall, R. Spang, G.Mann, S.Davies, K.Carslaw, Nitric acid distributions observed by the MIPAS on ENVISAT during the Vintersol campaign of 2002/3 and comparisons to a denitrification model, manuscript in preparation.

Schlager, H., et al., Observations of denitrification and renitrification in the 2002-2003 Arctic winter stratosphere, in preparation for Atmos. Chem. Phys., 2005.

Stroh, F., Marc von Hobe, Serhiy Hrechanyy, Ulf Winkler, Gebhard G?nther, Paul Konopka, Michael Volk, Hans Schlager, Francesco Cairo, Valentin Mitev and Renaud Matthey, Observations of Enhanced ClO in the Arctic Polar Winter UTLS in the Arctic Polar Winter UTLS, in preparation for Atmos. Chem. Phys, 2005.

### 6.10.3 Other publicatons from the project

A high number of talks and posters on the results obtained in the EUPLEX project have been given at a variety of scientific meetings and as seminar talks etc. For the sake of conciseness these are not listed here.
Meetings with significant contributions from the EUPLEX project were:

- EGU, Nice, April 2003
- Joint SOLVEII/VINTERSOL Science Meeting, Orlando, Oct. 2003
- AGU, San Francisco, Dec. 2003
- EGU, Nice, April 2004
- Quadrennial Ozone Symposium, Kos, June 2004

Also around ten Ph.D. thesis were completed at the partner institutions based on EUPLEX scientific objectives.

### 6.10.4 Project Reports and Planning Documents

All the documents prepared within EUPLEX for. Contractual, planning and reporting purposes are available from the restricted part of the EUPLEX web site at NILU:

1. EUPLEX Description of Work, 23.07.2001.
2. EUPLEX Campaign Preparation Document (White Book), January 2003.
3. EUPLEX Mid-Term Report, 14.07.2003.
4. EUPLEX Yearly Report, July 2004.
5. EUPLEX Final Report, January 2005.

Also Minutes of all planned project meetings listed in Table 6.2 are available from the same web site.